4. RESULTS AND DISCUSSION

The work done has been discussed under three heads:

4.1. 2-Aminobenzamide-based FXa inhibitors,

4.2. 1,3,4-Thiadiazole-based FXa inhibitors, and

4.3. Carbazole derivatives as FXa inhibitors

4.1. 2-Aminobenzamide-based Factor Xa Inhibitors

Designing aspects, synthesis, biological evaluation and molecular modeling studies of 2-aminobenzamide derivatives have been described under the following headings:

4.1.1. Designing of 2-aminobenzamide-based FXa Inhibitors

4.1.2. Synthesis of the designed 2-aminobenzamide derivatives

4.1.3. Biological evaluation

4.1.4. Docking and molecular dynamics studies

4.1.1. Designing of 2-Aminobenzamide-based Factor Xa Inhibitors

First crystal structure of FXa was reported in 1994 and till date 656 structures have been made available in protein data bank having 224 entries for Homosapiens. Availability of crystal structures of FXa bound to various inhibitors has encouraged researchers to identify suitable chemical groups worthy of binding to S1 and S4 pockets of FXa, employing structure-based drug design approach for the designing of better FXa inhibitors. A large number of FXa inhibitors containing different scaffolds as reported by various research groups have been discussed in detail in chapter-2. Among these, anthranilamide and *cis*-diamine based FXa inhibitors have been explored extensively for developing orally active antithrombotic drugs. These vicinal diamide-based FXa inhibitors with U or V shape of the molecule demonstrated good binding to FXa.

Inspired by the favorable biological profile of anthranilamide based FXa inhibitors, we selected betrixaban (**10**) as a lead molecule for further chemical modifications. It was planned to use anthranilamide as the central scaffold to connect it to the two different hydrophobic arms (S1 binding ligand

and S4 binding ligand). The neutral haloaromatics, particularly the chlorinated ones have proven their worth as successful S1 binding ligands as they bind effectively to Tyr228 of S1 pocket by Cl-π interaction, improving selectivity and oral bioavailability.[88] The highly basic amidine group, initially used as a successful S1 or S4 binding ligand, has been reported to be the culprit for poor oral bioavailability of these compounds.[89]

To develop orally active, small FXa inhibitors, it was contemplated to introduce alkyls, benzyls, biphenyls or substituted piperazines as S4 binding ligands in the anthranilamide scaffold as the replacements of highly basic amidine group of betrixaban (**10**) and maintain the 5-chloro-2-pyridyl group as such, as the S1 binding ligand as represented in **Figure 4.1**.

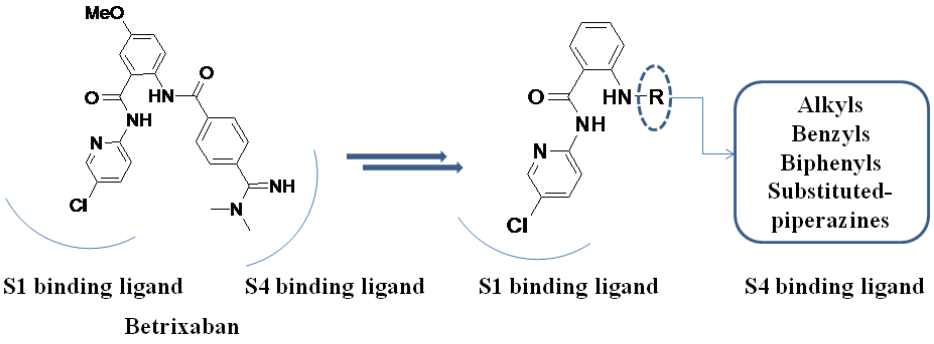

Figure 4.1. Anthranilamide derivatives possessing novel S4 binding ligands.

4.1.2. Synthesis of the designed 2-aminobenzamide derivatives

4.1.2.1. Synthesis of *N*-substituted isatoic anhydride (52-63)

Commercially available isatoic anhydride (**51**) was reacted with alkyl/arylalkyl halides in presence of some organic base to obtain *N*-substituted isatoic anhydrides (**52-63**) as illustrated in **Scheme 4.1**. All of the intermediates **(52-63)** were characterized on the basis of their physical and spectral data (**Table 4.1**) as reported in literature.[90–92] The -NH stretching vibration peak of isatoic anhydride disappeared in *N*-substituted isatoic anhydrides.

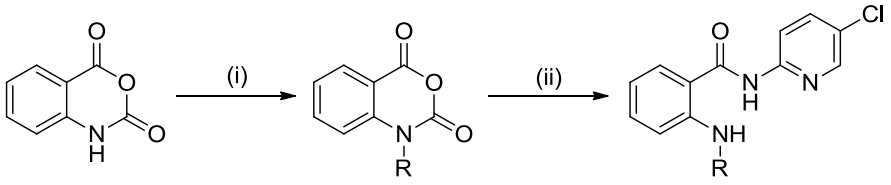

Scheme 4.1. Synthetic route for the preparation of compounds **(64-76)**. Reagents and conditions: (i) Alkyl/arylalkyl halide, DIPEA, DMA, rt; (ii) 2-Amino-5-chloropyridine, pot. *tert*-butoxide, THF, rt.

Table 4.1. Analytical data of *N*-substituted isatoic anhydride (**52-63**)

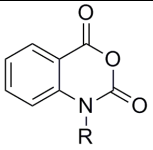

Comp	R	M.P.	IR characteristic peaks (cm^{-1})
52		160-162 °C (lit.[90] 164-166 °C)	1771, 1719, 1324, 1068, 1024, 762, 742
53		111-113 °C (lit.[91] 115-117 °C)	1773, 1726, 1323, 1050, 745
54	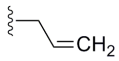	97-99 °C (lit.[92] 102-104)	1722, 1602, 1379, 1319, 1027, 759
55	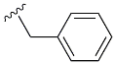	140-142 °C (lit.[90] 139-141 °C)	1779, 1719, 1379, 1317, 1025, 758
56	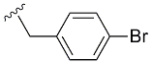	172-174 °C (lit.[92] 175-177 °C)	1777, 1719, 1379, 1322,1027, 839, 754
57	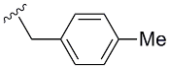	131-133 °C (lit.[92] 133-135 °C)	1786, 1716, 1376, 1325, 1025, 825, 761
58	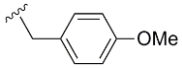	137-139 (lit.[92] 138-140)	2226, 1792, 1717, 1376, 1326, 1032, 858, 759
59	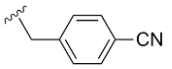	117-119 °C	1777, 1717, 1380, 1310, 1028, 816, 759
60	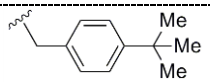	164-166 °C	1777, 1722, 1376, 1323, 1025, 805, 762
61	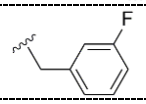	130-132 °C (lit.[92] 133-135 °C)	1785, 1713, 1377, 1321,1029, 759
62	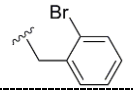	136-138 °C	1785, 1720, 1360,1328, 1033, 761
63	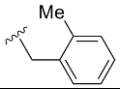	130-132 °C	1774, 1722, 1377, 1315, 1028, 768, 745

4.1.2.2. Synthesis of substituted 2-amino-*N*-(5-chloropyridin-2-yl)benzamides (64-76)

The synthesis of substituted 2-amino-*N*-(5-chloropyridin-2-yl)benzamides (**64-76**) was accomplished by adopting general **Scheme 4.1**. The *N*-substituted isatoic anhydrides (**52-63**) were subjected to ring opening by reacting with 2-amino-5-chloropyridine to afford the desired substituted 2-amino-*N*-(5-chloropyridin-2-yl)benzamides (**64-76**). IR spectra of these compounds showed peaks (cm^{-1}) at 3300-3490 (N-H stretch), 1640-1660 (C=O stretch), 1550-1575 and 1500-1520 (N-H bend) (**Table 4.2**).

Table 4.2. Analytical data of the compounds (**64-76**)

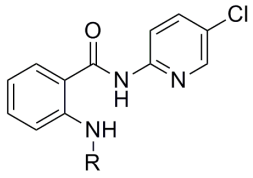

(64-76)

Comp	R	M.P.	IR characteristic peaks (cm^{-1})
64	H	188-190 °C	3486, 3376, 1657, 1552, 1515, 851, 747
65		143-145 °C	3387, 3219, 1654, 1572, 1514, 832, 743
66		126-128 °C	3352, 3229, 1660, 1572, 1512, 823, 743
67	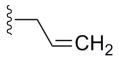	102-104 °C	3356, 3216, 1657, 1571, 1512, 829, 745
68	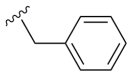	152-154 °C	3356 , 3257, 1653, 1571, 1509, 830, 748
69	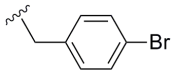	130-132 °C	3396, 3208, 1649, 1574, 1511, 834, 748
70	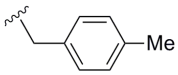	142-144 °C	3350, 3260, 1655, 1570, 1509, 825, 746
71	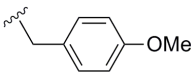	144-146 °C	3359, 3225, 1655, 1568, 1510, 835, 746
72	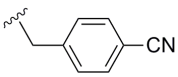	140-142 °C	3391, 3310, 2232, 1654, 1571, 1521, 836, 743
73	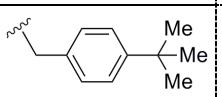	136-138 °C	3365, 3223, 1657, 1571, 1521, 832, 743

Comp	R	M.P.	IR characteristic peaks (cm^{-1})
74	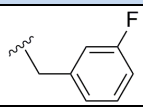	118-120 °C	3406, 3212, 1652, 1574, 1512, 750
75	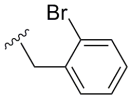	119-121 °C	3416, 3319, 1659, 1572, 1513, 739
76	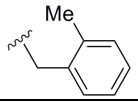	128-130 °C	3437, 3336, 1656, 1571, 1513, 740

The ^{1}H-NMR spectrum of compound (**64**) showed a broad singlet at δ 8.61 due to the proton (NH_e) attached to the amidic nitrogen and broad singlet at δ 5.62 for two amino protons (NH_i). The aromatic protons of pyridine ring appeared as doublet at δ 8.29 for one proton (ArH_f), doublet at δ 8.18 for one proton (ArH_h) and doublet of doublet at δ 7.68 for one proton (ArH_g). The other aromatic protons appeared as doublet of doublet at δ 7.49 for one proton (ArH_d), multiplet at δ 7.24-7.28 for one proton (ArH_b) and another multiplet at δ 6.68-6.73 for two hydrogens (Ar$H_{a,c}$). Its mass spectrum showed molecular ion $(M)^+$ peak at 247.9 m/z and $(M-127)^+$ ion peak at 119.9 m/z.

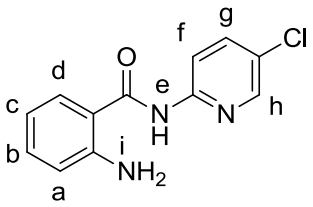

(64)

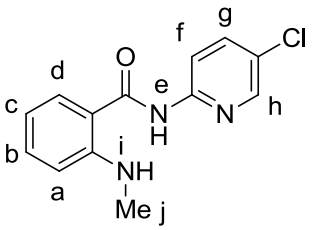

(65)

The ^{1}H-NMR spectrum of compound (**65**) showed a broad singlet at δ 8.58 due to the proton (NH_e) attached to the amidic nitrogen. The aromatic protons of pyridine ring appeared as doublet at δ 8.26 for one proton (ArH_f), doublet at δ 8.19 for one proton (ArH_h) and doublet of doublet at δ 7.68 for one proton (ArH_g). The other aromatic protons appeared as doublet of doublet at δ 7.51 for one proton (ArH_d), multiplet at δ 7.36-7.40 for one proton (ArH_b), doublet of doublet at δ 6.72 for one proton (ArH_a) and another multiplet at δ 6.61-6.65 for one proton (ArH_c). It also showed singlet at δ 7.51 for one amine

proton (NH_i) and singlet at δ 2.90 for three methyl protons (NHCH_{3k}). Its ^{13}C-NMR spectrum showed peak at 168.16 due to C=O carbon of the amide. Aromatic carbons appeared at δ 151.25, 150.09, 146.17, 138.15, 134.05, 127.80, 126.41, 114.83, 113.64 and 111.61 whereas the aliphatic carbon appeared at δ 29.73. Its mass spectrum showed molecular ion $(M)^+$ peak at 261.9 m/z and $(M-127)^+$ ion peak at 134.9 m/z.

The ^{1}H-NMR spectrum of compound (**66**) showed a broad singlet at δ 8.65 due to the proton (NH_e) attached to the amidic nitrogen. The aromatic protons of pyridine ring offered signals as doublet at δ 8.26 for one proton (ArH_f), doublet at δ 8.16 for one proton (ArH_h) and doublet of doublet at δ 7.67 for one proton (ArH_g). The other aromatic protons were observed as doublet of doublet at δ 7.51 for one proton (ArH_d), multiplet at δ 7.33-7.37 for one proton (ArH_b), doublet of doublet at δ 6.72 for one proton (ArH_a) and multiplet at δ 6.59-6.63 for one proton (ArH_c). It also showed singlet at δ 7.45 for one amine proton (NH_i). Aliphatic protons appeared as multiplet at δ 3.18-3.25 for methylene hydrogens (CH_{2j}) and triplet at δ 1.31 for three methyl protons (CH_{3k}). Its ^{13}C-NMR spectrum showed peak at δ 168.12 due to C=O carbon of the amide. Aromatic carbons appeared at δ 150.22, 150.06, 146.09, 138.21, 134.04, 127.90, 126.43, 114.99, 114.91, 113.55 and 112.29 whereas the aliphatic carbons appeared at δ 37.78 and 14.50. Its mass spectrum showed $(M-127)^+$ ion peak at 148.3 m/z.

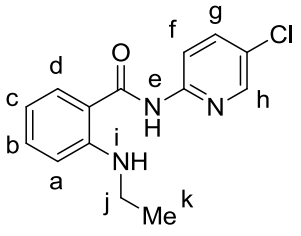

(66)

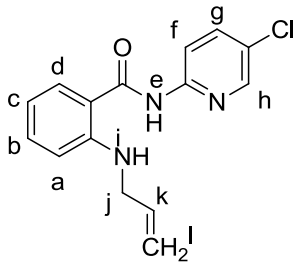

(67)

The ^{1}H-NMR spectrum of compound (**67**) showed a broad singlet at δ 8.66 due to the proton (NH_e) attached to the amidic nitrogen. The aromatic protons of pyridine ring were observed as doublet at δ 8.27 for one proton (ArH_f), doublet at δ 8.16 for one proton (ArH_h) and doublet of doublet at δ

7.67 for one proton (ArH_g). The other aromatic protons appeared as doublet of doublet at δ 7.52 for one proton (ArH_d), multiplet at δ 7.32-7.36 for one proton (ArH_b), doublet of doublet at δ 6.71 for one proton (ArH_a) and another multiplet at δ 6.61-6.65 for one proton (ArH_c). It also showed singlet at δ 7.74 for one amine proton (NH_i). The aliphatic protons were observed as multiplet at δ 5.90-6.00 for one allylic proton (CH_k), two multiplets at δ 5.28-5.33 and δ 5.17-5.20 for two allylic protons (CH_{2l}) and multiplet at δ 3.18-3.25 for two methylene hydrogens (CH_{2j}). Its mass spectrum showed molecular ion $(M)^+$ peak at 287.9 m/z and $(M-127)^+$ ion peak at 160.9 m/z.

The ^{1}H-NMR spectrum of compound (**68**) showed a broad singlet at δ 9.06 due to the proton (NH_e) attached to the amidic nitrogen. The aromatic protons of pyridine ring were observed as doublet at δ 8.38 for one proton (ArH_f), doublet at δ 8.23 for one proton (ArH_h) and doublet of doublet at δ 7.76 for one proton (ArH_g). It also displayed doublet of doublet at δ 7.67 for one aromatic proton (ArH_d) and multiplet at δ 7.27-7.41 for six aromatic protons (Ar$H_{b,k,l,m}$) and one amino proton (NH_i). A multiplet was observed at δ 6.67-6.73 for two aromatic protons (Ar$H_{a,c}$). A singlet at δ 4.48 was obtained for two benzylic hydrogens (CH_{2j}). The mass spectrum showed molecular ion $(M)^+$ peak at 337.9 m/z and (M-127) ion peak at 210.9 m/z.

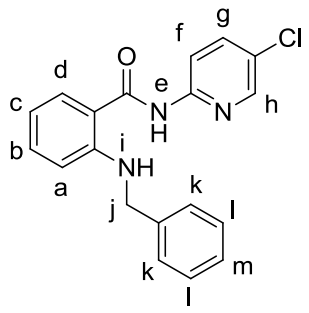

(68)

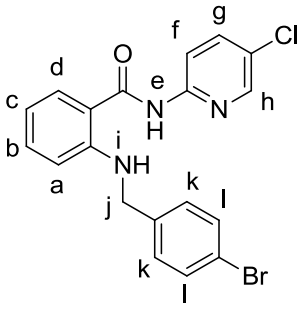

(69)

The ^{1}H-NMR spectrum of compound (**69**) showed a broad singlet at δ 8.59 due to the proton (NH_e) attached to the amidic nitrogen. The aromatic protons of pyridine ring appeared as doublet at δ 8.28 for one proton (ArH_f), doublet at δ 8.26 for one proton (ArH_h) and doublet of doublet at δ 7.70 for one proton (ArH_g). It also showed triplet at δ 8.12 for one amine proton (NH_i). The other aromatic protons appeared as doublet of doublet at δ 7.57 for one

proton (ArH_d), doublet at δ 7.48 for two protons (ArH_l), multiplet at δ 7.25-7.34 for three protons (Ar$H_{b,k}$) and multiplet at δ 6.63-6.71 for two protons (Ar$H_{a,c}$). A doublet at δ 4.42 was accounted for two benzylic hydrogens (CH_{2j}). The mass spectrum showed molecular ion $(M)^+$ peak at 416.6 m/z, $(M+2)^+$ ion peak at 418.5 m/z and $(M-127)^+$ ion peak at 290.4 m/z.

The ^{1}H-NMR spectrum of compound (**70**) showed a broad singlet at δ 8.52 due to the proton (NH_e) attached to the amidic nitrogen. The aromatic protons of pyridine ring were observed as doublet at δ 8.26 for one proton (ArH_f), doublet at δ 8.23 for one proton (ArH_h) and doublet of doublet at δ 7.67 for one proton (ArH_g). The other aromatic protons appeared as doublet of doublet at δ 7.54 for one proton (ArH_d), multiplet at δ 7.24-7.32 for four protons (Ar$H_{k,l}$), multiplet at δ 7.13-7.15 for one proton (ArH_b), doublet at δ 6.69 for (ArH_a) and multiplet at δ 6.62-6.66 for one proton (ArH_c). It also showed triplet at δ 8.03 for one amine proton (NH_i). The aliphatic protons offered signals as doublet at δ 4.40 for two benzylic hydrogens (CH_{2j}) and a singlet at δ 2.33 for three methyl protons (CH_{3m}). Its mass spectrum showed molecular ion $(M)^+$ peak at 351.9 m/z and (M-127) ion peak at 223.9 m/z.

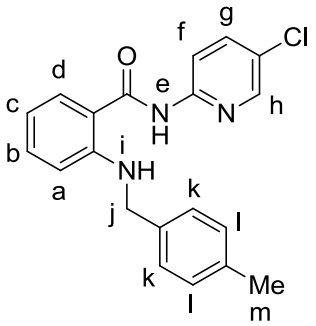

(70)

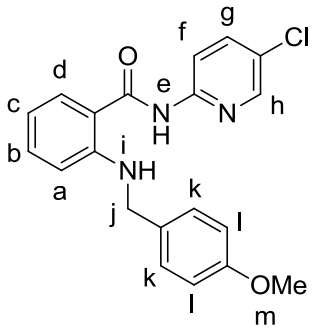

(71)

The ^{1}H-NMR spectrum of compound (**71**) showed a broad singlet at δ 8.54 due to the proton (NH_e) attached to the amidic nitrogen. The aromatic protons of pyridine ring were observed as doublet at δ 8.25 for one proton (ArH_f), doublet at δ 8.22 for one proton (ArH_h) and doublet of doublet at δ 7.67 for one proton (ArH_g). The other aromatic protons were observed as doublet of doublet at δ 7.54 for one proton (ArH_d), multiplet at δ 7.25-7.33 for four protons (Ar$H_{k,l}$), multiplet at δ 6.87-6.89 for one proton (ArH_b), doublet at

δ 6.70 for (ArH_a) and multiplet at δ 6.62-6.66 for one proton (ArH_c). It also displayed triplet at δ 7.98 for one amine proton (NH_i). The aliphatic protons were observed as doublet at δ 4.38 for two benzylic hydrogens (CH_{2j}) and a singlet at δ 3.79 for three methyl protons (CH_{3m}). Its mass spectrum showed $(M+Na)^+$ ion peak at 389.9 m/z, (M-127) ion peak at 241 m/z and (M-156) ion peak at 212 m/z.

The ^{1}H-NMR spectrum of (**72**) showed a broad singlet at δ 11.58 due to the proton (NH_e) attached to the amidic nitrogen. The aromatic protons of pyridine ring were observed as doublet at δ 8.84 for one proton (ArH_f), doublet at δ 8.22 for one proton (ArH_h) and doublet of doublet at δ 8.11 for one proton (ArH_g). The other aromatic protons appeared as multiplet at δ 7.32-7.69 for six protons (Ar$H_{b,d,k,l}$). One amine proton (NH_i) was merged in aromatic region at δ 7.32-7.69. It also displayed a multiplet at δ 6.81-6.85 for (ArH_c) and doublet at δ 6.59 for one proton (ArH_a). The aliphatic protons were observed as doublet at δ 4.56 for the two benzylic hydrogens (CH_{2j}). The mass spectrum showed molecular ion $(M)^+$ peak at 362.5 m/z and $(M-127)^+$ ion peak at 235.2 m/z.

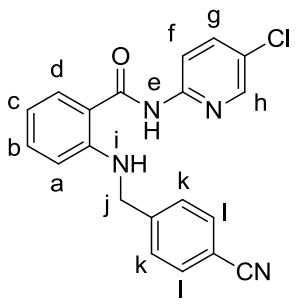

(72)

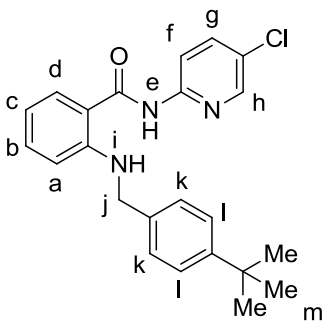

(73)

The ^{1}H-NMR spectrum of compound (**73**) showed a broad singlet at δ 8.59 due to the proton (NH_e) attached to the amidic nitrogen. The aromatic protons of pyridine ring were observed as doublet at δ 8.25 for one proton (ArH_f), doublet at δ 8.20 for one proton (ArH_h) and doublet of doublet at δ 7.67 for one proton (ArH_g). It also showed a triplet at δ 8.01 for one amine proton (NH_i). The other aromatic protons appeared as doublet at δ 7.54 for one proton (ArH_d), multiplet at δ 7.29-7.37 for five protons (Ar$H_{b,k,l}$), doublet at δ

6.72 for (ArH_a) and multiplet at δ 6.62-6.66 for one proton (ArH_c). The aliphatic protons were observed as doublet at δ 4.39 for two benzylic hydrogens (CH_{2j}) and singlet at δ 1.31 for nine methyl protons (CH_{3m}). Its mass spectrum showed molecular ion peak at 394.6 m/z and (M-127) ion peak at 267.6 m/z.

The ^{1}H-NMR spectrum of compound (**74**) showed a broad singlet at δ 8.56 due to the proton (NH_e) attached to the amidic nitrogen. The aromatic protons of pyridine ring appeared as doublet at δ 8.27 for one proton (ArH_f), doublet at δ 8.23 for one proton (ArH_h) and doublet of doublet at δ 7.69 for one proton (ArH_g). It also showed a triplet at δ 8.14 for one amine proton (NH_i). The other aromatic protons were observed as doublet of doublet at δ 7.55 for one proton (ArH_d), multiplet at δ 7.25-7.32 for two protons (Ar$H_{n,l}$), doublet at δ 7.14 for one proton (ArH_m), doublet at δ 7.07 for one proton (ArH_k), multiplet at δ 6.92-6.96 one proton (ArH_b) and multiplet at δ 6.61-6.69 two protons (Ar$H_{a,c}$). The aliphatic protons were observed as a doublet at δ 4.45 for two benzylic protons (CH_{2j}). Its mass spectrum showed molecular ion $(M)^+$ peak at 355.9 m/z, $(M+Na)^+$ ion peak at 377.9 m/z and (M-127) ion peak at 227 m/z.

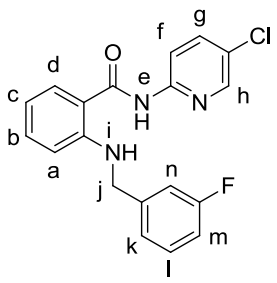

(74)

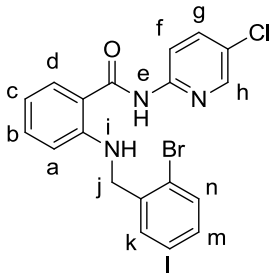

(75)

The ^{1}H-NMR spectrum of compound (**75**) showed a broad singlet at δ 9.86 due to the proton (NH_e) attached to the amidic nitrogen. It also showed a triplet at δ 8.58 for one amine proton (NH_i). The aromatic protons of pyridine ring were observed as doublet at δ 8.47 for one proton (ArH_f), doublet at δ 8.15 for one proton (ArH_h) and doublet of doublet at δ 7.82 for one proton (ArH_g). The other aromatic protons were observed as doublet of

doublet at δ 7.77 for one proton (ArH_d), doublet at δ 7.50 for one protons (ArH_n), multiplet at δ 7.25-7.34 for three protons (Ar$H_{k,l,m}$), multiplet at δ 7.04-7.08 for one proton (ArH_b), multiplet at δ 6.64-6.68 for one proton (ArH_c) and doublet at δ 6.53 for one protons (ArH_a). A doublet at δ 4.44 accounted for two benzylic protons (CH_{2j}). The mass spectrum showed molecular ion $(M)^+$ peak at 416.5 m/z and $(M+2)^+$ ion peak at 418.6 m/z.

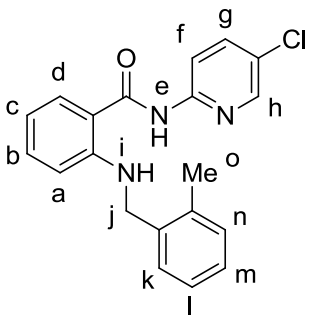

(76)

The ^{1}H-NMR spectrum of compound (**76**) showed a broad singlet at δ 8.49 due to the proton (NH_e) attached to the amidic nitrogen. The aromatic protons of pyridine ring were observed as doublet at δ 8.25 for one proton (ArH_f), doublet at δ 8.23 for one proton (ArH_h) and doublet of doublet at δ 7.67 for one proton (ArH_g). The other aromatic protons were observed as doublet at δ 7.55 for one proton (ArH_d), multiplet at δ 7.14-7.35 for five protons (Ar$H_{b,k,l,m,n}$) and multiplet at δ 6.64-6.70 for two protons (Ar$H_{a,c}$). It also showed a triplet at δ 7.92 for one amine proton (NH_i). The aliphatic protons were observed as doublet at δ 4.37 for two benzylic protons (CH_{2j}) and singlet at δ 2.38 for three methyl protons (CH_{3o}). Its mass spectrum showed molecular ion $(M)^+$ peak at 351.9 m/z and (M-127) ion peak at 223.9 m/z.

4.1.2.3. Synthesis of 2-(2-chloroacetamido)-*N*-(5-chloropyridin-2-yl) benzamide (77)

Compound (**64**) was reacted with chloroacetyl chloride to offer the intermediate (**77**) as illustrated in **Scheme 4.2**.

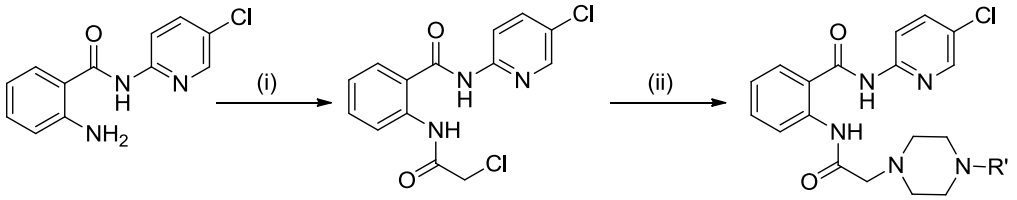

(64) **(77)** **(78-83)**

Scheme 4.2. Synthetic route for the preparation of compounds (**78-83**). Reagents and conditions: (i) Chloroacetyl chloride, K_2CO_3, dry DCM, 0-5 °C; (ii) Substituted piperazines, DMF, 120 °C, 4-6 h.

The IR spectrum of intermediate (**77**) showed peaks (cm^{-1}) at 3401, 3285 (N-H stretch) and 1663 (C=O stretch) for amide functional group. Its ^{1}H-NMR spectrum showed two broad singlets at δ 11.57 and δ 8.73 due to the two protons (N$H_{e,i}$) attached to the amidic nitrogens. The aromatic protons of pyridine ring were observed as doublet at δ 8.61 for one proton (ArH_f), doublet of doublet at δ 8.32 for one proton (ArH_g) and doublet at δ 8.25 for one proton (ArH_h). The other aromatic protons appeared as multiplet at δ 7.69-7.75 for (Ar$H_{a,d}$) multiplet at δ 7.54-7.59 for one proton (ArH_b) and multiplet at δ 7.19-7.26 for one proton (ArH_c). The aliphatic protons were observed as singlet at δ 4.20 for two methylene protons (CH_{2j}). The mass spectrum showed molecular ion $(M)^+$ peak at 324.0 m/z and $(M+2)^+$ ion peak at 326.0 m/z.

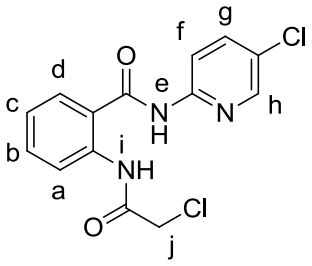

(77)

4.1.2.4. 2-(2-(*N*-Substituted piperazin-1-yl)acetamido)-*N*-(5-chloropyridin-2-yl)benzamides (78-83)

2-(2-(*N*-Substitutedpiperazin-1-yl)acetamido)-*N*-(5-chloropyridin-2-yl) benzamides (**78-83**) were synthesized using synthetic route as depicted in **Scheme 4.2**. The chloro group of the intermediate (**77**) was displaced by different substituted piperazines to get the desired piperazinyl compounds (**78-**

83). The IR spectra of these compounds showed one characteristic peak around 1670 cm^{-1} for C=O stretching of amide and another one in the range of 3500-3200 cm^{-1} (N-H stretch).

Table 4.3. Analytical data of piperazinyl compounds (**78-83**)

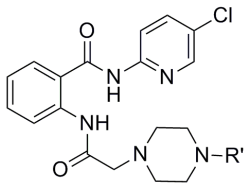

(78-83)

Comp	R	M.P.	IR characteristic peaks (cm^{-1})
78	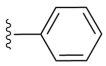	148-150 °C	3431, 3200, 1693, 1666, 1573, 1516, 842, 754
79	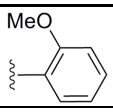	140-142 °C	3430, 3223,1666, 1578, 1503, 834, 751
80	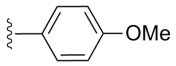	100-102 °C	3443, 3200, 1683, 1604, 1572, 1510, 827, 773
81	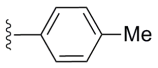	183-185 °C	3274, 1687, 1580, 1509, 843, 765
82	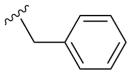	150-152 °C	3435, 3233, 1667, 1576, 1511, 830, 751
83	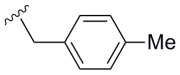	154-156 °C	3434, 3190, 1693, 1665, 1579, 1515, 840, 762

The ^{1}H-NMR spectrum of compound (**78**) showed two singlets at δ 11.70 and δ 8.83 due to the protons (N$H_{e,i}$) attached to the amidic nitrogens. The aromatic protons of pyridine ring were observed as doublet at δ 8.24 for one proton (ArH_f), doublet of doublet at δ 8.14 for one proton (ArH_g) and doublet at δ 7.61 for one proton (ArH_h). Other signals appeared as doublet of doublet at δ 8.70 for one aromatic proton (ArH_d), multiplet at δ 7.50-7.54 for one aromatic proton (ArH_b), multiplet at δ 7.28-7.37 for three aromatic protons (Ar$H_{a,n}$), multiplet at δ 7.10-7.14 for one aromatic proton (ArH_c) and multiplet at δ 6.90-6.94 for three aromatic protons (Ar$H_{m,o}$). Aliphatic protons appeared as singlet at δ 3.23 for two methylene protons (CH_{2j}), triplet at δ 3.33 for four methylene protons (NCH_{2l}) and triplet at δ 2.78 for four methylene

protons (NCH_{2k}). Its mass spectrum showed molecular ion $(M)^+$ peak at 450.1 m/z and $(M+2)^+$ ion peak at 452.1 m/z.

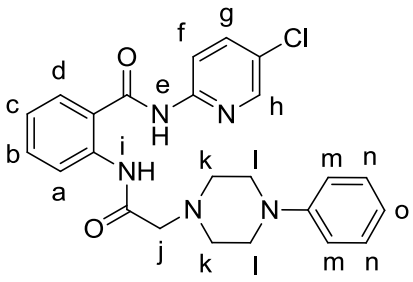

(78)

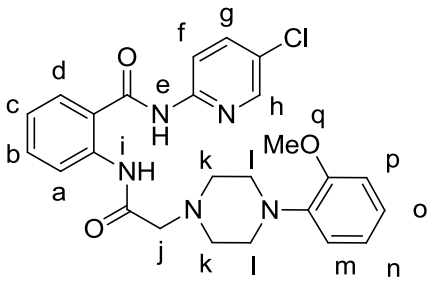

(79)

The ^{1}H-NMR spectrum of compound (**79**) showed a singlet at δ 11.76 due to the protons (NH_e) attached to the amidic nitrogen. The aromatic protons of pyridine ring were observed as doublet at δ 8.36 for one proton (ArH_f), doublet of doublet at δ 7.64 for one proton (ArH_g) and doublet at δ 8.21 for one proton (ArH_h). It showed multiplet at δ 8.70-8.74 for two protons (ArH_d and NH_i), multiplet at δ 7.52-7.56 for two aromatic protons (Ar$H_{a,p}$), multiplet at δ 7.13-7.17 for one aromatic proton (ArH_n), multiplet at δ 7.04-7.08 for one aromatic proton (ArH_b), multiplet at δ 6.95-6.99 for one aromatic proton (ArH_c) and multiplet at δ 6.90-6.92 for two aromatic protons (Ar$H_{m,o}$). Aliphatic protons were observed as singlet at δ 3.87 for three methyl protons (CH_{3q}) and a singlet at δ 3.24 for two methylene protons (CH_{2j}). It also displayed one multiplet at δ 3.22-3.24 for four methylene protons (NCH_{2l}) and another multiplet at δ 2.83-2.85 for four methylene protons (NCH_{2k}). Its mass spectrum showed molecular ion $(M)^+$ peak at 480.7 m/z and $(M+2)^+$ ion peak at 482.7 m/z.

The ^{1}H-NMR spectrum of compound (**80**) showed a doublet at δ 8.55 for one aromatic proton (ArH_h), two doublets of doublet at δ 8.30 and δ 7.42 for two aromatic protons (ArH_g) and (ArH_a) respectively. It also displayed multiplet at δ 7.74-7.84 for three aromatic protons (Ar$H_{f,d,b}$), multiplet at δ 7.50-7.54 for one proton (ArH_c) and multiplet at δ 6.80-6.82 for four aromatic protons (Ar$H_{m,n}$). The aliphatic protons were observed as singlet at δ 3.75 for three methyl protons (CH_{3o}), singlet at δ 3.63 for two methylene protons

(CH_{2j}), multiplet at δ 2.78-2.80 for four methylene protons (NCH_{2l}) and multiplet at δ 2.39-2.41 for four methylene protons (NCH_{2k}). Its ^{13}C-NMR spectrum showed peak at δ 162.22 due to C=O carbon of the amide. Aromatic carbons appeared at δ 152.38, 149.03, 147.69, 146.84, 137.26, 134.95, 132.20, 127.62, 127.51, 127.05, 126.25, 121.21, 118.29 and 114.48 whereas the aliphatic carbons appeared at δ 61.19, 55.57, 52.61 and 50.46. The mass spectrum showed molecular ion $(M)^+$ peak at 480.7 m/z and $(M+2)^+$ ion peak at 482.7 m/z.

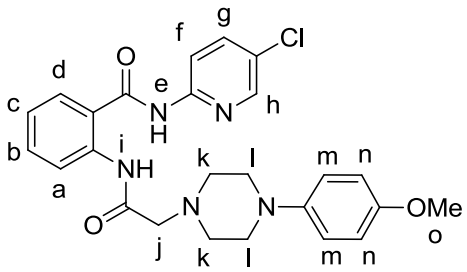

(80)

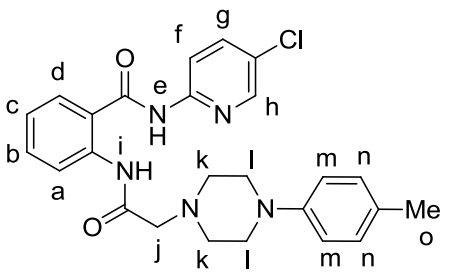

(81)

The ^{1}H-NMR spectrum of compound (**81**) showed two singlets at δ 11.74 and δ 8.55 due to the protons (N$H_{e,i}$) attached to the amidic nitrogens. The aromatic protons of pyridine ring were observed as doublet at δ 8.24 for one proton (ArH_f), doublet of doublet at δ 7.63 for one proton (ArH_g) and doublet at δ 8.22 for one proton (ArH_h). The other aromatic protons appeared as doublet of doublet at δ 8.73 for one aromatic proton (ArH_d), multiplet at δ 7.52-7.56 for one proton (ArH_b), multiplet at δ 7.32-7.35 for one proton (ArH_a), multiplet at δ 7.14-7.18 for one proton (ArH_c), doublet at δ 7.11 for two protons (ArH_n) and doublet at δ 6.83 for two protons (ArH_m). The aliphatic protons were observed as singlet at δ 2.32 for three methyl protons (CH_{3o}), singlet at δ 3.24 for two methylene protons (CH_{2j}), triplet at δ 3.28 for four methylene protons (NCH_{2l}) and multiplet at δ 2.77-2.80 for four methylene protons (NCH_{2k}). Its mass spectrum showed molecular ion $(M)^+$ peak at 464.8 m/z and $(M+2)^+$ ion peak at 466.8 m/z.

The ^{1}H-NMR spectrum of compound (**82**) showed two singlets at δ 11.51 and δ 8.74 due to the protons (N$H_{e,i}$) attached to the amidic nitrogens.

The aromatic protons of pyridine ring were observed as doublet at δ 8.44 for one proton (ArH_f), doublet of doublet at δ 7.63 for one proton (ArH_g) and doublet at δ 8.24 for one proton (ArH_h). The other aromatic protons were observed as doublet of doublet at δ 8.64 for one aromatic proton (ArH_d), doublet of doublet at δ 7.78 for one aromatic proton (ArH_a), multiplet at δ 7.48-7.53 for one proton (ArH_b), multiplet at δ 7.11-7.15 for one proton (ArH_c) and multiplet at δ 7.24-7.26 for five protons (Ar$H_{n,o,p}$). The aliphatic protons were observed as singlet at δ 3.52 for two methylene protons (CH_{2m}), singlet at δ 3.16 for two methylene protons (CH_{2j}) and multiplet δ 2.59-2.63 for eight methylene protons (NC$H_{2k,l}$). Its mass spectrum showed molecular ion $(M)^+$ peak at 463.8 m/z and $(M+2)^+$ ion peak at 465.8 m/z.

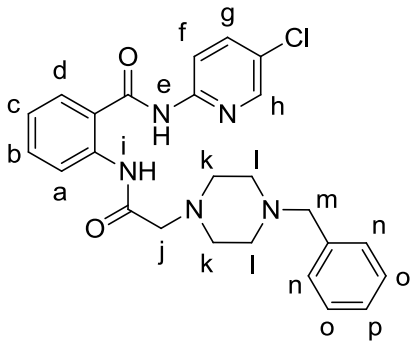

(82)

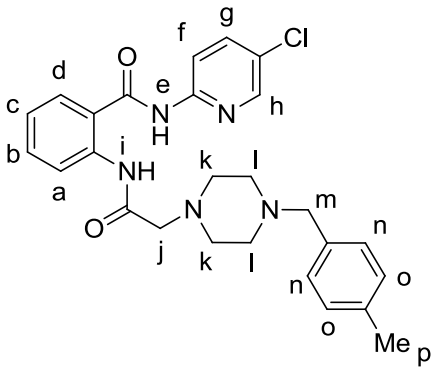

(83)

The ^{1}H-NMR spectrum of compound (**83**) showed two singlets at δ 11.50 and δ 8.73 due to the protons (N$H_{e,i}$) attached to the amidic nitrogens. The aromatic protons of pyridine ring were observed as doublet at δ 8.44 for one proton (ArH_f), doublet of doublet at δ 7.62 for one proton (ArH_g) and doublet at δ 8.23 for one proton (ArH_h). The other aromatic protons were observed as doublet of doublet at δ 8.64 for one aromatic proton (ArH_d), doublet of doublet at δ 7.76 for one aromatic proton (ArH_a), multiplet at δ 7.48-7.53 for one proton (ArH_b) and multiplet at δ 7.11-7.20 for five protons (Ar$H_{c,n.o}$). The aliphatic protons were observed as singlet at δ 3.48 for three methylene protons (CH_{2m}), singlet at δ 3.16 for two methylene protons (CH_{2j}), multiplet 2.58-2.62 for eight methylene protons (NC$H_{2k,l}$) and singlet at δ 2.34 for three methyl protons (CH_{3p}). Its mass spectrum showed molecular ion $(M)^+$ peak at 478.0 m/z.

4.1.2.5. Synthesis of substituted 4-bromomethyl-1,1'-biphenyls (93-101)

Substituted 4-bromomethyl-1,1'-biphenyls (**93-101**) required for the preparation of the target compounds (**102-110**) were synthesized in two steps (**Scheme 4.3**). A Suzuki cross-coupling reaction was performed using X-substituted (X = H, F) 4-bromotoluene and Y-substituted phenylboronic acid as per the reported green synthetic procedure[93,94] to obtain compounds (**84-92**). Characterization data for all the synthesized compounds (**84-92**) were in accordance with the reported compounds.[95–97] These biphenyls (**84-92**) were subjected to benzylic bromination to get the desired bromomethyl derivatives (**93-101**) which were used in the next step without further purification.

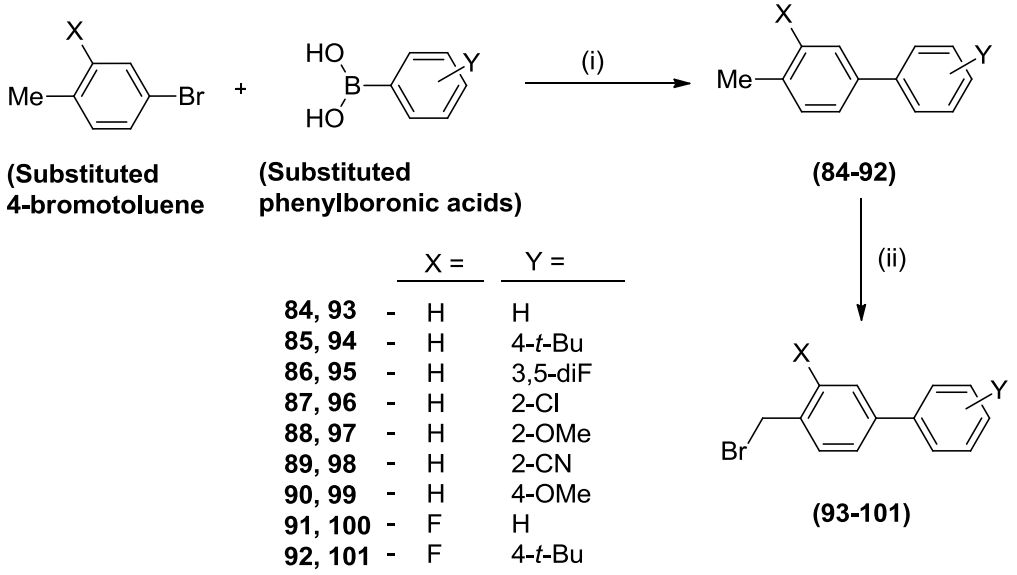

	X =	Y =
84, 93	H	H
85, 94	H	4-*t*-Bu
86, 95	H	3,5-diF
87, 96	H	2-Cl
88, 97	H	2-OMe
89, 98	H	2-CN
90, 99	H	4-OMe
91, 100	F	H
92, 101	F	4-*t*-Bu

Scheme 4.3. Synthetic route for the preparation of 4-bromomethyl-1,1'-biphenyls (**93-101**). Reagents and conditions: (i) K_2CO_3, $Pd(OAc)_2$, PEG 4000, H_2O, 50 °C, 30 mins (ii) *N*-Bromosuccinimide, AIBN, CCl_4, reflux, 20 h.

4.1.2.6. Synthesis of 2-(4-(2-/3-/4-substituted phenyl)benzylamino)-*N*-(5-chloropyridin-2-yl)benzamides (102-110)

Compound (**64**) was reacted with different 4-bromomethyl-1,1'-biphenyls (**93-101**) to obtain the targeted compounds (**102-110**) as depicted in **Scheme 4.4**. These compounds displayed one peak around 1660 cm^{-1} for C=O stretching of amide and another one in the range of 3500-3200 cm^{-1} (N-H stretch) in their IR spectra.

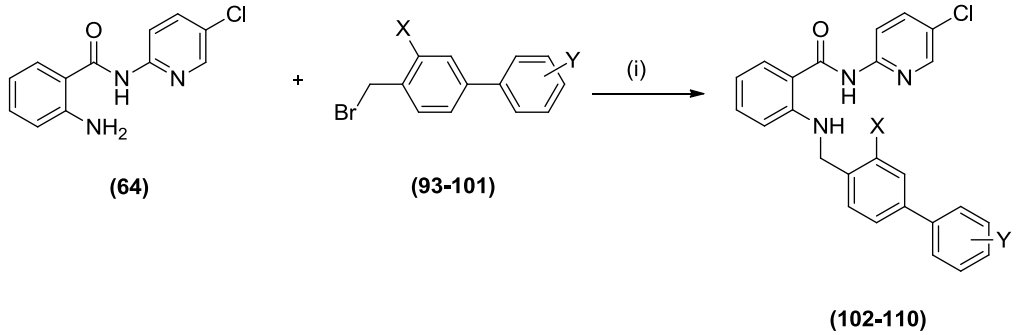

Scheme 4.4. Synthetic route for the preparation of compounds (**102-110**). Reagents and conditions: (i) K_2CO_3, DMF, 120 °C, 4-6 h.

Table 4.4. Analytical data of compounds (**102-110**)

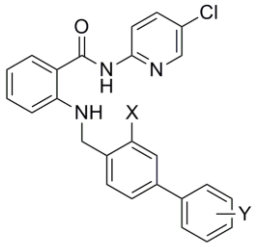

(102-110)

Comp	X	Y	M.P. (°C)	IR characteristic peaks (cm^{-1})
102	H	H	190-192	3435, 3350, 1649, 1572, 1509, 742
103	H	4-*t*-Bu	167-169	3372, 3226, 2962,1653, 1573, 1510, 814, 749
104	H	3,5-diF	162-164	3396, 3212, 3082,1651, 1573, 1513, 837, 750
105	H	2-Cl	110-112	3368, 3229, 2227, 1650, 1572, 1511, 828, 760
106	H	2-OMe	174-176	3368, 3229, 2227, 1650, 1572, 1511, 828, 760
107	H	2-CN	185-187	3368, 3229, 2227, 1650, 1572, 1511, 828, 760
108	H	4-OMe	187-189	3368, 3218, 1650, 1578, 1516, 836, 749
109	F	H	162-164	3400, 3210,1651, 1572, 1514, 829, 742
110	F	4-*t*-Bu	135-137	3398, 3226, 1657, 1576, 1511, 824, 746

The ^{1}H-NMR spectrum of compound (**102**) showed singlet at δ 8.47 due to the proton (NH_e) attached to the amidic nitrogen and triplet at δ 8.06 for one amine proton (NH_i). The aromatic protons of pyridine ring appeared as doublet at δ 8.20 for one proton (ArH_f), doublet at δ 8.17 for one proton (ArH_h) and doublet of doublet at δ 7.61 for one proton (ArH_g). It also showed multiplet at δ 7.48-7.52 for five aromatic protons (Ar$H_{m,n,o}$), multiplet at δ 7.33-7.39 for four protons (Ar$H_{k,l}$), multiplet at δ 7.23-7.28 for two aromatic protons (Ar$H_{b,d}$) and multiplet at δ 6.58-6.66 for two aromatic protons (Ar$H_{a,c}$). The aliphatic protons appeared as doublet at δ 4.42 for two methylene protons (CH_{2j}). Its mass spectrum displayed molecular ion $(M)^+$ and $(M+2)^+$ peaks at 414.7 and 416.5 m/z respectively.

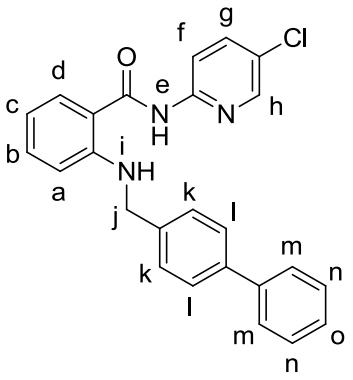

(102)

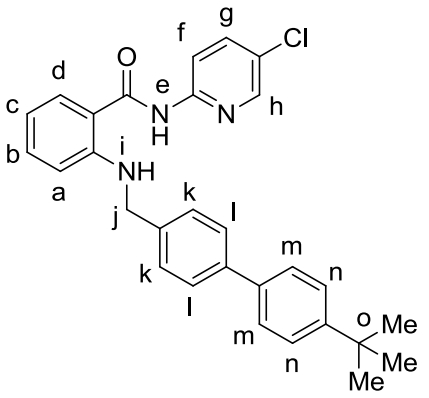

(103)

The ^{1}H-NMR spectrum of compound (**103**) showed singlet at δ 8.53 due to the proton (NH_e) attached to the amidic nitrogen and triplet at δ 8.11 for one amino proton (NH_i). The aromatic protons of pyridine ring were observed as doublet at δ 8.27 for one proton (ArH_f), doublet at δ 8.24 for one proton (ArH_h) and doublet of doublet at δ 7.68 for one proton (ArH_g). The other aromatic protons offered signals as multiplet at δ 7.51-7.57 for five aromatic protons (Ar$H_{d,m,n}$), multiplet at δ 7.41-7.46 for four aromatic protons (Ar$H_{k,l}$), multiplet at δ 7.30-7.32 for one proton (ArH_b), doublet at δ 6.73 for one aromatic proton (ArH_a) and multiplet at δ 6.64-6.68 for one aromatic proton (ArH_c). The aliphatic protons appeared as doublet at δ 4.48 for two methylene protons (CH_{2j}) and singlet at δ 1.35 for nine methyl protons (CH_{3o}). Its mass

spectrum showed molecular ion (M^+) peak at 470.7 m/z and $(M+2)^+$ peak at 472.7 m/z.

The ^{1}H-NMR spectrum of compound (**104**) showed singlet at δ 8.54 due to the proton (NH_e) attached to the amidic nitrogen and triplet at δ 8.15 for amino proton (NH_i). The aromatic protons of pyridine ring were observed as doublet at δ 8.27 for one proton (ArH_f), doublet at δ 8.25 for one proton (ArH_h) and doublet of doublet at δ 7.69 for one proton (ArH_g). It showed doublet of doublet at δ 7.57 for one aromatic proton (ArH_d), doublet at δ 7.51 for two aromatic protons (ArH_k) and doublet at δ 7.45 for two aromatic protons (ArH_l). It also displayed multiplet at δ 7.29-7.33 for one aromatic proton (ArH_b), multiplet at δ 7.06-7.11 for two aromatic protons (ArH_m), multiplet at δ 6.74-6.79 for one aromatic proton (ArH_n) and multiplet at δ 6.62-6.69 for two aromatic protons (Ar$H_{a,c}$). The aliphatic protons appeared as doublet at δ 4.49 for two methylene protons (CH_{2j}). Its mass spectrum showed molecular ion $(M)^+$ peak at 450.8 m/z.

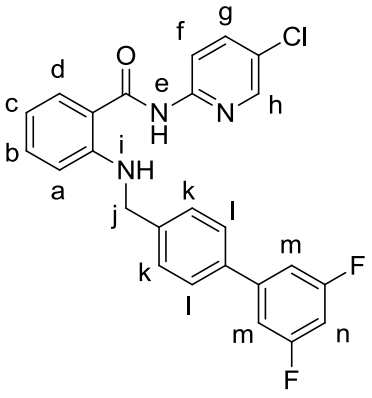

(104)

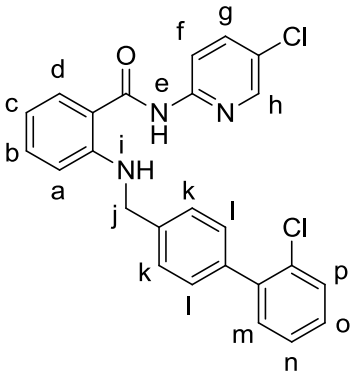

(105)

The ^{1}H-NMR spectrum of compound (**105**) showed singlet at δ 8.53 due to the proton (NH_e) attached to the amidic nitrogen and triplet at δ 8.14 for one amino proton (NH_i). The aromatic protons of pyridine ring were observed as doublet at δ 8.28 for one proton (ArH_f), doublet at δ 8.24 for one proton (ArH_h) and doublet of doublet at δ 7.68 for one proton (ArH_g). It showed doublet of doublet at δ 7.57 for one aromatic proton (ArH_d) and doublet at δ 6.75 for one aromatic proton (ArH_a). It also displayed one multiplet at

δ 7.40-7.47 for five aromatic protons (Ar$H_{b,m,n,o,p}$) and multiplet at δ 7.41-7.46 for four aromatic protons (Ar$H_{k,l}$). It also displayed multiplet at δ 6.66-6.68 for one aromatic proton (ArH_c). The aliphatic protons appeared as doublet at δ 4.50 for two methylene protons (CH_{2j}). Its mass spectrum showed molecular ion (M^+) and $(M+2)^+$ peaks at 448.8 and 450.8 m/z respectively.

The ^{1}H-NMR spectrum of compound (**106**) showed singlet at δ 10.46 due to the proton (NH_e) attached to the amidic nitrogen and triplet at δ 8.08 for one amino proton (NH_i). The aromatic protons of pyridine ring were observed as doublet at δ 8.17 for one proton (ArH_f), doublet at δ 8.31 for one proton (ArH_h) and doublet of doublet at δ 7.76 for one proton (ArH_g). It showed doublet of doublet at δ 7.82 for one aromatic proton (ArH_d), doublet at δ 7.46 for two aromatic protons (ArH_l), doublet at δ 7.39 for two aromatic protons (ArH_k) and doublet at δ 6.72 for one aromatic proton (ArH_a). It also displayed multiplet at δ 7.25-7.32 for three aromatic protons (Ar$H_{b,m,p}$), multiplet at δ 6.97-7.03 for two aromatic protons (Ar$H_{n,o}$) and multiplet at δ 6.61-6.65 for one aromatic proton (ArH_c). The aliphatic protons appeared as doublet at δ 4.45 for two methylene protons (CH_{2j}) and singlet at δ 3.78 for three methyl protons (CH_{3q}). The mass spectrum showed molecular ion $(M)^+$ peak at 444.1 m/z and $(M-127)^+$ ion peak at 317.2 m/z.

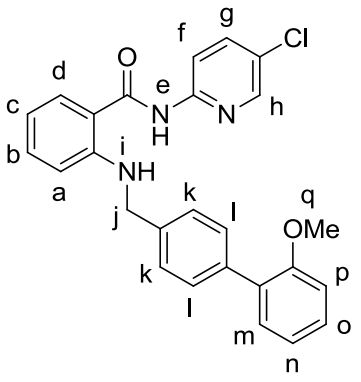

(106)

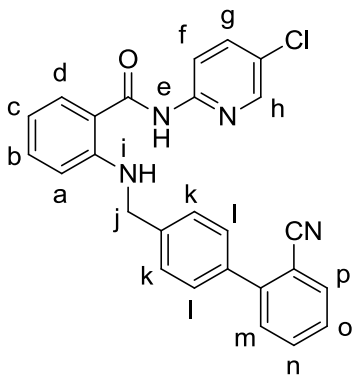

(107)

The ^{1}H-NMR spectrum of compound (**107**) showed singlet at δ 8.56 due to the proton (NH_e) attached to the amidic nitrogen and triplet at δ 8.18 for one amino proton (NH_i). The aromatic protons of pyridine ring were observed as doublet at δ 8.28 for one proton (ArH_f), doublet at δ 8.23 for one proton

(ArH_h) and doublet of doublet at δ 7.69 for one proton (ArH_g). It showed doublet of doublet at δ 7.75 for one aromatic proton (ArH_d), multiplet at δ 7.31-7.35 for one aromatic proton (ArH_b) and multiplet at δ 6.66-6.72 for two aromatic protons (Ar$H_{a,c}$). It also displayed multiplet at δ 7.62-7.65 for one aromatic proton (ArH_m), multiplet at δ 7.41-7.45 for one aromatic proton (ArH_o) and multiplet at δ 7.48-7.58 for six aromatic protons (Ar$H_{k,l,n,p}$). The aliphatic protons appeared as a doublet at δ 4.52 for two methylene protons (CH_{2j}). Its ^{13}C-NMR spectrum showed peak at δ 168.02 due to C=O carbon of the amide. The aromatic carbons appeared at δ 150.45, 149.60, 145.12, 143.15, 140.37, 139.31, 137.12, 134.64, 133.80, 132.88, 130.05, 129.43, 129.14, 128.36, 127.56, 127.46, 126.45, 118.80, 115.90, 113.15, 112.77 and 111.17 whereas the aliphatic carbon appeared at δ 46.90. Its mass spectrum showed molecular ion $(M)^+$ peak at 438.9 m/z and $(M+2)^+$ peak at 440.9 m/z.

The NMR spectrum of compound (**108**) showed singlet at δ 10.45 due to the proton (NH_e) attached to the amidic nitrogen and triplet at δ 8.08 for one amino proton (NH_i). The aromatic protons of pyridine ring were observed as doublet at δ 8.17 for one proton (ArH_f), doublet at δ 8.32 for one proton (ArH_h) and doublet of doublet at δ 7.76 for one proton (ArH_g). The other aromatic protons appeared as doublet of doublet at δ 7.82 for one aromatic proton (ArH_d), doublet at δ 6.69 for one aromatic proton (ArH_a), doublet at δ 7.41 for two aromatic protons (ArH_m), doublet at δ 6.96 for two aromatic protons (ArH_n), multiplet at δ 7.52-7.54 for four aromatic protons (Ar$H_{k,l}$), multiplet at δ 7.26-7.29 for one aromatic proton (ArH_b) and multiplet at δ 6.60-6.64 for one aromatic proton (ArH_c). The aliphatic protons appeared as doublet at δ 4.45 for two methylene protons (CH_{2j}) and singlet at δ 3.81 for three methyl protons (CH_{3o}). The mass spectrum showed molecular ion $(M)^+$ peak at 444 m/z and $(M-127)^+$ ion peak at 317 m/z.

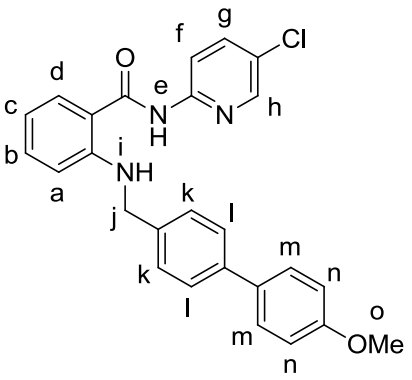

(108)

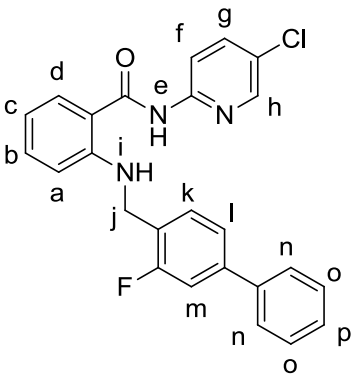

(109)

The ^{1}H-NMR spectrum of compound (**109**) showed singlet at δ 8.53 due to the proton (NH_e) attached to the amidic nitrogen and triplet at δ 8.12 for one amino proton (NH_i). The aromatic protons of pyridine ring were observed as doublet at δ 8.28 for one proton (ArH_f), doublet at δ 8.25 for one proton (ArH_h) and doublet of doublet at δ 7.69 for one proton (ArH_g). It also displayed multiplet at δ 7.54-7.58 for three aromatic protons (Ar$H_{d,m,p}$), multiplet at δ 7.40-7.45 for three aromatic protons (Ar$H_{b,k,l}$), multiplet at δ 7.29-7.37 for four aromatic protons (Ar$H_{n,o}$) and multiplet at δ 6.67-6.75 for two aromatic protons (Ar$H_{a,c}$). The aliphatic protons appeared as doublet at δ 4.54 for two methylene protons (CH_{2j}). Its mass spectrum showed molecular ion $(M)^+$ peak at 431.78 m/z.

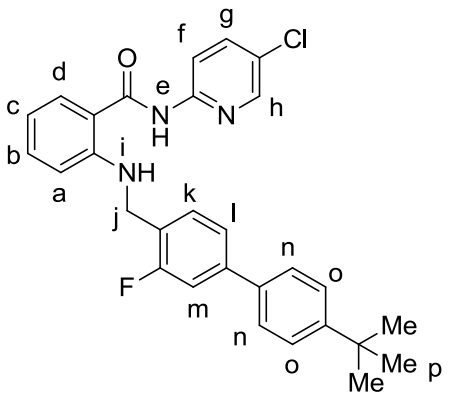

(110)

The ^{1}H-NMR spectrum of compound (**110**) showed singlet at δ 8.52 due to the proton (NH_e) attached to the amidic nitrogen and triplet at δ 8.10 for one amino proton (NH_i). The aromatic protons of pyridine ring were observed

as doublet at δ 8.28 for one proton (ArH_f), doublet at δ 8.25 for one proton (ArH_h) and doublet of doublet at δ 7.69 for one proton (ArH_g). It also displayed doublet of doublet at δ 7.57 for one aromatic proton (ArH_d), doublet of doublet at δ 6.74 for one aromatic proton (ArH_a), multiplet at δ 7.44-7.50 for four aromatic protons (Ar$H_{n,o}$), multiplet at δ 7.38-7.42 for one aromatic proton (ArH_b), multiplet at δ 7.27-7.36 for three aromatic protons (Ar$H_{k,l,m}$) and multiplet at δ 6.66-6.70 for one aromatic proton (ArH_c). The aliphatic protons appeared as doublet at δ 4.54 for two methylene protons (CH_{2j}) and singlet at δ 1.33 for nine methyl protons (CH_{3p}). Its mass spectrum showed molecular ion $(M)^+$ peak at 488.9 m/z and $(M+2)^+$ peak at 490.9 m/z.

4.1.3. Biological evaluation

All the synthesized compounds were tested *in vitro* for FXa inhibitory activity by chromogenic substrate hydrolysis assay. Compounds showing good *in vitro* FXa inhibitory activity were subjected to measurement of *ex vivo* prothrombin time and clotting time. Based on its promising *in vitro* and *ex vivo* profile, the most active compound **(107)** was selected for further *in vivo* evaluation of its antithrombotic potential.

4.1.3.1. *In vitro* FXa and thrombin inhibition assays

In vitro enzyme inhibition assays for FXa and thrombin were performed for the synthesized compounds at a fixed concentration of 100 µM by using a chromogenic substrate (Spectrozyme TH for thrombin and S-2222 for FXa) as per the previously reported procedure.[82] The residual enzyme activity was determined from the change in the absorbance at 405 nm with hydrolysis of the substrate by the enzyme. Compounds offering less than 60 % of the residual FXa activity were chosen for determination of their IC_{50} values. Compounds (**69-71, 73-75**, **82** and **102**, **104-107**, **109** and **110**) showed more than 40 % inhibition of FXa in the preliminary screening (**Figure 4.2**). All the synthesized compounds showed more than 50 % thrombin residual activity at this concentration (**Figure 4.3**). All the selected compounds demonstrated good selectivity for FXa over thrombin (IC_{50} values of >100 µM). **Table 4.5**

represents IC_{50} values of compounds (**69-71, 73-75, 82** and **102, 104-107, 109** and **110**) against both the enzymes.

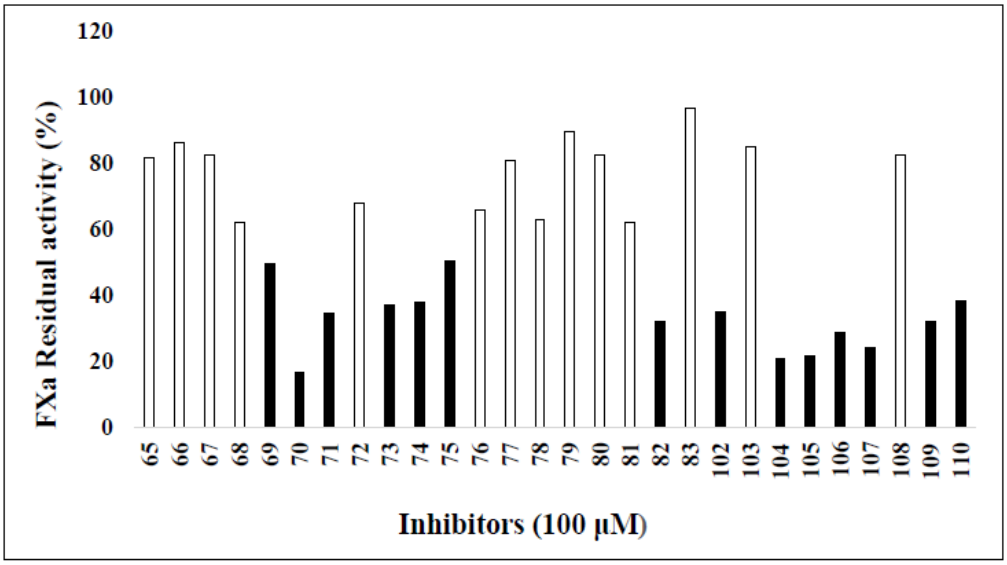

Figure 4.2. FXa residual activity (%) after treatment with the synthesized compounds. Experiments were performed at 100 µM in duplicate. Mean of % FXa residual activity values are represented (SE < 20 %).

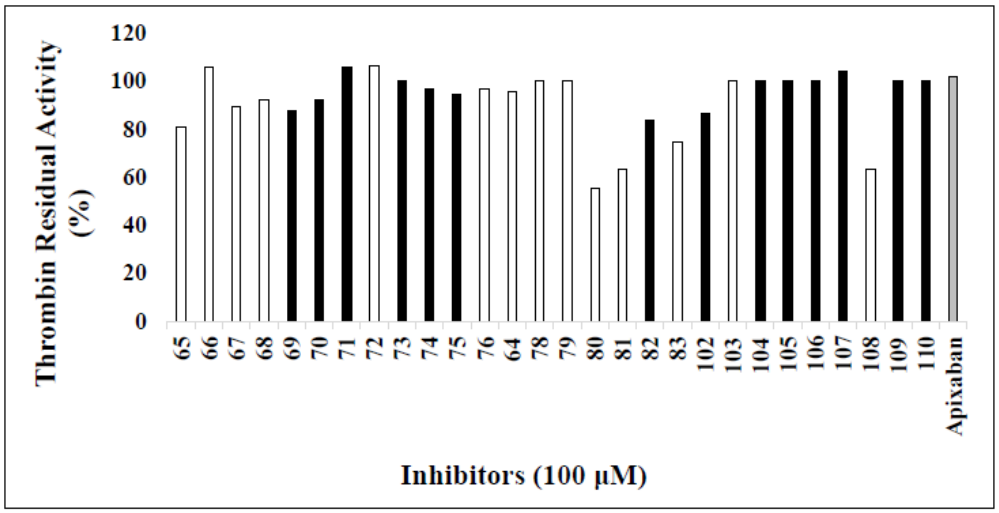

Figure 4.3. Thrombin residual activity (%) after treatment with the synthesized compounds. Experiments were performed at 100 µM in duplicate. Mean of % FXa residual activity values are represented (SE < 20 %).

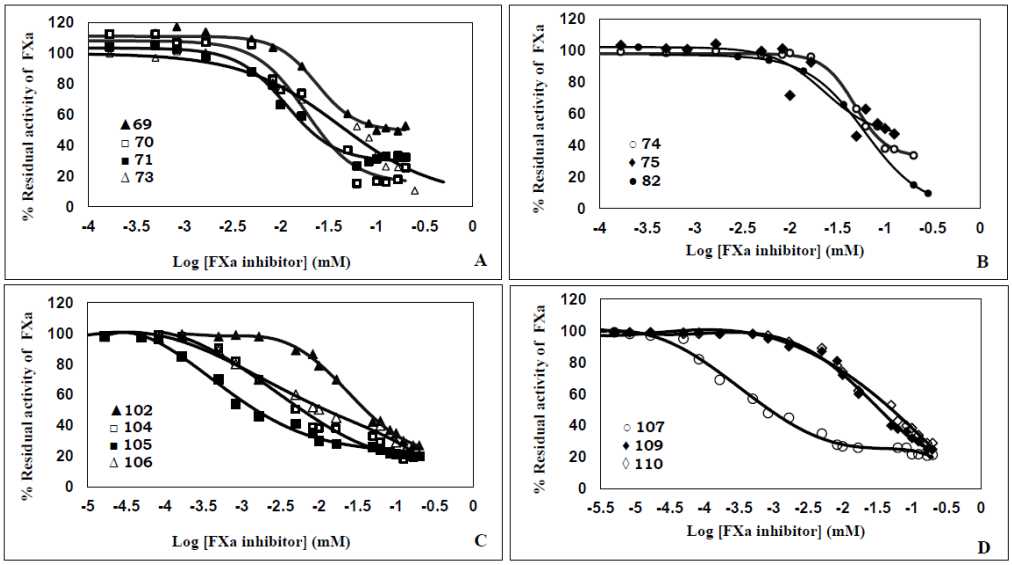

Figure 4.4. Direct inhibition of FXa by compounds (**69-71** and **73**) (A), **74**, **75** and **82** (B) (**102**, **104**, **105**, **106)** (C) and (**107**, **109**, **110**) (D). Solid lines represent sigmoidal fits to the data to obtain IC_{50} as described in experimental section. Experiments were performed in triplicate (SE <20%).

4.1.3.2. *Ex vivo* PT prolongation and clotting time

The coagulation cascade is composed of three pathways: extrinsic, intrinsic and common. Clotting is the general phenomena involving orderly activation of extrinsic and intrinsic factors, ultimately leading to clot formation via common pathway. Clotting time is therefore a general quantitative test to check the integrity of coagulation cascade, while the prothrombin time emphasizes the integrity of extrinsic pathway.

Compounds showing significant inhibition of the enzyme FXa in the preliminary screening were evaluated further using *ex vivo* measurements of prothrombin time and clotting time (for more details, refer supporting information). The PT prolonging activity and clotting time of compounds (**69-71, 73-75**, **82** and **102**, **104-107**, **109** and **110**) along with control group and the standard drug apixaban were determined at 2 h after oral administration in rat (30 mg/kg dose) and the data are shown in **Table 4.5**. Most of the tested compounds indicated slightly higher prolongation in prothrombin time than that of control (7.7 sec). Compounds (**104**, **105**, **107** and **74**) showed significant change in the prothrombin time. The selected test compounds also showed much higher clotting time than the control (12.5 sec). Compound

(**107**) (45 sec) exhibited a significant change in clotting time offering the highest value among the selected compounds. However, this was lesser than that of the standard drug apixaban (60 sec).

Table 4.5. IC_{50} values, PT time and Clotting time for the test compounds

Comp	IC_{50} value (μM)[a]		PT time (sec)[b]	Clotting time (sec)[b]
	FXa	Thrombin		
69	23.7 ± 3.4	>100	9.2	15
70	18.4 ± 2.6	>100	8.7	30
71	11.5 ± 1.3	>100	8.9	30
73	41.0 ± 3.2	>100	8.6	30
74	48.3 ± 2.9	>100	9.9	30
75	23.2 ± 8.4	>100	9.4	37.5
82	57.5 ± 8.6	>100	9.4	30
102	35.3 ± 2.3	>100	8.8	35
104	5.4 ± 1.0	>100	9.8	40
105	1.3 ± 0.8	>100	9.9	40
106	12.5 ± 2.2	>100	9.1	35
107	**0.7 ± 0.2**	**>100**	**10.1**	**45**
109	30.0 ± 6.4	>100	8.7	30
110	52.5 ± 5.7	>100	9.5	35
Apixaban	0.35 ± 0.1	12.8 ± 2.2	12.8	60
Control	-	-	7.7	12.5

[a] IC_{50} values shown are the mean of triplicate measurements.

[b] The *ex vivo* PT time and Clotting time were determined 2 h after oral administration of the test compounds to rats at a dose of 30 mg/kg (n = 3).

4.1.3.3. *In vivo* $FeCl_3$ induced arterial thrombosis

Based on *in vitro* FXa inhibitory activity and *ex vivo* PT prolongation time of compound (**107**), it was selected for *in vivo* evaluation of antithrombotic potential by $FeCl_3$ induced arterial thrombosis model in rats. The reduction in thrombus weight was considered as a preventive measure for *in vivo* efficacy of a compound. Compound (**107**) reduced thrombus weight by

46 % at 30 mg/kg in rats. In the case of standard drug (apixaban) at dose of 30 mg/kg, the reduction in thrombus weight was found to be 69 %.

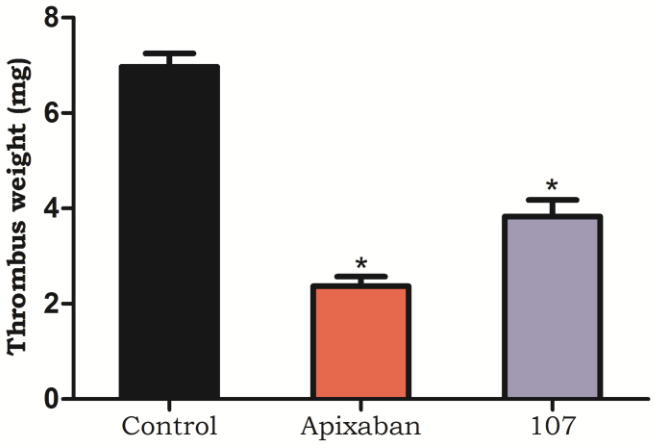

Figure 4.5. Effect of compound (**107**) and apixaban (30 mg/kg) on thrombus weight ($FeCl_3$ induced arterial thrombosis model). Statistical analysis was performed by One way ANOVA using Graph-pad prism 5.0 $^{*}p < 0.01$ vs. vehicle control. (n = 3).

4.1.4. Molecular modeling studies

4.1.4.1. Docking studies

To have a view of the molecular interactions of the synthesized compounds with the enzyme, docking studies were performed with FXa. All the synthesized compounds were docked in the active site of FXa. Docking of betrixaban (**10**) was also done as a standard. The docking scores are given in the **Table 4.6**. Compound (**107**) offered the highest docking score which indicated its high binding interactions with the enzyme.

Table 4.6. Docking scores of active compounds

Comp	IC_{50} value (µM) FXa	Docking score (Kcal/mole)
69	23.7 ± 3.4	-7.51
70	18.4 ± 2.6	-7.78
71	11.5 ± 1.3	-7.33
73	41.0 ± 3.2	-7.87
74	48.3 ± 2.9	-7.29

Comp	IC_{50} value (µM) FXa	Docking score (Kcal/mole)
75	23.2 ± 8.4	-6.62
82	57.5 ± 8.6	-7.70
102	35.3 ± 2.3	-8.81
104	5.4 ± 1.0	-9.10
105	1.3 ± 0.8	-9.38
106	12.5 ± 2.2	-8.91
107	**0.7 ± 0.2**	**-10.43**
109	30.0 ± 6.4	-8.71
110	52.5 ± 5.7	-7.72
Betrixaban	ND[a]	-9.44

[a]Not determined

The intermolecular interactions of the highest binding compound (**107**) and betrixaban (**10**) as a standard drug are shown in **Figure 4.6**. In betrixaban (**10**), the pyridine ring occupied the S1 pocket, indicating a good lipophilic interaction. In addition to this, chloro group of pyridine and π-system of Tyr228 of S1 pocket exhibited a non-covalent lipophilic interaction. Interestingly, compound (**107**) also demonstrated similar interactions and the chloro group of pyridine in compound (**107**) was observed to be stabilized at 3.82 Å from the centroid of Tyr228 aromatic ring which indicated high stability of the ligand-enzyme complex. In case of betrixaban, -C=O of Gly219 (2.1 Å) and disulfide linkage of Cys191 and Cys220 (2.4 Å) displayed good hydrogen bonding interactions with the pyridine amide–NH to form a stable complex. Whereas in case of compound (**107**), the –C=O and -NH of the amide interacted with -NH of Gln192 (2.12 Å) and –C=O of Gly219 (1.92 Å), respectively by hydrogen bonding to form a stable complex. The aromatic ring of 2-aminobenzamide exhibited the strong π-cation interactions with the Arg222. Generally the π-cation interaction is considered stronger than hydrogen bond or any other physical interactions, and this has been observed here to impart ligand receptor stability. Further, the *ortho* substituted biphenyl group in compound (**107**) exhibited excellent π-π interaction with Tyr99,

Phe174 and Trp215 triad in the S4 pocket. From the obtained results we clearly get an idea that occupying S1 and S4 sites by specific lipophilic functionalities is of utmost importance for enhanced binding affinity of the ligands within the enzyme active site.

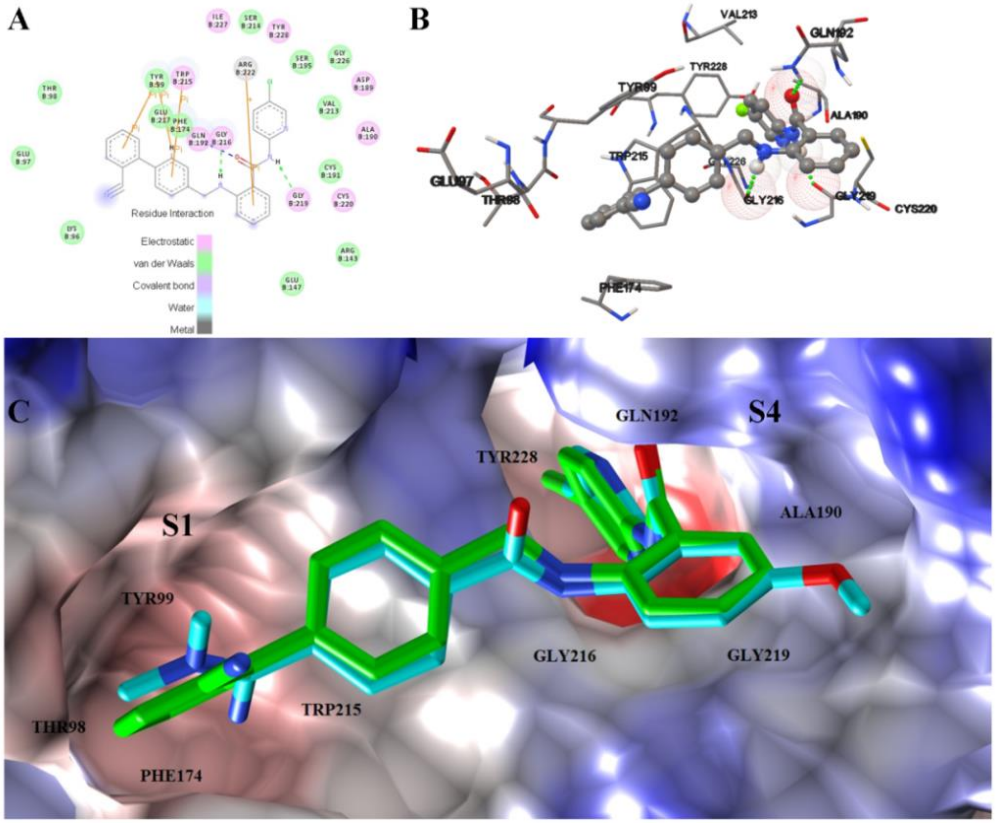

Figure 4.6. (A) 2D representation of interactions between compound (**107**) and the active site of FXa enzyme. (B) Docking pose of compound (**107**) within the active site of FXa. (C) Overlay of the 3D structures of compound (**107**) and betrixaban (**10**) within the active site of FXa (PDB code: 4A7I[8]). Color code: betrixaban = Cyan, compound (**107**) = Green.

To check selectivity, we also performed docking of the most active compound (**107**) with thrombin (FIIa), FIXa and FXIa. For this purpose the protein structures were obtained from RCSB database (PDB code: 1SL3, 3CL5, 5QCK respectively). The docking scores suggest the selectivity of compound (**107**) for FXa over Thrombin, FIXa and FXIa. Docking scores and IC_{50} values of compound (**107**) and Apixaban over other serine proteases were represented in **Table 4.6.**

Table 4.7. Docking score and IC_{50} values of compound (**107**) and apixaban (**8**) over other serine proteases

Enzyme	Compd (107)		Apixaban (8)	
	Glide XP docking score	IC_{50} value (µM)[a]	Glide XP docking score	IC_{50} value (µM)[a]
FXa	-10.43	0.7 ± 0.2	-9.075	0.35 ± 0.1
Thrombin (FIIa)	-7.88	> 100	-5.284	12.8 ± 2.2
FIXa	-6.98	ND[b]	-4.626	ND[b]
FXIa	-8.07	ND[b]	-5.584	ND[b]

[a]Inhibitory activity against human FXa and FIIa. IC_{50} values shown are the mean of triplicate measurements.

[b]ND = Not Determined

4.1.4.2. Molecular dynamics simulations

In the molecular docking studies, compound (**107**) exhibited highly favorable interactions within the active site of FXa. Thus, to confirm and validate the stability of the proposed complex of the active compound (**107**) and FXa, molecular dynamics was performed. The dynamic stability of the ligand (**107**) with FXa was studied in the complex over a period of 10 ns duration. Post dynamic analysis was carried out to understand stability of the ligand-receptor complex by average root mean square deviation (RMSD).[98,99] To examine the binding stability of the complex over the predefined period of time, RMSD-P, RMSF-P and RMSD-L (P = Protein; L = Ligand) were scrutinized to support the docking results. Initial pose of the ligand-receptor complex was considered as the reference frame to calculate these values. RMSD-P was calculated to understand the large scale movements in the protein in presence of the ligand in the active site. This gives insight into the structural conformation of the protein throughout the simulation time. The RMSD-P for the FXa-ligand (**107**) complex was observed in the range of 0.7 to 1.6 Å. This observation suggested that the presence of ligand (**107**) in the active site of FXa receptor has not influenced the stability of the protein backbone throughout the simulation run. To identify the stability of the ligand with respect to the protein and its binding site, the RMSD-L of compound (**107**) was computed. The Ligfit on Prot RMSD-L for the ligand was observed

in the range of 0.4 to 3.2 Å. Here, the major fluctuation was observed within the first 1 ns duration and afterwards the ligand in the complex was quite stable with RMSD in the range of 0.4 to 1.8 Å with an average value of 1.1 Å. The average RMSD value observed here is significantly less than the RMSD-P, indicating that the ligand is stable inside the binding pocket and it has not diffused away from the active site during the entire simulation period. Further, the Ligfit on Lig RMSD was measured to understand the internal fluctuation of the ligand atoms. It was observed in the acceptable range of 0.3 to 1.3 Å and no deviation was observed during the study period (**Figure 4.7a**).

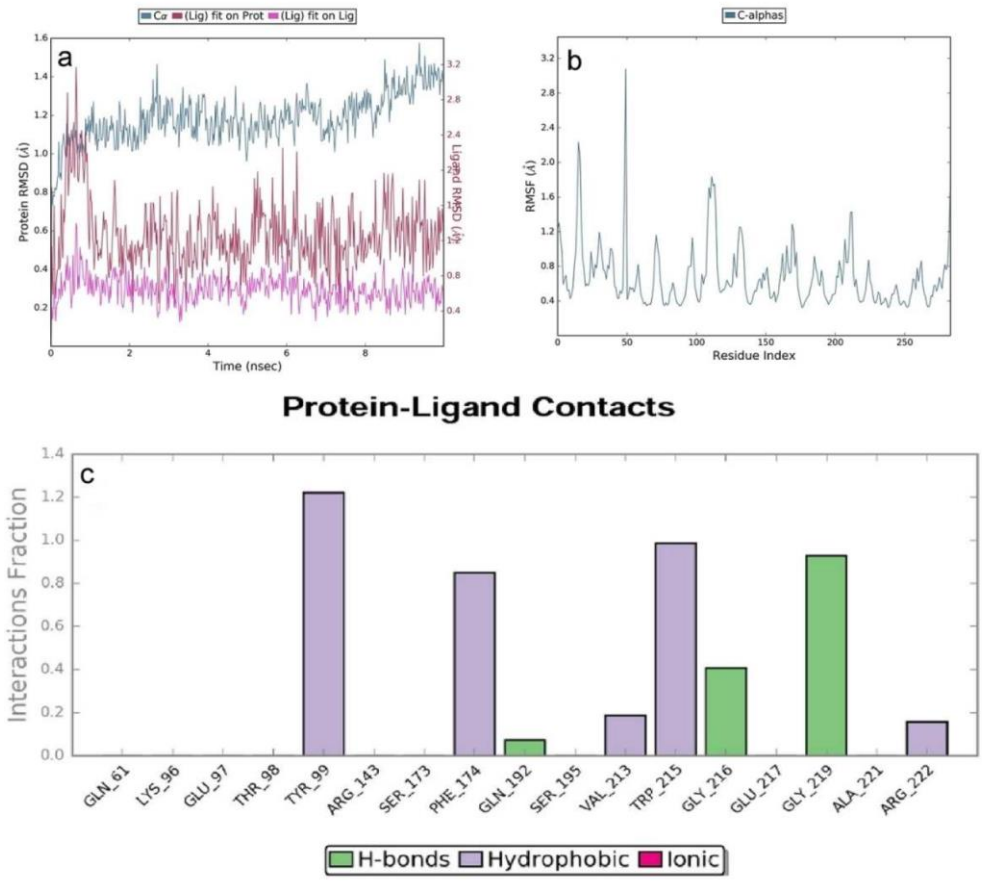

Figure 4.7. (**a**) RMSD-P, RMSD-L plot for FXa with **107**; (**b**) RMSF-P for FXa with **107**; (**c**) Ligand and receptor residue contact diagram for FXa with **107**.

The structural integrity of the protein and the residual mobility of the ligand were quantified in terms of RMSF-P (**Figure 4.7b**). For almost all residues including loop residues and the terminal residues of the protein in complexation with **107**, in the active site, the RMSF-P was below 3.2 Å. In the

protein ligand stability the interaction study was also evaluated over a period of time. In the docking study, the NH and C=O of the carboxamide group and NH of 2-aminobenzamide scaffold of compound (**107**) form H-bond with Gly219, Gln192 and Gly216 respectively. From the simulation study it was confirmed that the amide NH and 2-amino -NH formed two H-bonds with Gly219 and Gly216. These were maintained stable over 92 % and 29 % of simulation time respectively with the respective amino acids. All these H-bonds were having distances within 2.5 Å, and donor angle of ≥ 120° and acceptor angle of ≥ 90°. Further, the H-bond with Gln192 was not observed to be stable within these limits during the simulation time. Additionally, the amine –NH and amide –C=O of 2-aminobenzamide showed 23 % stable intra-molecular H-bond over the total simulation period. Further, the MD study showed that the π-cation interaction between Arg222 and 2-aminobenzamide was stable only for approximately 20 % of the total duration of simulation. The hydrophobic interactions including π-π interaction with Tyr99, Phe174 and Trp215 played vital role in the stability of the ligand-receptor complex wherein all the residues were involved in hydrophobic interaction for more than 80% of the total simulation time (**Figure 4.7c**).

4.2. 1,3,4-Thiadiazole-based FXa inhibitors

Design, synthesis, biological evaluation and molecular modeling studies of 1,3,4-thiadiazole derivatives have been discussed under the following headings:

4.2.1. Designing of 1,3,4-thiadiazole derivatives as FXa inhibitors,

4.2.2. Synthesis of 1,3,4-thiadiazole derivatives,

4.2.3. Biological evaluation and

4.2.4. Molecular modeling studies

4.2.1. Designing of 1,3,4-thiadiazole derivatives as FXa inhibitors

Pharmacophore modeling helps to identify a set of common features that interacts with a set of complementary sites in the biological target. Structurally diverse scaffold exhibits the desired biological activity by acting on same receptor active site. With structurally different scaffolds, the

alignment becomes the bottleneck for pharmacophore model development. At the beginning of this study, 224 PDB structures of FXa from Homosapiens were identified in Protein data bank. All these structures were analyzed for their resolution, protein and co-crystallized ligand consistency and co-crystallized ligand reported biological activity. First of all, on the basis of resolution, all the PDB structures were screened and only the structures with resolution 3 Å or better were selected. The reported IC_{50} or K_i values of co-crystallized ligands were considered as the second filter and the PDB structures with co-crystallized ligand activity of 10 nM or better were selected for further use in model development. After second filter, 47 PDB structures were obtained. All these PDB structures were optimized and processed using protein preparation wizard within Schrodinger Suit using OPLS_2005 force field. All these protein structures with co-crystallized ligand structures were aligned using software and after getting all the ligands aligned in same X, Y, Z coordinates in the active site of the receptors, all the protein structures were knocked out to obtain all the active site aligned ligands. This type of alignment gave us the structural feature based alignment of structurally diverse scaffolds. Structural feature based pharmacophore was developed on these aligned ligands by using PHASE module of Schrodinger. Here we obtained three point pharmacophore models from which we selected the top ranked two models based on the receptor knowledge. The selected pharmacophore models were HRR and HHR (H = hydrophobic; R = aromatic ring) (**Figure 4.8 and 4.9**). When the obtained pharmacophoric features were overlaid on the receptor active site, one of the aromatic feature and hydrophobic feature was observed in S1 binding pocket. In S1 binding site, the observed hydrophobic feature was near to the Tyr228. Whereas the remaining aromatic/hydrophobic features of the two selected models was observed in S4 pocket (**Figure 4.10 and 4.11**).

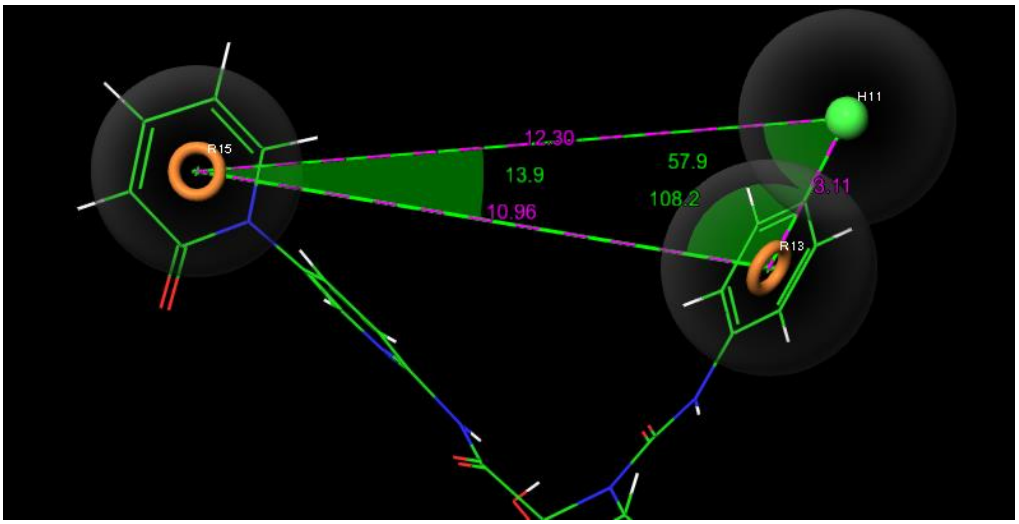

Figure 4.8. Pharmacophore model 1 (HRR) with distances and angles in the features.

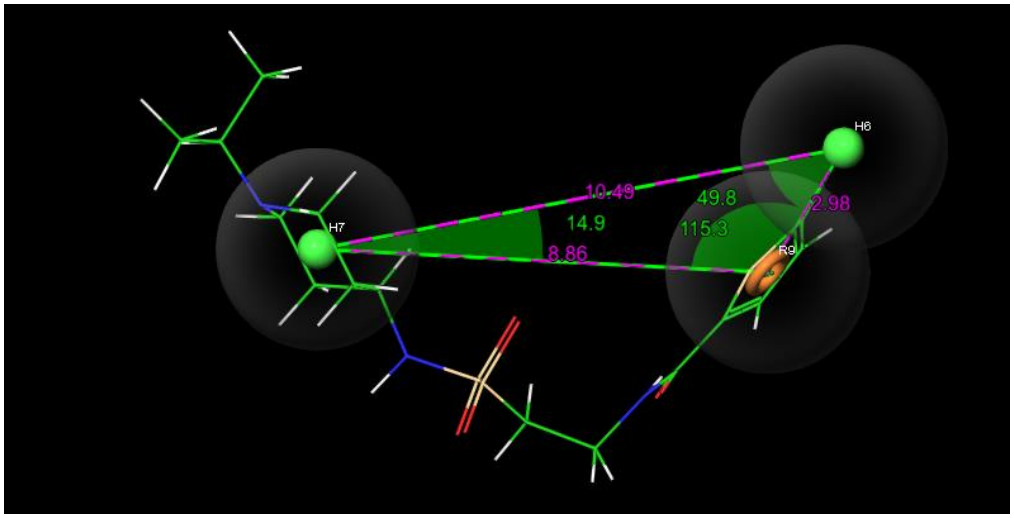

Figure 4.9. Pharmacophore model 2 (HHR) with distances and angles in the features.

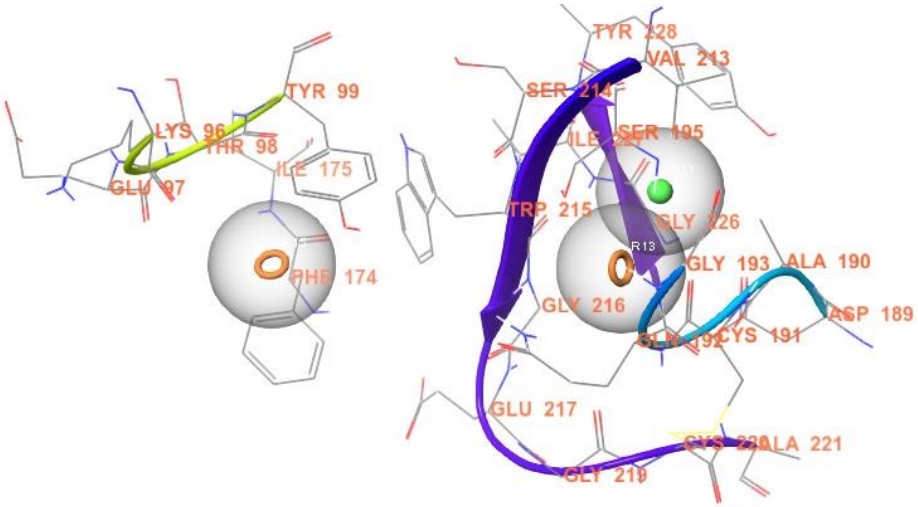

Figure 4.10. Alignment of the developed pharmacophore model 1in the active site of FXa enzyme.

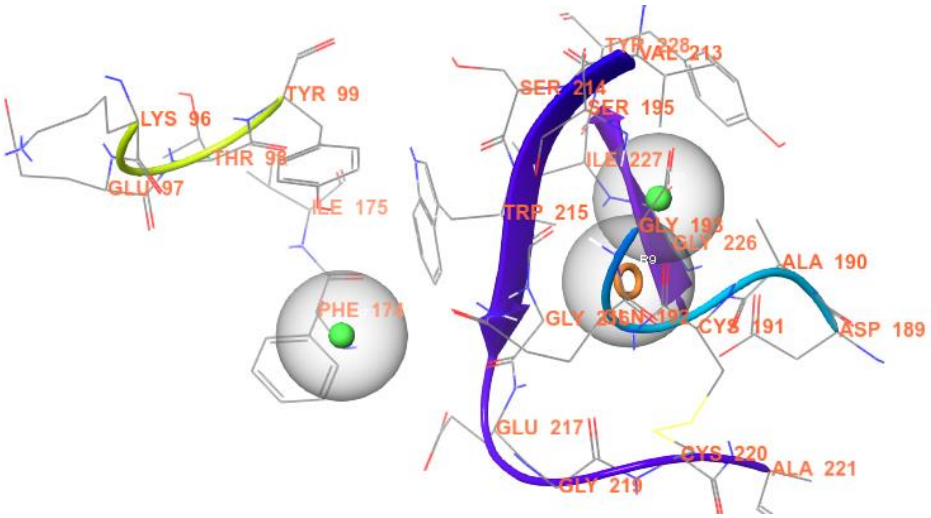

Figure 4.11. Alignment of developed pharmacophore model 2 in the active site of FXa enzyme.

To identify the hits or leads, "Clean Drug-Like" molecules data base (13,195,609 molecules) was retrieved from the Zinc-12 library, structures were prepared and primarily screened by using Lipinski rule of five. The obtained molecules were used for screening by using the two selected pharmacophore models. The molecules matching with either of the pharmacophore models were identified in this filter and top 10,000 molecules were selected for next step of screening. These molecules were taken up for receptor based virtual screening. To carry out receptor based virtual screening four receptor structures (PDB code: 4A7I, 3FFG, 2Y5F, 2P16) were selected and HTVS was carried out using Glide module of Schrodinger. The common top 10 % molecules from HTVS were selected for SP docking with all four receptors and top 10 % of the compounds were taken forward for XP docking. Finally top 10 % molecules from XP docking were identified as possible hits.

After the systematic multi-stage screening, a few hits were obtained from the Zinc library. Based on persistent high performance, novelty and synthetic feasibility, the obtained hit (A) was selected and modified to generate a lead molecule (**158**). The *p*-chlorophenyl group was introduced at S1 binding site of the enzyme as neutral haloaromatic group, as the chlorinated aromatics, have proven their worth as successful P1 motifs. The molecular interactions of the designed lead molecule (**158**) were assessed theoretically by means of docking the compound within the active sites of

FXa. The thienopyrimidinone part of the scaffold was observed in the S4 binding pocket of the receptor active site. To confirm the reliability of the strategy, compound (**158**) was firstly synthesized (**Scheme 4.6**) and evaluated for *in vitro* inhibition of FXa (IC_{50} = 14.96 µM) and anticoagulant activity (nPT = 1.56, naPTT = 1.26). Considering the activity observed for the lead compound (**158**), it was contemplated to introduce substituted benzyls, biaryls or amidoalkyls as S4 binding ligands in the novel 1,3,4-thiadiazole scaffold and maintain the chloroaromatic group as such, as the S1 binding ligand as represented in **Figure 4.12**.

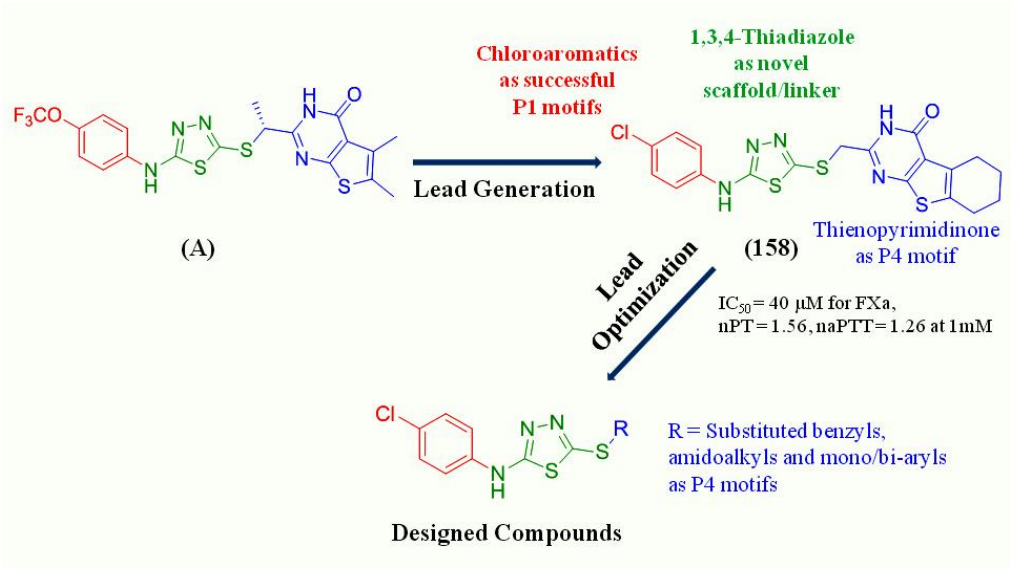

Figure 4.12. Designing of 1,3,4-thiadiazole derivatives as FXa inhibitors.

4.2.2. Synthesis of 1,3,4-thiadiazole derivatives

4.2.2.1. Synthesis of thiosemicarbazide derivatives (126-140) and 5-substituted amino-1,3,4-thiadiazole-2-thiols (141-155)

Synthesis of 5-substituted amino-1,3,4-thiadiazole-2-thiols (**141-155**) was carried out as depicted in **Scheme 4.5**. Commercially available substituted anilines were reacted with carbon disulphide in presence of sodium hydroxide followed by treatment with hydrazine hydrate to obtain the corresponding thiosemicarbazides (**126-134**). For the synthesis of benzylthiosemicarbazides (**135-140**), substituted benzylamines were initially reacted with carbon disulphide in presence of triethylamine and methyl iodide and then refluxed with hydrazine hydrate. All these thiosemicarbazides were characterized

according to their physical data and spectral data as given in **Table 4.8**. Their IR spectra showed C=S stretching at 1200-1300 cm^{-1} and $NHNH_2$ stretching at 3200-3350 cm^{-1}. Some of these compounds were characterized by mass spectrometry.

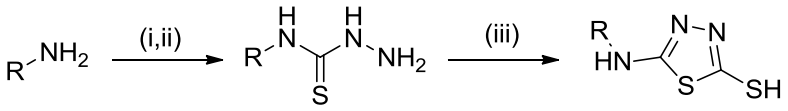

(111-125) **(126-140)** **(141-155)**

Scheme-4.5. Synthetic route for the preparation of thiosemicarbazides (**126-140**) and thiols (**141-155**). Reagents and conditions: For (**126-134**) (i) Carbon disulphide, sodium hydroxide, DMF, 20-30 °C, 2-3 h; (ii) Hydrazine hydrate, 70 °C, 1.5 h; For (**135-140**) (i) Carbon disulphide, triethylamine, methanol, 20-30 °C, 2-3 h and iodomethane in methanol at -10 °C (ii) Hydrazine hydrate, methanol, reflux; (iii) Carbon disulphide, potassium hydroxide, methanol, reflux, 5-6 h.

Table 4.8. Analytical data of thiosemicarbazide derivatives (**126-140**)

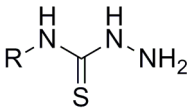

(126-140)

Comp	R	M.P.	IR characteristic peaks (cm^{-1})	Mass (m/z)
126	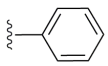	136-138 °C (lit.[100] 138-140 °C)	3304, 3166, 1638, 1528, 1287, 1070, 898	-
127	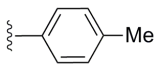	137-139 °C (lit.[100] 140-142 °C)	3252, 3193, 3032, 1619, 1544, 1276, 1063, 806	-
128	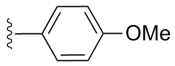	157-159 °C (lit.[100] 154-156 °C)	3317, 3167, 1636, 1528, 1244, 1033, 833	-
129	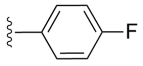	173-175 °C (lit.[100] 176-178 °C)	3313, 3163, 2971, 1638, 1529, 1289, 1071, 840	-
130	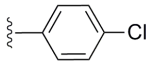	166-168 °C (lit.[101] 162-164 °C)	3360, 3249, 3083, 1550, 1263, 831	-
131	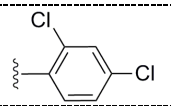	167-169 °C (lit.[100] 169-171 °C)	3244, 3129, 1608, 1538, 1472, 1204, 1015, 820	-
132	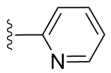	188-190 °C	3241, 3158, 1607, 1510, 1207, 1008, 761	169.0 $(M)^+$

Comp	R	M.P.	IR characteristic peaks (cm-1)	Mass (m/z)
133	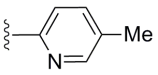	153-155 °C	3252, 3006, 1617, 1525, 1237, 1017, 819	183.0 $(M)^+$
134	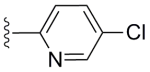	212-214 °C	3243, 3128, 1609, 1538, 1203, 1014, 820	203.0 $(M)^+$ 205.0 $(M+2)^+$
135	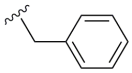	126-128 °C	3328, 3292, 3026, 1617, 1537, 1225, 1084, 791	182.0 $(M)^+$
136	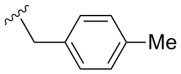	154-156 °C	3294, 2918, 1615, 1541, 1270, 1075, 823	195.75 $(M)^+$
137	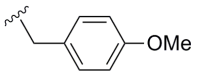	112-114 °C	3332, 3230, 2914, 1615, 1538, 1248, 1029, 843	212.0 $(M)^+$
138	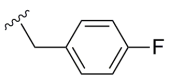	138-140 °C	3328, 3292, 2920, 1617, 1541, 1223, 1074, 847	200.0 $(M)^+$
139	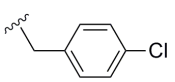	178-180 °C	3317, 3200, 2925, 1615, 1549, 1238, 1083, 808	216.0 $(M)^+$ 218.0 $(M+2)^+$
140	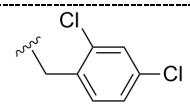	140-142 °C	3311, 3194, 2987, 1621, 1551, 1236, 1083, 869	292.0 $(M)^+$ 294.0 $(M+2)^+$

The thiosemicarbazides (**126-140**) were further cyclized using carbon disulphide and potassium hydroxide to get 5-substituted amino-1,3,4-thiadiazole-2-thiols (**141-155**). The IR spectrum of these compound revealed the disappearance of C=S stretching. All of these intermediates were also confirmed by mass spectrometry (**Table 4.9**).

Table 4.9. Analytical data of intermediate thiols (**141-155**)

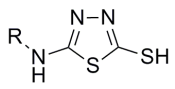

(141-155)

Comp	R	M.P.	IR characteristic peaks (cm^{-1})	Mass (m/z)
141	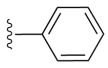	209-211 °C (lit.[102] 214-216 °C)	3215, 3128, 3027, 1600, 1569, 1056, 871	210.0 $(M)^+$
142	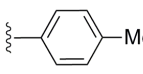	218-220 °C (lit.[102] 220-222 °C)	3230, 3114, 2910, 1606, 1564, 1326, 1056, 812	224.0 $(M)^+$
143	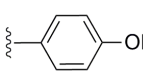	160-162 °C	3201, 3077, 2948, 1605, 1567, 1496, 1056, 852	240.0 $(M)^+$

Comp	R	M.P.	IR characteristic peaks (cm^{-1})	Mass (m/z)
144	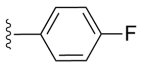	204-206 °C	3239, 3110, 2928, 1615, 1570, 1057, 824	228.0 $(M)^+$
145	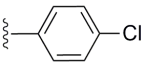	201-203 °C (lit.[102] 200-202 °C)	3230, 3115, 2926, 1602, 1565, 1488, 1057, 820	243.4 $(M)^+$ 245.4 $(M+2)^+$
146	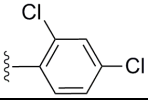	209-211 °C	3230, 3115, 2927, 1603, 1564, 1326, 1057, 843	278.0 $(M)^+$ 280.0 $(M+2)^+$
147	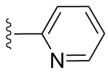	237-239 °C	3251, 3114, 2929, 1619, 1558, 1479, 865	211.0 $(M)^+$
148	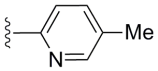	243-245 °C	3228, 3134, 2973, 1617, 1492, 818	225.0 $(M)^+$
149	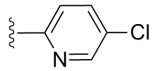	>250 °C	3223, 3115, 2964, 1611, 1555, 1475, 819	245.0 $(M)^+$ 247.0$(M+2)^+$
150	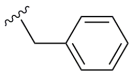	132-134 °C (lit.[103] 136-138 °C)	3255, 3033, 2871, 1552, 1458, 1299, 1045, 746	224.0 $(M)^+$
151	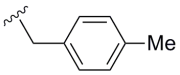	155-157 °C	3302, 3049, 1556, 1461, 1046, 807	238.0 $(M)^+$
152	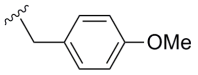	119-121 °C	3209, 3077, 2886, 1566, 1467, 1311, 1251, 824	253.0 $(M)^+$
153	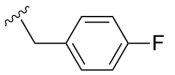	165-167 °C	3296, 3048, 2875, 1557, 1463, 1302, 1228, 827	242.0 $(M)^+$
154	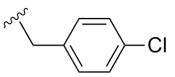	152-154 °C	3276, 3050, 2874, 1562, 1484, 1095, 810	258.0 $(M)^+$ 260.0 $(M+2)^+$
155	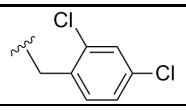	175-177 °C	3276, 3050, 2874, 1562, 1484, 1095, 810	292.0 $(M)^+$ 294.0 $(M+2)^+$

4.2.2.2. Synthesis of lead molecule (158)

The desired lead molecule (**158**) was prepared by following the synthetic route as depicted in **Scheme 4.6**. The starting material required for the synthesis of compound (**158**) was prepared using classical Gewald reaction as per previously reported procedure.[104] Cyclohexanone was treated with ethyl cyanoacetate in the presence of diethylamine to get compound (**156**). Its IR spectrum showed peaks (cm^{-1}) at 3405, 3298 (N-H stretch), 2937 (C-H stretch) and 1647 (C=O stretch). Compound (**156**) reacted with chloroacetonitrile in the presence of catalytic HCl to get condensed product (**157**).[105] The IR

spectrum of compound (**157**) displayed peaks (cm^{-1}) at 3074 (C-H stretch) and 1681 (C=O stretch). Its mass spectrum also showed molecular $(M)^+$ peak at 254.79 m/z and $(M+2)^+$ ion peak 256.70 m/z. The key intermediate (**145**) was reacted with thienopyrimidinone moiety (**157**) to get lead molecule (**158**). The IR spectrum of compound (**158**) showed peaks (cm^{-1}) at 3185 (N-H stretch) and 1664 (C=O stretch) for amide functional group.

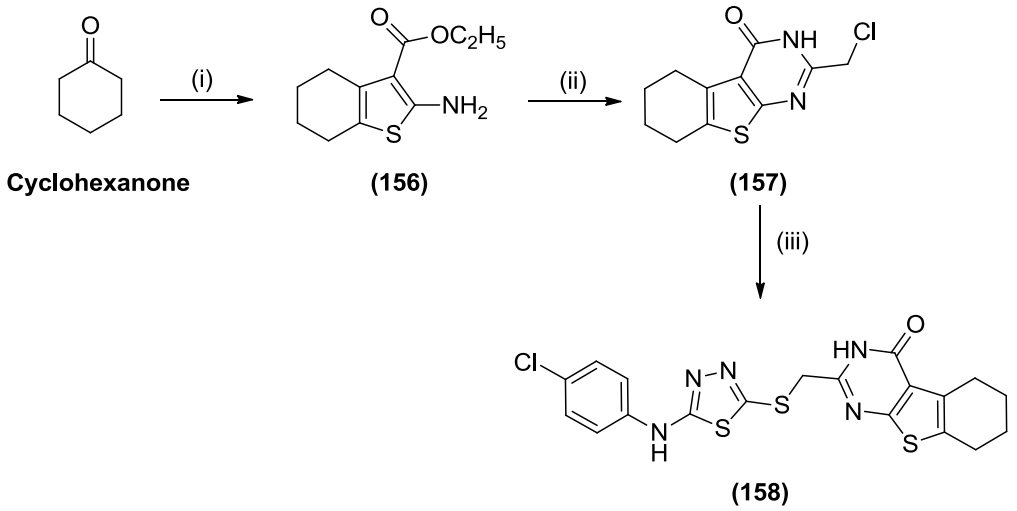

Scheme 4.6. Synthetic route for the preparation of lead molecule (**158**). Reagents and conditions: (i) Ethyl cyanoacetate, powdered sulfur, diethylamine, methanol (ii) Chloroacetonitrile, HCl in dioxane (iii) Compound (**145**), potassium carbonate, DMF, rt, 2-3 h.

Its ^{1}H-NMR spectrum of compound (**158**) showed two singlets at δ 12.42 and δ 10.52 for amide proton (NH_e) and amine proton (NH_c) respectively. It showed signals as doublet at δ 7.59 for two aromatic protons (ArH_b), doublet at δ 7.33 for two aromatic protons (ArH_a) confirming total four aromatic protons. Aliphatic protons appeared as singlet at δ 4.27 for two methylene protons (C$H_{2/d}$) attached to carbon near thio group, triplet at δ 2.82 for two methylene protons (C$H_{2/f}$) triplet at δ 2.72 for two methylene protons (C$H_{2/i}$) and multiplet at δ 1.76-1.81 for two methylene protons (C$H_{2/g,h}$). Its mass spectrum showed molecular ion $(M)^+$peak at 462.60 m/z and $(M+2)^+$ ion peak at 464.60 m/z.

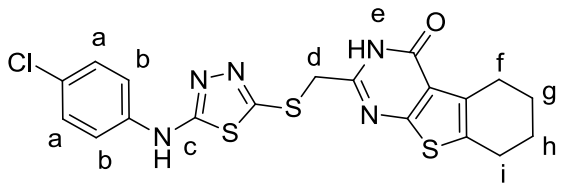

(158)

Based on this encouraging activity of the lead compound (**158**), chemical modifications were carried out in the novel 1,3,4-thiadiazole scaffold to come up with some potential leads and to establish a SAR for the series. It was decided initially to keep the chloroaromatic group as such, as the S1 binding ligand. So the key intermediate (**145**) having *p*-chlorophenyl group was reacted with different substituted benzyls, monoaryls, biaryls or amidoalkyls as S4 binding ligands.

4.2.2.3. Synthesis of 5-(substituted-benzylthio)-*N*-(4-chlorophenyl)-1,3,4-thiadiazol-2-amines (159-165)

The first set of 1,3,4-thiadiazole derivatives (**159-165**) were synthesized by reacting **(145)** with different benzyl halides as illustrated in **Scheme 4.7**. The IR spectrum of these compounds displayed common characteristic peak at 3200-3300 cm^{-1} assigned to NH group. The mass spectra and HPLC data (**Table 4.10**) confirmed the molecular weight and purity of the compounds (**159-165**).

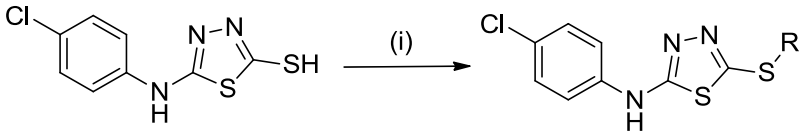

(145) **(159-165)**

Scheme 4.7. Synthetic route for the preparation of compounds (**159-165**). Reagents and conditions: (i) Substituted benzyl halides, potassium carbonate, DMF, rt, 2-3 h.

Table 4.10. Analytical data of compounds **(159-165)**

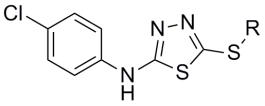

(159-165)

Comp	R	M.P. (°C)	IR characteristic peaks (cm^{-1})	Mass (m/z)	HPLC Data
159		185-187	3258, 3057, 2837, 1658, 1599, 1491, 1401, 806	334.37 $(M)^+$ 336.36 $(M+2)^+$	Purity: 97.1% t_R = 6.03 min
160	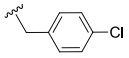	183-185	3252, 3025, 2819, 1609, 1565, 1489, 1413, 819;	368.38 $(M)^+$ 370.39 $(M+2)^+$	Purity: 97.9% t_R = 5.37 min
161	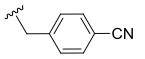	201-203	3250, 3039, 2917, 2227, 1619, 1494, 1411, 820	359.43 $(M)^+$, 361.44 $(M+2)^+$	Purity: 98.2% t_R = 4.50 min
162	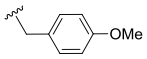	190-192	3262, 3024, 2836, 1607, 1548, 1494, 1404, 1030, 814	364.38 $(M)^+$ 366.39 (M+2)	Purity: 97.4% t_R = 4.21 min
163	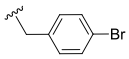	179-181	3249, 3036, 2822, 1618, 1494, 1412, 827	412.43 $(M)^+$ 414.48 $(M+2)^+$	Purity: 96.1% t_R = 5.16 min
164	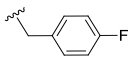	178-180	3246, 3189, 2824, 1891, 1618, 1455, 1224, 823	352.36 $(M)^+$, 354.35 $(M+2)^+$	Purity: 99.5% t_R = 4.82 min
165	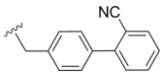	171-173	3303, 3084, 2849, 2233, 1605, 1486, 1400, 810	435.52 $(M)^+$, 437.52 $(M+2)^+$	Purity: 98.5% t_R = 6.56 min

The ^{1}H-NMR spectrum of compound (**159**) showed a broad singlet at δ 10.34 for the amine proton (NH_c). It showed signals as doublet at δ 7.60 for two aromatic protons (ArH_b), doublet at δ 7.39 for two aromatic protons (ArH_e) and then multiplet at δ 7.25-7.34 for the remaining five aromatic protons (Ar$H_{a,f,g}$), confirming to a total of nine aromatic protons. A singlet at δ 4.39 was accounted for the two methylene protons (C$H_{2/d}$) attached to carbon near thio group.

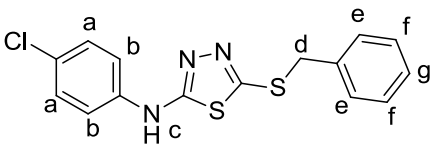

(159)

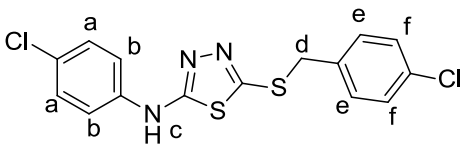

(160)

The ^{1}H-NMR spectrum of compound (**160**) showed a broad singlet at δ 10.29 for the amine proton (NH_c). It displayed signals as doublet at δ 7.59

for two aromatic protons (ArH_b), doublet at δ 7.38 for two protons (ArH_f), doublet at δ 7.30 for two protons (ArH_e) and another doublet at δ 7.26 for two protons (ArH_a). It also showed a singlet at δ 4.36 for the two methylene protons (C$H_{2/d}$) attached to carbon near thio group.

The ^{1}H-NMR spectrum of compound (**161**) showed a broad singlet at δ 10.35 for the amine proton (NH_c). It offered signals as doublet at δ 7.70 for two protons (ArH_b), multiplet at δ 7.58-7.60 for four protons (Ar$H_{e,f}$) and then doublet at δ 7.26 for two protons (ArH_a). Aliphatic protons appeared as singlet at δ 4.36 was for the two methylene protons (C$H_{2/d}$) attached to carbon near thio group.

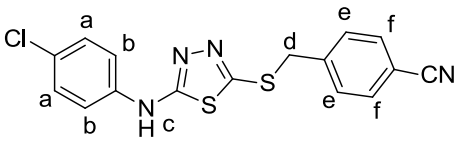

(161)

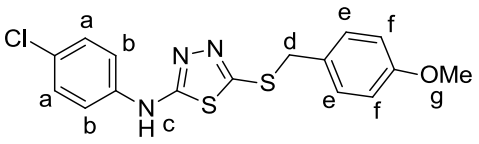

(162)

The ^{1}H-NMR spectrum of compound (**162**) showed a broad singlet at δ 10.52 for the amine proton (NH_c). The aromatic protons appeared as doublet at δ 7.62 for two protons (ArH_b), doublet at δ 7.40 for two protons (ArH_a), doublet at δ 7.34 for two protons (ArH_e) and doublet at δ 6.91 for two protons (ArH_f). The aliphatic protons were observed as singlet at δ 4.38 for the two methylene protons (C$H_{2/d}$) attached to carbon near thio group and singlet at δ 3.74 for three protons of methoxy group (OC$H_{3/g}$).

The ^{1}H-NMR spectrum of compound (**163**) showed a broad singlet at δ 10.52 for the amine proton (NH_c). It displayed signals as doublet at δ 7.60 for two protons (ArH_f), doublet at δ 7.52 for two protons (ArH_b), doublet at δ 7.39 for two protons (ArH_a) and doublet at δ 7.37 for two protons (ArH_e). The aliphatic protons appeared as singlet at δ 4.40 for the two methylene protons (C$H_{2/d}$) attached to carbon near thio group.

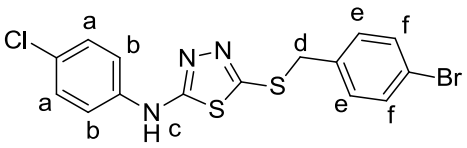

(163)

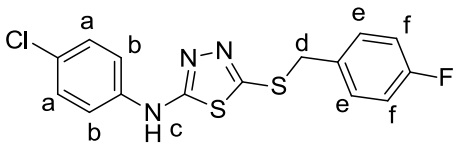

(164)

The ^{1}H-NMR spectrum of compound (**164**) showed a broad singlet at δ 10.52 for the amine proton (N*H*$_c$). It displayed signals as doublet at δ 7.61 for two protons (Ar*H*$_b$), multiplet at δ 7.39-7.48 for four protons (Ar*H*$_{a,e}$) and multiplet at δ 7.21-7.16 for two protons (Ar*H*$_f$). The aliphatic protons appeared as singlet at δ 4.40 for the two methylene protons (C*H*$_{2/d}$) attached to carbon near thio group.

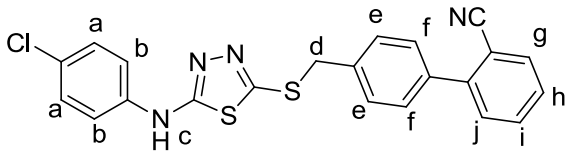

(165)

The ^{1}H-NMR spectrum of compound (**165**) showed a broad singlet at δ 10.43 for the amine proton (N*H*$_c$). It also showed doublet at δ 7.87 for one proton (Ar*H*$_j$), doublet of triplet at δ 7.74 for one proton (Ar*H*$_i$), multiplets at δ 7.52-7.62 and at δ 7.29-7.32 for eight and two protons respectively. A singlet at δ 4.50 accounted for two methylene protons (C*H*$_{2/d}$) attached to carbon near thio group. Its ^{13}C-NMR spectrum showed peak at δ 118.41 due to carbon of the nitrile group. The aromatic carbons appeared at δ 164.45, 152.63, 143.93, 139.10, 137.62, 136.86, 133.76, 133.41, 129.97, 129.27, 128.80, 128.77, 128.13, 125.30, 118.82, 118.41 and 109.99 whereas the aliphatic carbon appeared at δ 37.26.

4.2.2.4. Synthesis of 5-(thiosubstituted)-*N*-(4-chlorophenyl)-1,3,4-thiadiazol-2-amines (178-186)

Some secondary amines (morpholine, piperidine and pyrrolidine) were reacted with various acid chlorides (**166-168**) to offer the intermediates (**169-177**). These intermediates **(169-177)** without further purification were reacted with compound (**145**) to get the desired 5-thiosubstituted 1,3,4-thiadiazoles

(**178-186**) (**Scheme 4.8**). Some physical and spectral data is shown in **Table 4.11** for these compounds (**178-186**).

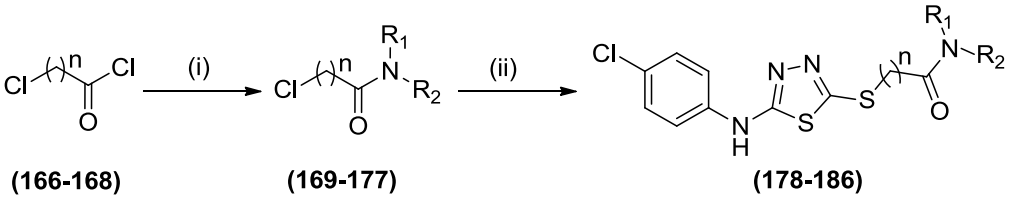

Scheme 4.8. Synthetic route for the preparation of compounds (**178-186**). Reagents and conditions: (i) Secondary amines, anhydrous potassium carbonate, dry DCM, rt, 6-7 h; (ii) Compound (**145**), potassium carbonate, DMF, rt, 3-4 h.

Table 4.11. Analytical data of compounds (**178-186**)

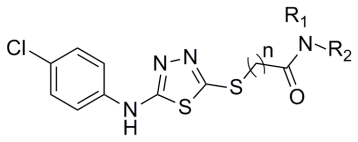
(178-186)

Comp	n	NR^1R^2	M.P. (°C)	IR characteristic peaks (cm^{-1})	Mass (m/z)	HPLC Data
178	1		228-230	3246, 3048, 2881, 1642, 1516, 1406, 1244, 815	355.4 $(M)^+$ 357.4 $(M+2)^+$	Purity: 97.0% t_R = 3.36 min
179	1		201-203	3259, 3038, 2856, 1632, 1495, 1406, 1215, 823	369.5 $(M)^+$ 371.5 $(M+2)^+$	Purity: 96.8% t_R = 3.65 min
180	1		200-202	3250, 3050, 2865, 1641, 1494, 1407, 1216, 818	371.4 $(M)^+$, 373.4 $(M+2)^+$	Purity: 97.9% t_R = 3.07 min
181	2		194-196	3254, 3055, 2875, 1638, 1517, 1410, 846	369.0 $(M)^+$ 371.0 (M+2)	Purity: 95.9% t_R = 4.04 min
182	2		178-180	3242, 3035, 2857, 1646, 1608, 1412, 825	383.5 $(M)^+$ 385.4 $(M+2)^+$	Purity: 97.2%, t_R = 4.77 min
183	2		214-216	3236, 3035, 2865, 1647, 1523, 1412, 847	385.5 $(M)^+$, 387.5 $(M+2)^+$	Purity: 98.1%, t_R = 3.24 min
184	3		156-158	3245, 3048, 1634, 1517, 829	383.5 $(M)^+$, 385.5 $(M+2)^+$	Purity: 99.7%, t_R = 3.56 min
185	3		145-147	3252, 2996, 2859, 1630, 1512, 1401, 823	397.5 $(M)^+$, 399.5 $(M+2)^+$	Purity: 96.3%, t_R = 3.93 min
186	3		178-180	3237, 3038, 1641, 1521, 1441, 819	399.5 $(M)^+$, 401.5 $(M+2)^+$	Purity: 96.8%, t_R = 3.25 min

The ^{1}H-NMR spectrum of compound (**178**) showed a broad singlet at δ 10.53 for the amine proton (NH_c), a doublet at δ 7.62 for two protons (ArH_b) and another doublet at δ 7.40 for two protons (ArH_a). The aliphatic protons were observed as a singlet at δ 4.22 for two methylene protons (C$H_{2/d}$) attached to the carbon near thio group, multiplet at δ 3.30-3.50 for four protons (NC$H_{2/e}$) and multiplet at δ 1.76-1.94 for four aliphatic protons (C$H_{2/f}$).

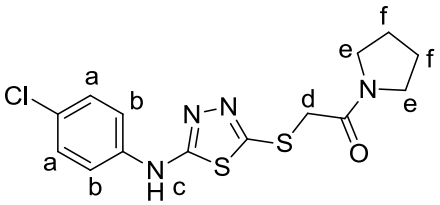

(178)

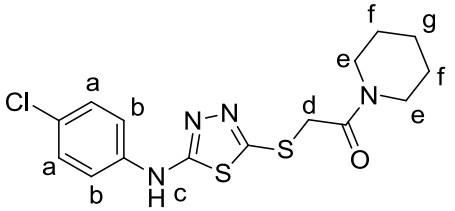

(179)

The ^{1}H-NMR spectrum of compound (**179**) showed a broad singlet at δ 10.53 for the amine proton (NH_c), a doublet at δ 7.60 for two protons (ArH_b) and another doublet at δ 7.39 for two protons (ArH_a). It also offered a singlet at δ 4.30 accounting for two methylene protons (C$H_{2/d}$) attached to the carbon near thio group, a multiplet at δ 3.35-3.43 appeared for four protons (NC$H_{2/e}$) and another multiplet at δ 1.44-1.56 accounted for six aliphatic protons (C$H_{2/f,g}$).

The ^{1}H-NMR spectrum of compound (**180**) showed a broad singlet at δ 10.54 for the amine proton (NH_c), a doublet at δ 7.62 for two protons (ArH_b) and another doublet at δ 7.40 for two protons (ArH_a). The aliphatic protons appeared as a singlet at δ 4.32 for two methylene protons (C$H_{2/d}$) attached to the carbon near thio group, a multiplet at δ 3.52-3.62 for four protons (OC$H_{2/f}$) and another multiplet at 3.36-3.51 for four protons (NC$H_{2/e}$).

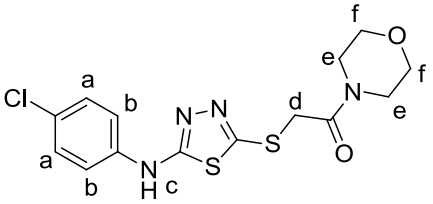

(180)

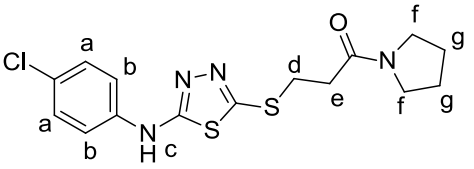

(181)

The ^{1}H-NMR spectrum of compound (**181**) showed a broad singlet at δ 10.54 for the amine proton (NH_c), a doublet at δ 7.62 for two protons (ArH_b) and another doublet at δ 7.40 for two protons (ArH_a). The aliphatic protons were observed as multiplet at δ 3.34-3.39 for four protons (NC$H_{2/f}$) attached to carbon near nitrogen, triplet at δ 3.29 for two protons attached to the carbon near thio group (C$H_{2/d}$), triplet at δ 2.74 for two methylene protons attached to carbon near carbonyl group (COC$H_{2/e}$), multiplet at δ 1.75-1.88 for four aliphatic protons (C$H_{2/g}$).

The ^{1}H-NMR spectrum of compound (**182**) showed a broad singlet at δ 10.48 for the amine proton (NH_c), a doublet at δ 7.60 for two protons (ArH_b) and another doublet at δ 7.37 for two protons (ArH_a). It showed a triplet at δ 3.42 for two methylene protons attached to the carbon near thio group (SC$H_{2/d}$). Other aliphatic protons appeared as multiplet at δ 3.29-3.35 for four protons (NC$H_{2/f}$) attached to the carbon near nitrogen, triplet at δ 2.78 for four protons (COC$H_{2/e}$), multiplet at δ 1.54-1.58 for four aliphatic protons (C$H_{2/g}$) and multiplet at δ 1.46-1.37 for two aliphatic protons (C$H_{2/h}$).

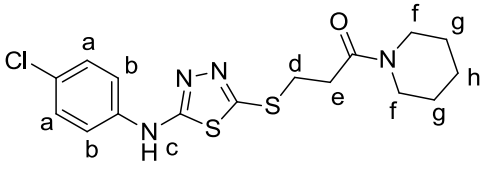

(182)

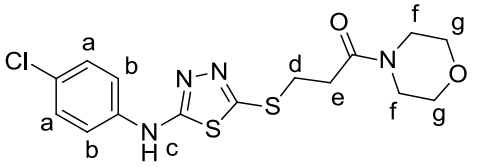

(183)

The ^{1}H-NMR spectrum of compound (**183**) displayed a broad singlet at δ 10.53 for the amine proton (NH_c), a doublet at δ 7.62 for two protons (ArH_b) and another doublet at δ 7.39 for two protons (ArH_a). The aliphatic protons appeared as a triplet at δ 3.55 for four protons (OC$H_{2/g}$) attached to the carbon near oxygen, triplet at δ 3.40 for four protons (NC$H_{2/f}$), triplet at δ 3.37 for two methylene protons attached to the carbon near thio group (SC$H_{2/d}$) and triplet at δ 2.83 for two aliphatic protons (COC$H_{2/e}$).

The ^{1}H-NMR spectrum of compound (**184**) showed a broad singlet at δ 10.54 for the amine proton (NH_c), a doublet at δ 7.62 for two protons (ArH_b) and another doublet at δ 7.37 for two protons (ArH_a). The aliphatic protons

appeared as a multiplet at δ 3.24-3.34 for four protons (NC$H_{2/g}$), triplet at δ 3.19 for two methylene protons attached to the the carbon near thio group (SC$H_{2/d}$), triplet at δ 2.32 for two aliphatic protons (COC$H_{2/f}$), multiplet at δ 2.02-2.09 for four aliphatic protons (C$H_{2/h}$) and multiplet at δ 1.91-1.94 for two aliphatic protons (C$H_{2/e}$). Its ^{13}C-NMR spectrum showed peak at δ 169.23 due to C=O carbon of the amide. Aromatic carbons appeared at δ 164.20, 153.36, 139.18, 128.81, 125.29 and 118.81 whereas the aliphatic carbons appeared at δ 45.68, 45.12, 33.74, 32.0, 23.47, 24.42 and 23.80.

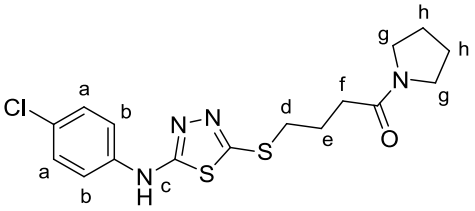

(184)

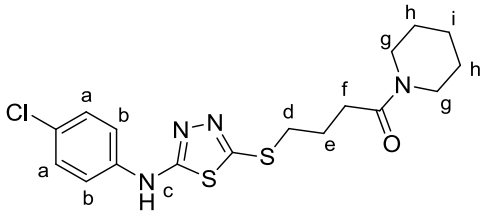

(185)

The ^{1}H-NMR spectrum of compound (**185**) showed a broad singlet at δ 10.51 for the amine proton (NH_c), a doublet at δ 7.60 for two protons (ArH_b) and another doublet at δ 7.40 for two protons (ArH_a). The aliphatic protons were observed as multiplet at δ 3.33-3.40 for four protons (NC$H_{2/g}$), triplet at δ 3.17 for two methylene protons attached to the carbon near thio group (SC$H_{2/d}$), triplet at δ 2.42 for two protons (COC$H_{2/f}$), multiplet at δ 1.84-1.92 for two protons (C$H_{2/e}$), multiplet at δ 1.51-1.56 for two protons (C$H_{2/i}$) and multiplet at δ 1.38-1.45 for four protons (C$H_{2/h}$).

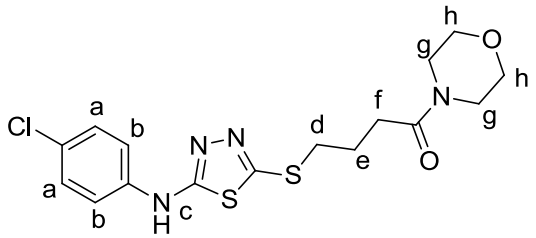

(186)

The ^{1}H-NMR spectrum of compound (**186**) showed a broad singlet at δ 10.55 for the amine proton (NH_c), a doublet at δ 7.61 for two protons (ArH_b) and another doublet at δ 7.38 for two protons (ArH_a). The aliphatic protons appeared as multiplet at δ 3.48-3.53 for four protons (OC$H_{2/h}$) attached to the

carbon near oxygen, multiplet at δ 3.35-3.41 for four protons (NC$H_{2/g}$), triplet at δ 3.18 for two methylene protons attached to the carbon near thio group (SC$H_{2/d}$), triplet at δ 2.45 for two aliphatic protons (COC$H_{2/f}$) and multiplet at δ 1.88-1.92 for two protons (C$H_{2/e}$).

4.2.2.5. Synthesis of substituted anilines (197-204, 208, 210)

The synthesis of necessary amines was carried out as per **Scheme 4.9**. Commercially available 4-fluoro-1-nitrobenzene (**187**) and 4-bromo-1-nitrobenzene (**188**) were used as the starting materials for the preparation of substituted anilines (**197-204**). 4-Fluoro-1-nitrobenzene (**187**) was refluxed with different secondary amines i.e. pyrrolidine, piperidine, morpholine and *N*-methylpiperazine, respectively to get intermediates (**189-192**). Compounds (**193-196**) were synthesized by reacting 4-bromo-1-nitrobenzene (**188**) with different secondary amides like 2-pyrrolidinone, δ-valerolactam, ε-caprolactam and 2-hydoxypyridine respectively in the presence of K_2CO_3 as a base, CuI as a metal catalyst and DMEDA as a ligand. Structures of these compounds were confirmed by their physical data and IR spectroscopy given in **Table 4.12**. These intermediates (**189-196**) were reduced with the help of Pd/C and hydrazine hydrate to obtain the corresponding anilines (**197-204**).

4-Phenylmorpholin-3-one (**206**) was prepared by cyclization of 2-anilinoethanol **(205)** with chloroacetyl chloride. Further nitration of the morpholinone derivative (**206**) was done using conc. sulphuric acid and nitric acid to afford the 4-(4-nitrophenyl)morpholin-3-one (**207**). Thereafter, the intermediate (**207**) was reduced with the help of Pd/C and hydrazine hydrate to obtain 4-(4-aminophenyl)morpholin-3-one (**208**).

To synthesize 1-(4-amino-3-fluorophenyl)pyridin-2(1*H*)-one (**210**), 2-fluoro-4-iodoaniline (**209**) was reacted with 2-hydoxypyridine as shown in **Scheme 4.9**. All the synthesized substituted anilines (**197-204**, **208**, and **210**) were characterized by their melting points and IR spectra given in **Table 4.13**.

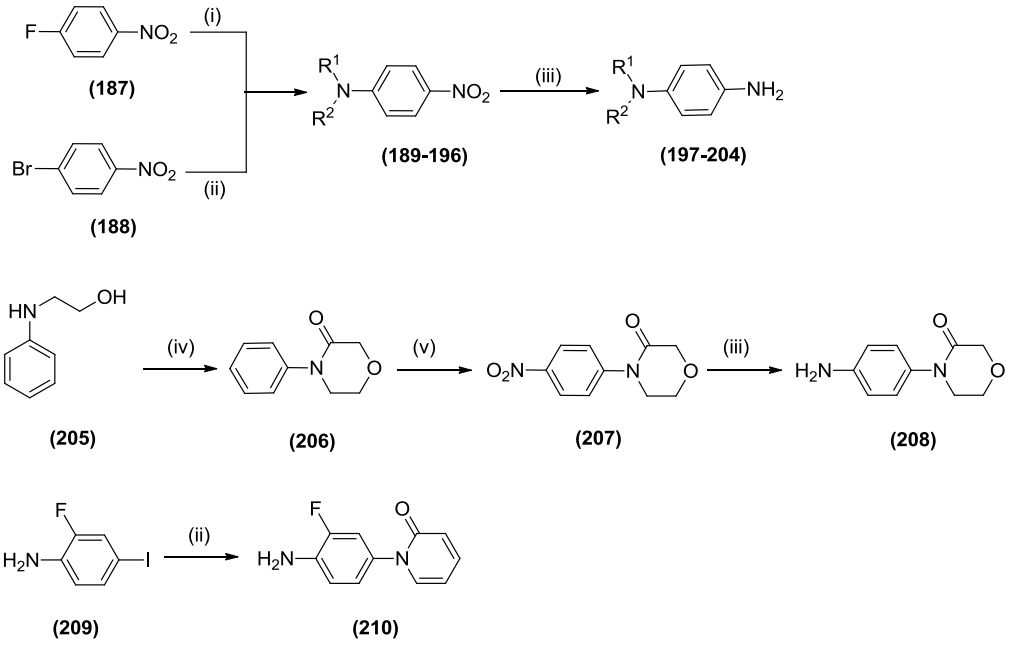

Scheme 4.9. Synthetic routes for the preparation of compounds **(197-204, 208** and **210)**. Reagents and conditions: (i) Secondary amines, potassium carbonate, DMF, 110 °C, 12-15 h; (ii) Secondary amides, CuI, DMEDA, K_2CO_3, dioxane, in pressure tube at 140-150 °C, 4-5 h. (iii) Pd/C, Ethanol, hydrazine hydrate, reflux 2-3 h.; (iv) Chloroacetyl chloride, 10N sodium hydroxide, IPA, 40 °C, 1 h.; (v) 98% Sulphuric acid, nitric acid, 0 °C, 2-3 h.

Table 4.12. Analytical data of nitro compounds (**189-196** and **207**)

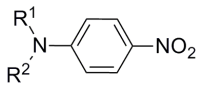

(189-196,207)

Comp	NR^1R^2	M.P.	IR characteristic peaks (cm^{-1})
189		163-165 °C (lit.[106] 167-169 °C)	2972, 2859, 1520, 1297, 821
190	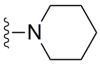	100-102 °C (lit.[107] 104-106 °C)	2940, 2846, 1598, 1321, 818
191	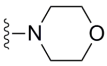	154-156 °C (lit.[108] 152-154 °C)	3111, 1583, 1057, 848
192	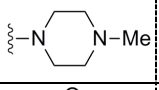	101-103 °C (lit.[109] 102-104 °C)	2937, 2888, 1594, 1328, 851
193		128-130 °C (lit.[110] 129-131 °C)	3119, 2893, 1703, 1596, 1388, 849
194	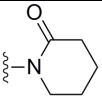	97-99 °C (lit.[80] 96-98 °C)	3099, 2954, 1657, 1591 1344, 858

Comp	NR^1R^2	M.P.	IR characteristic peaks (cm^{-1})
195	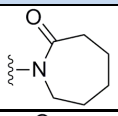	157-159 °C	2932, 1659, 1522, 1346, 862
196	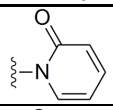	187-189 °C (lit.[111] 188-190 °C)	3058, 1671, 1524, 1351, 862
207	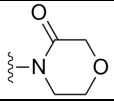	147-149 °C (lit.[112] 148-152 °C)	3064, 1673, 1593, 1000, 855

Table 4.13. Analytical data of substituted anilines (**197-204, 208** and **210**)

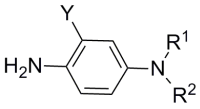

(197-204, 208, 210)

Comp Id	Y	NR^1R^2	M.P.	IR characteristic peaks (cm^{-1})
197	H		Semisolid	3423, 3320, 2926,1517, 1266
198	H	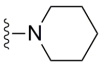	Semisolid	3430, 3350, 2931,1512, 823
199	H	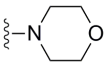	124-126 °C (lit.[113] 124-126 °C)	3384, 3326, 3012, 1517, 1264, 832
200	H	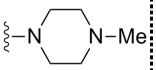	85-87 °C (lit.[114] 88-90 °C)	3358, 3030, 2929, 1512, 1278, 821
201	H	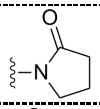	122-124 °C	3428, 3334, 3214, 2982, 1665, 1511, 1291, 840
202	H	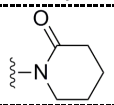	115-117 °C (lit.[115] 118-120 °C)	3440, 3325, 3212, 2953, 1608, 1516,1298, 823
203	H	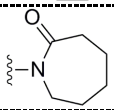	157-159 °C	3408, 3329, 3230, 2931, 1626, 1513, 1282, 826
204	H	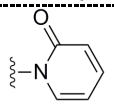	125-127 °C (lit.[115] 128-130 °C)	3462, 3307, 3201, 1654, 1573 and 825
208	H	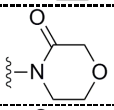	127-129 °C (lit.[115] 115-128 °C)	3459, 3340, 2886, 1639, 1517, 1120, 829
210	F	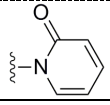	192-194 °C (lit.[115] 196-198 °C)	3465, 3302, 1654, 1574, 1518, 1325, 763

The commercially available 4-chloroaniline (**211**), 4-fluoroaniline (**212**) and *p*-anisidine (**213**) were used as such in the next step.

4.2.2.6. Synthesis of 2-((5-((4-chlorophenyl)amino)-1,3,4-thiadiazol-2-yl)thio)-*N*-phenylacetamides (227-239)

Substituted anilines (**197-204, 208, 210-213**) were reacted with chloroacetyl chloride or bromoacetyl bromide to obtain the intermediates (**214-226**). These compounds were characterized by their physical and spectral data (**Table 4.14**). All of these compounds (**214-226**) showed common characteristic peak around 1650-1700 cm^{-1} for amide stretching. Some of them were also confirmed by mass spectrometry.

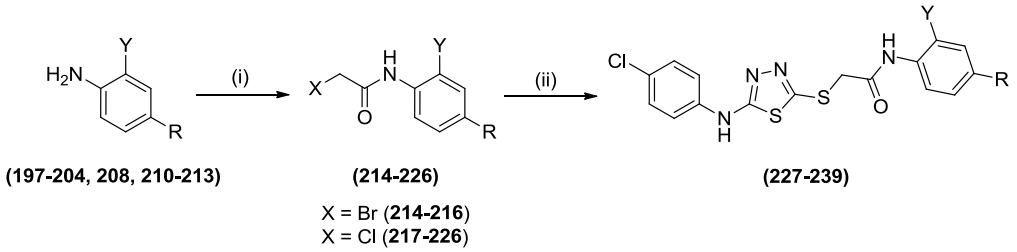

Scheme 4.10. Synthetic route for the preparation of compounds (**227-239**). Reagents and conditions: (i) Chloroacetyl chloride, anhydrous potassium carbonate, dry DCM, rt, 2-3 h; (ii) Compound (**145**), potassium carbonate, DMF, rt, 3-4 h.

Table 4.14. Analytical data of compounds **(214-226)**

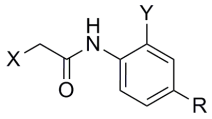

(214-226)

Comp	X	Y	R	M.P.	IR characteristic peaks (cm^{-1})	Mass (m/z)
214	Br	H		150-152 °C (lit.[116] 153-155 °C)	3291, 3068, 2956, 1660, 1546, 1248, 830	-
215	Br	H		138-140 °C (lit.[116] 137-139 °C)	3273, 3102, 2836, 1653, 1506, 1210, 837	-
216	Br	H		127-129 °C (lit.[116] 128-130 °C)	3297, 3024, 2972, 1652, 1554, 1485, 798	-
217	Cl	H		196-198 °C	3329, 2956, 1662, 1519, 1326, 827	-

Comp	X	Y	R	M.P.	IR characteristic peaks (cm^{-1})	Mass (m/z)
218	Cl	H	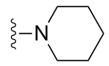	210-212 °C	3185, 3058, 2936, 1663, 1572, 804	-
219	Cl	H	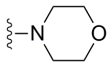	167-169 °C (lit.[117] 170-172 °C)	3317, 2963, 2818, 1658, 1521, 1119, 820	-
220	Cl	H	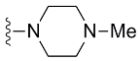	249-251 °C	3265, 3038, 2843, 1675, 1515, 1251, 922	268.0 $(M)^+$, 270.0 $(M+2)^+$
221	Cl	H	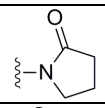	203-205 °C	3315, 3194, 2960, 1707, 1669, 1328, 846	253.4 $(M)^+$, 255.1 $(M+2)^+$
222	Cl	H	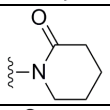	207-209 °C	3258, 3123, 3011, 1699, 1610, 1334, 839	267.5 $(M)^+$, 269.1 $(M+2)^+$
223	Cl	H	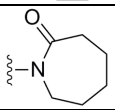	165-167 °C	3267, 3125, 2930, 1692, 1629, 1327, 838	280.8 $(M)^+$ 283.1 $(M+2)^+$
224	Cl	H	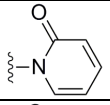	>250 °C	3275, 3129, 3084, 1704, 1660, 1332, 839	263.4 $(M)^+$ 265.1 $(M+2)^+$
225	Cl	H	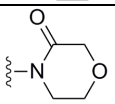	216-218 °C	3274, 3134, 2984, 1712, 1635, 1006, 846	269.4 $(M)^+$, 271.1 $(M+2)^+$
226	Cl	F	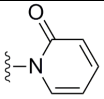	>250 °C	3265, 3020, 1711, 1658, 1535, 1427, 769	281.2 $(M)^+$ 283.2 (M+2)

The acylated compounds (**214-226**) were further reacted with the key intermediate (**145**) to get the desired compounds (**227-239**). **Table 4.15** represents melting points, spectral (IR and Mass) and HPLC data of all the final compounds (**227-239**).

Table 4.15. Analytical data of compounds **(227-239)**

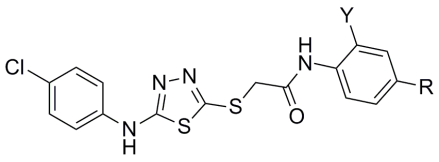

(227-239)

Comp	X	R	M.P.	IR characteristic peaks (cm^{-1})	HPLC Data
227	H		203-205 °C	3299, 3046, 2826, 1671, 1528, 1494, 822	Purity: 96.5% t_R = 4.47 min
228	H		201-203 °C	3310, 3055, 2829, 1668, 1416, 1215, 829	Purity: 99.1% t_R = 3.80 min

Comp	X	R	M.P.	IR characteristic peaks (cm^{-1})	HPLC Data
229	H		241-243 °C	3324, 3018, 2837, 1601, 1409, 1248, 826	Purity: 98.4 % t_R = 3.62 min
230	H		226-228 °C	3312, 3056, 2839, 1650, 1543, 1403, 817	Purity: 98.8% t_R = 4.86 min
231	H	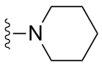	227-229 °C	3313, 3056, 2854, 1651, 1541, 1402, 817	Purity: 97.1%, t_R = 4.99 min
232	H	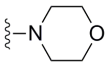	238-240 °C	3319, 3053, 1649, 1510, 1406, 819	Purity: 96.6% t_R = 3.50 min
233	H	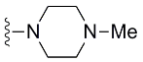	240-242 °C	3314, 3184, 3059, 2936, 1652, 1620, 1402, 816	Purity: 99.2% t_R = 3.56 min
234	H	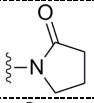	>250 °C	3296, 3188, 3071, 1654, 1605, 1405, 827	Purity: 98.9% t_R = 3.26 min
235	H	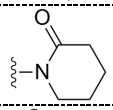	>250 °C	3272, 3123, 3059, 2868, 1683, 1620, 1408, 831	Purity: 98.4% t_R = 3.35 min
236	H	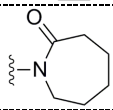	227-229 °C	3275, 3123, 2949, 1686, 1620, 1516, 1406, 827	Purity: 95.9%, t_R = 4.04 min
237	H	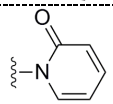	>250 °C	3318, 1659, 1530, 1620, 1409, 832	Purity: 99.1%, t_R = 3.20 min
238	H	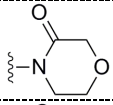	224-226 °C	3192, 3046, 2907, 1665, 1603, 1514, 1414, 832	Purity: 97.4%, t_R = 3.04 min
239	F	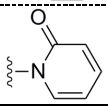	>250 °C	3269, 3069, 1662, 1533, 1620, 1400, 822	Purity: 99.5%, t_R = 3.10 min

The ^{1}H-NMR spectrum of compound (**227**) showed two broad singlets at δ 10.49 and at δ 10.43 for two amine protons (N$H_{c,e}$). The aromatic protons appeared as doublet at δ 7.61 for two protons (ArH_f), doublet at δ 7.59 for two protons (ArH_b), doublet at δ 7.38 for two protons (ArH_a) and doublet at δ 7.37 for two protons (ArH_g). It also showed a singlet at δ 4.12 for two protons attached to the carbon near thio group (C$H_{2/d}$). Its mass spectrum showed $(M)^+$ peak at 411.43 m/z and $(M+2)^+$ peak at 413.41 m/z.

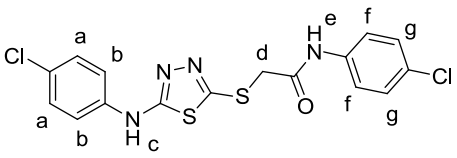

(227)

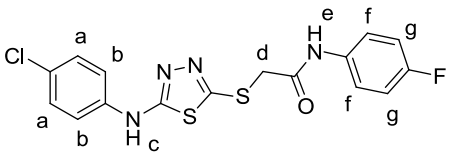

(228)

The ^{1}H-NMR spectrum of compound (**228**) showed a broad singlet at δ 10.36 for the amine proton (NH_c). The aromatic protons appeared as multiplet at δ 7.58-7.60 for four protons (Ar$H_{b,f}$) , doublet at δ 7.36 for two protons (ArH_a) and another multiplet at δ 7.13-7.18 for two protons (ArH_g). It also displayed a singlet at δ 4.10 for two protons attached to the carbon near thio group (C$H_{2/d}$). Its mass spectrum showed $(M)^+$ peak at 395.45 m/z and $(M+2)^+$ peak at 397.45 m/z.

The ^{1}H-NMR spectrum of compound (**229**) showed two broad singlets at δ 10.50 and at δ 10.15 for two amine protons (N$H_{c,e}$). The aromatic protons were observed as doublet at δ 7.59 for two protons (ArH_b), doublet at δ 7.48 for two protons (ArH_f), doublet at δ 7.37 for two protons (ArH_a) and another doublet at δ 6.89 for two protons (ArH_g). It also displayed a singlet at δ 4.08 for two protons attached to the carbon near thio group (C$H_{2/d}$) and another singlet at δ 3.71 for three aliphatic protons of methoxy group (OC$H_{3/h}$). Its mass spectrum showed $(M)^+$ peak at 407.52 m/z and $(M+2)^+$ peak at 409.52 m/z. .

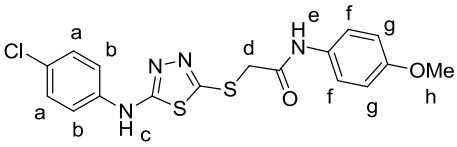

(229)

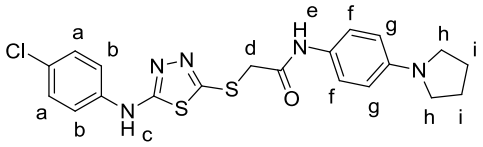

(230)

The ^{1}H-NMR spectrum of compound (**230**) showed a broad singlet at δ 9.94 for the amine proton (NH_c). The aromatic protons appeared as doublet at δ 7.59 for two protons (ArH_b), doublet at δ 7.38 for two protons (ArH_f), doublet at δ 7.37 for two protons (ArH_a) and another doublet at δ 6.48 for two protons (ArH_g). The aliphatic protons appeared as singlet at δ 4.02 for two protons (C$H_{2/f}$) attached to carbon near thio group, multiplet at δ 3.16-3.19

accounted for five protons, among them four protons are of the carbon attached near nitrogen group (NC$H_{2/h}$) and one proton accounted for the amine group (NH_g). It also showed a triplet at δ 1.93 for four aliphatic protons (C$H_{2/i}$). Its mass spectrum showed $(M)^+$ peak at at 376.68 m/z and $(M+2)^+$ peak at at 378.69 m/z.

The ^{1}H-NMR spectrum of compound (**231**) showed a broad singlet at δ 10.10 for one amine proton (NH_c). The aromatic protons appeared as doublet at δ 7.59 for two protons (ArH_b), doublet at δ 7.40 for two protons (ArH_f), doublet at δ 7.38 for two protons (ArH_a) and another doublet at δ 6.87 for two protons (ArH_g). Aliphatic protons were observed as singlet at δ 4.06 for two protons (C$H_{2/d}$) attached to the carbon near thio group, multiplet at δ 3.03-3.05 for four protons of carbon attached near nitrogen (NC$H_{2/h}$) and multiplet at δ 1.49-1.59 for six aliphatic protons (C$H_{2/i,j}$). Its mass spectrum showed $(M)^+$ peak at at 460.36 m/z and $(M+2)^+$ peak at at 462.42 m/z .

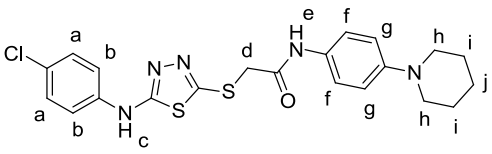

(231)

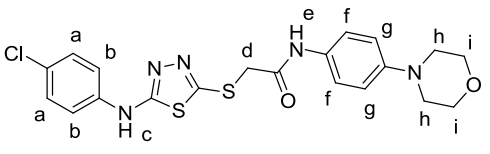

(232)

The ^{1}H-NMR spectrum of compound (**232**) showed two broad singlets at δ 10.52 and δ 10.11 for two amine proton (N$H_{c,e}$). The aromatic protons were observed as doublet at δ 7.60 for two protons (ArH_b), doublet at δ 7.45 for two protons (ArH_f), doublet at δ 7.38 for two protons (ArH_a) and doublet at δ 6.90 for two protons (ArH_g). The aliphatic protons appeared as singlet at δ 4.08 for two protons (C$H_{2/d}$) attached to carbon near thio group, multiplet at δ 3.72-3.74 for four protons of carbon attached near oxygen (OC$H_{2/i}$) and multiplet at δ 3.03-3.05 for four protons of the carbon attached near nitrogen (NC$H_{2/h}$). Its mass spectrum showed $(M)^+$ peak at 462.64 m/z and $(M+2)^+$ peak at 464.61 m/z.

The ^{1}H-NMR spectrum of compound (**233**) showed two broad singlets at δ 10.52 and at δ 10.08 for two amine protons (N$H_{c,e}$). The aromatic protons appeared as doublet at δ 7.61 for two protons (ArH_b), doublet at δ 7.44 for two

protons (ArH_f), doublet at δ 7.39 for two protons (ArH_a) and doublet at δ 6.90 for two protons (ArH_g). Aliphatic protons appeared as singlet at δ 4.08 for two protons (C$H_{2/d}$) attached to the carbon near thio group, triplet at δ 3.08 for four protons of carbon attached near nitrogen (NC$H_{2/h}$) and triplet at δ 2.45 for four aliphatic protons (C$H_{2/i}$) and singlet at δ 2.23 for three protons (C$H_{3/j}$). The mass spectrum showed $(M)^+$ peak at at 475.0 m/z and $(M+2)^+$ peak at at 477.0 m/z .

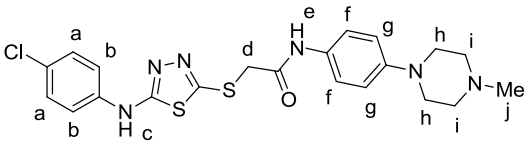

(233)

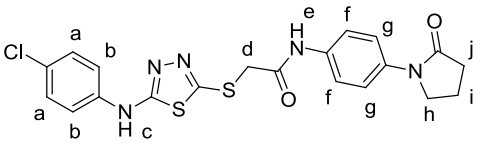

(234)

The ^{1}H-NMR spectrum of compound (**234**) displayed two broad singlets at δ 10.52 and at δ 10.32 for two amine protons (N$H_{c,e}$). The aromatic protons appeared as multiplet at δ 7.56-7.62 for six protons (Ar$H_{a,b,f}$), and doublet at 7.38 for two protons (ArH_g). Aliphatic protons were observed as singlet at δ 4.12 for two protons attached to the carbon near thio group (C$H_{2/d}$), triplet at δ 3.80 for two aliphatic protons (NC$H_{2/h}$), triplet at δ 2.47 for two aliphatic protons (COC$H_{2/j}$) attached to carbon near carbonyl group and multiplet at δ 2.02-2.08 for two aliphatic protons (C$H_{2/i}$). The mass spectrum showed $(M)^+$ peak at 458.48 m/z and $(M+2)^+$ peak at 460.21 m/z.

The ^{1}H-NMR spectrum of compound (**235**) showed two broad singlets at δ 10.53 and at δ 10.37 for two amine protons (N$H_{c,e}$). The aromatic protons were appeared as doublet at δ 7.60 for two protons (ArH_f), doublet at δ 7.57 for two protons (ArH_b), doublet at δ 7.38 for two protons (ArH_a), and doublet at δ 7.21 for two protons (ArH_h). It also displayed a singlet at δ 4.12 for two protons attached to the carbon near thio group (C$H_{2/d}$), triplet at δ 3.56 for two aliphatic protons (NC$H_{2/h}$), triplet at δ 2.37 for two aliphatic protons (COC$H_{2/k}$) and multiplet at δ 1.83-1.84 for four aliphatic protons (C$H_{2/i,j}$). Its ^{13}C-NMR spectrum showed peak at δ 168.68 and δ 165.44 due to C=O carbon of the amide. Aromatic carbons appeared at δ 164.66, 152.61, 139.11, 139.03, 138.45, 128.82, 126.52, 125.30, 119.30 and 118.82 whereas the aliphatic

carbons appeared at δ 50.79, 32.45, 22.90 and 20.81. Its mass spectrum showed $(M)^+$ peak at 474.22 m/z and $(M+2)^+$ peak at 476.22 m/z.

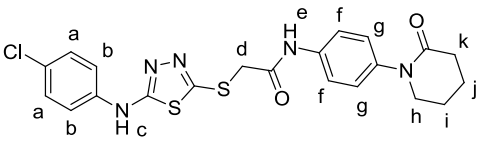

(235)

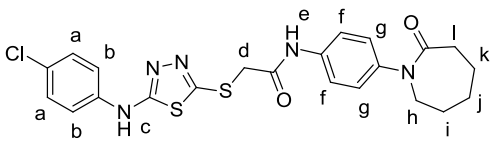

(236)

The ^{1}H-NMR spectrum of compound (**236**) showed two broad singlets at δ 10.50 and δ 10.33 for two amine protons (N$H_{c,e}$). The aromatic protons were observed as doublet at δ 7.59 for two protons (ArH_f), doublet at δ 7.57 for two protons (ArH_b), doublet at δ 7.37 for two protons (ArH_a) and doublet at δ 7.14 for two protons (ArH_h). The aliphatic protons appeared as singlet at δ 4.11 for two protons attached to the carbon near thio group (C$H_{2/d}$), multiplet at δ 3.68-3.69 for two protons (NC$H_{2/h}$), multiplet at δ 2.56-2.59 for two protons (COC$H_{2/l}$) and multiplet at δ 1.69-1.72 for six protons (C$H_{2/i,j,k}$). The mass spectrum showed $(M)^+$ peak at 488.32 m/z and $(M+2)^+$ peak at 490.31 m/z.

The ^{1}H-NMR spectrum of compound (**237**) showed broad singlets at δ 10.51 and and δ 10.50 for two amine protons (N$H_{c,e}$). The aromatic protons appeared as multiplet at δ 7.68-7.70 for two protons (ArH_b), multiplet at δ 7.59-7.61 for three protons (Ar$H_{f,h}$), multiplet at δ 7.47-7.51 for one proton (ArH_j), multiplet at δ 7.34-7.39 for four protons (Ar$H_{a,g}$), multiplet at δ 6.45-6.47 for one proton (ArH_k) and multiplet at δ 6.28-6.31 for one proton (ArH_i). It also displayed a singlet at δ 4.15 for two aliphatic protons attached to the carbon near thio group (C$H_{2/d}$). Its ^{13}C-NMR spectrum showed peak at δ 165.74 and δ 164.66 due to C=O carbon of the amide. Aromatic carbons appeared at δ 161.14, 152.54, 140.37, 139.09, 138.98, 138.31, 135.98, 128.80, 127.08, 125.29, 120.33, 119.30, 118.81, and 105.39 whereas the aliphatic carbons appeared at δ 38.05. Its mass spectrum showed $(M)^+$ peak at 470.0 m/z and $(M+2)^+$ peak at 472.0 m/z.

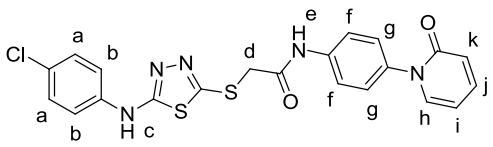

(237)

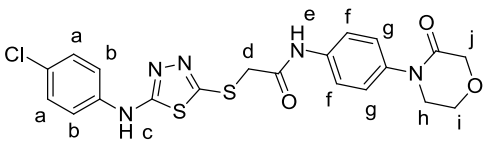

(238)

The ^{1}H-NMR spectrum of compound (**238**) showed two broad singlets at δ 10.53 and at δ 10.41 for two amine protons (N*H*$_{c,e}$). The aromatic protons appeared as doublet at δ 7.60 for two protons (Ar*H*$_{f}$), doublet at δ 7.59 for two protons (Ar*H*$_{b}$), doublet at δ 7.37 for two protons (Ar*H*$_{a}$) and doublet at δ 7.33 for two protons (Ar*H*$_{g}$). The aliphatic protons were obtained as singlet at δ 4.18 for two protons (C*H*$_{2/j}$) attached to the carbon near carbonyl group, singlet at δ 4.12 for two protons attached to carbon near thio group (C*H*$_{2/d}$), triplet at δ 3.95 for two protons (C*H*$_{2/h}$) and triplet at δ 3.69 for two protons (C*H*$_{2/i}$). Its ^{13}C-NMR spectrum showed peak at δ 166.44 and δ 166.11 due to C=O carbon of the amide. Aromatic carbons appeared at δ 165.24, 153.18, 139.67, 137.53, 137.39, 129.39, 126.43, 125.89, 119.95 and 119.40 whereas the aliphatic carbons appeared at δ 68.18, 63.94, 49.52 and 38.86. Its mass spectrum showed $(M)^{+}$ peak at 476.68 m/z and $(M+2)^{+}$ peak at 478.69 m/z.

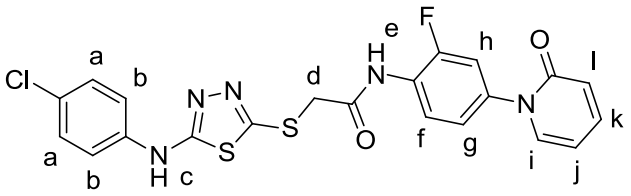

(239)

The ^{1}H-NMR spectrum of compound (**239**) showed two broad singlets at δ 10.49 and at δ 10.33 for two amine protons (N*H*$_{c,e}$). The aromatic protons were observed as multiplet at δ 8.04-8.08 for one proton (Ar*H*$_{i}$), multiplet at δ 7.60-7.67 for three protons (Ar*H*$_{f,g,h}$), multiplet at δ 7.50-7.54 for two protons (Ar*H*$_{b}$), multiplet at δ 7.38-7.41 for two protons (Ar*H*$_{a}$), multiplet at δ 7.24-7.26 for one protons (Ar*H*$_{k}$), multiplet at δ 6.48-6.51 for one proton (Ar*H*$_{l}$) and multiplet at δ 6.31-6.35 for one proton (Ar*H*$_{j}$). It also displayed a singlet at δ 4.15 for two protons attached to the carbon near thio group (C*H*$_{2/d}$). Its ^{13}C-NMR spectrum showed peak at δ 166.39 and δ 164.78 due to C=O

carbon of the amide. Aromatic carbons appeared at δ 160.97, 153.50, 152.49, 151.54, 140.61, 139.15, 138.77, 137.07, 136.98, 128.83, 125.70, 125.61, 125.32, 123.34, 122.80, 122.78, 120.42, 118.85,114.75, 114.57 and 105.58 whereas the aliphatic carbons appeared at δ 37.93. Its mass spectrum showed $(M)^+$ peak at 488.0 m/z and $(M+2)^+$ peak at 490.0 m/z.

4.2.2.7. Synthesis of 2-((5-(substituted phenyl or benzylamino)-1,3,4-thiadiazol-2-yl)thio)-*N*-(4-(2-oxopyridin-1(2*H*)-yl)phenyl)acetamides (240-253)

As per **Scheme 4.11**, 5-(substituted amino)-1,3,4-thiadiazole-2-thiols (**141-144, 146-155**) were reacted with 2-chloro-*N*-(4-(2-oxopyridin-1(2*H*)-yl)phenyl)acetamide (**224**) to get desired compounds (**240-253**). Analytical data of compounds (**240-253**) is shown in **Table 4.16**.

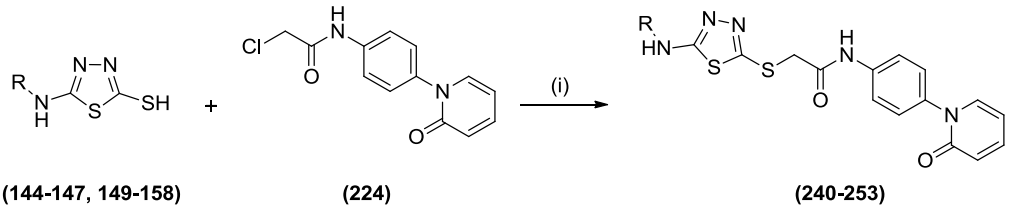

Scheme 4.11. Synthetic route for the preparation of compounds (**240-253**). Reagents and conditions: (i) Potassium carbonate, DMF, rt, 3-4 h.

Table 4.16. Analytical data of compounds (**240-253**)

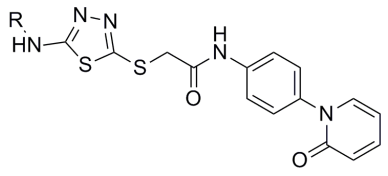

(240-253)

Comp	R	M.P.	IR characteristic peaks (cm^{-1})	HPLC Data
240	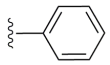	>250 °C	3315, 3061, 1660, 1532, 1411, 835	Purity: 99.1% t_R = 2.83 min
241	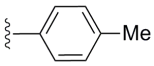	240-242 °C	3328, 3032, 2855, 1662, 1536, 1409, 833	Purity: 99.7% t_R = 3.04 min
242	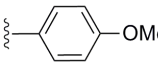	228-230 °C	3332, 2946, 1662, 1540, 1411, 830	Purity: 99.8 % t_R = 2.76 min
243	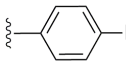	>250 °C	3321, 2944, 1661, 1538, 1411, 836	Purity: 99.5% t_R = 2.82 min

Comp	R	M.P.	IR characteristic peaks (cm^{-1})	HPLC Data
244	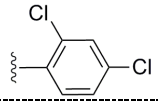	248-250 °C	3315, 3061, 1660, 1532, 1411, 835	Purity: 97.7% t_R = 3.67 min
245	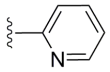	>250 °C	3189, 2769, 1665, 1531, 1412, 845	Purity: 99.0% t_R = 2.85 min
246	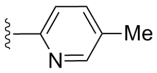	>250 °C	3258, 3041, 2829, 1680, 1654, 829	Purity: 99.4% t_R = 3.21 min
247	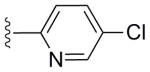	>250 °C	3263, 3069, 2923, 1662, 1537, 1413, 843	Purity: 96.8% t_R = 3.38 min
248	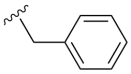	206-208 °C	3262, 3062, 1682, 1650, 1508, 850	Purity: 96.1% t_R = 2.59 min
249	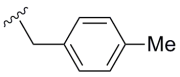	231-233 °C	3272, 3081, 2874, 1657, 1513, 836	Purity: 99.3% t_R = 2.30 min
250	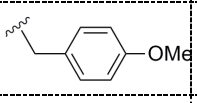	194-196 °C	3261, 3076, 2835, 1657, 1413, 1286, 1032, 835	Purity: 97.8% t_R = 2.71 min
251	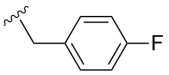	211-213 °C	3262, 3130, 3075, 1658, 1509, 1411, 833	Purity: 100% t_R = 2.72 min
252	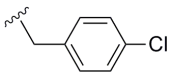	204-206 °C	3264, 3120, 2869, 1656, 1573, 839	Purity: 99.7%, t_R = 2.91 min
253	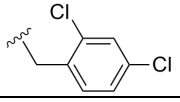	176-178 °C	3264, 3070, 1657, 1529, 1413, 833	Purity: 99.3% t_R = 3.25 min

The ^{1}H-NMR spectrum of compound (**240**) showed a broad singlet at δ 10.48 and another singlet at δ 10.36 for two NH protons (N$H_{d,f}$). The aromatic protons were observed as multiplet at δ 7.67-7.69 for two protons (ArH_c), multiplet at δ 7.58-7.60 for one proton (ArH_i), multiplet at δ 7.53-7.56 for two protons (ArH_g), multiplet at δ 7.46-7.50 for one proton (ArH_k), multiplet at δ 7.30-7.36 for four protons (Ar$H_{b,h}$), multiplet at δ 6.96-7.00 for one proton (ArH_a), doublet at δ 6.45 for one proton (ArH_l) and multiplet at δ 6.26-6.30 for one proton (ArH_j). It also displayed a singlet at δ 4.13 for two protons attached to the carbon near the thio group (C$H_{2/e}$). Its mass spectrum showed $(M)^+$ peak at 436.0 m/z.

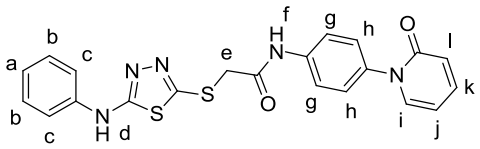

(240)

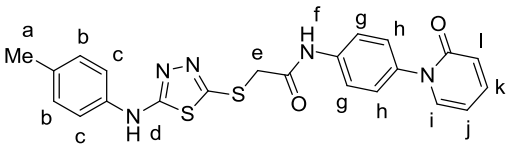

(241)

The ^{1}H-NMR spectrum of compound (**241**) showed two broad singlets at δ 10.52 and at δ 10.28 for two NH protons (N$H_{d,f}$). The aromatic protons were observed as multiplet at δ 7.70-7.72 for two protons (ArH_c), multiplet at δ 7.61-7.63 for one proton (ArH_i), multiplet at δ 7.44-7.51 for three protons (Ar$H_{g,k}$), multiplet at δ 7.36-7.38 for two protons (ArH_b), multiplet at δ 7.14-7.16 for two protons (ArH_h), multiplet at δ 6.47-6.49 for one proton (ArH_l) and multiplet at δ 6.29-6.33 for one proton (ArH_j). It also displayed a singlet at δ 4.14 for two aliphatic protons attached to the carbon near the thio group (C$H_{2/e}$) and another singlet at δ 2.26 for three methyl protons (C$H_{3/a}$). Its mass spectrum showed $(M)^+$ peak at 450.36 m/z.

The ^{1}H-NMR spectrum of compound (**242**) showed two broad singlets at δ 10.49 and at δ 10.19 for two NH protons (N$H_{d,f}$). The aromatic protons appeared as multiplet at δ 7.69-7.72 for two protons (ArH_c), multiplet at δ 7.61-7.63 for one proton (ArH_i), multiplet at δ 7.46-7.53 for three protons (Ar$H_{g,k}$), multiplet at δ 7.35-7.39 for two protons (ArH_h), multiplet at δ 6.91-6.95 for two protons (ArH_b), multiplet at δ 6.46-6.49 for one proton (ArH_l) and multiplet at δ 6.29-6.33 for one proton (ArH_j). It also displayed a singlet at δ 4.12 for two aliphatic protons attached to the carbon near the thio group (C$H_{2/e}$) and another singlet at δ 3.74 for three protons of methoxy group (OC$H_{3/a}$). The mass spectrum showed $(M)^+$ peak at 467.36 m/z.

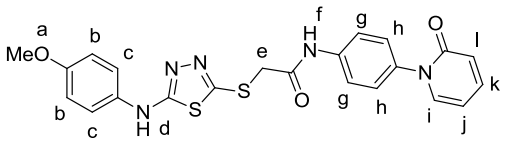

(242)

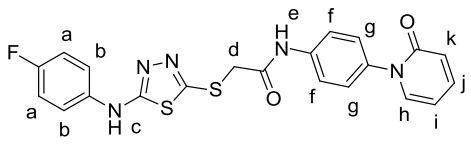

(243)

The ^{1}H-NMR spectrum of compound (**243**) showed broad a singlet at δ 10.51 and another singlet at δ 10.40 for two NH protons (N$H_{c,e}$). The

aromatic protons were observed as multiplet at δ 7.69-7.73 for two protons (ArH_b), multiplet at δ 7.57-7.69 for three protons (Ar$H_{f,h}$), multiplet at δ 7.49-7.53 for one proton (ArH_j), multiplet at δ 7.35-7.39 for two protons (ArH_g), multiplet at δ 7.15-7.22 for two protons (ArH_a), multiplet at δ 6.46-6.49 for one proton (ArH_k) and multiplet at δ 6.29-6.33 for one proton (ArH_i). It also displayed a singlet at δ 4.15 for two protons attached to the carbon near the thio group (C$H_{2/d}$). The mass spectrum showed $(M)^+$ peak at 454.32 m/z.

The ^{1}H-NMR spectrum of compound (**244**) showed a broad singlet at δ 10.51 and another singlet at δ 9.97 for two NH protons (N$H_{d,f}$). The aromatic protons appeared as multiplet at δ 8.34-8.37 for one proton (ArH_c), multiplet at δ 7.69-7.73 for two protons (ArH_g), multiplet at δ 7.63-7.65 for one proton (ArH_i), multiplet at δ 7.61-7.63 for one proton (ArH_b), multiplet at δ 7.48-7.53 for one proton (ArH_k), multiplet at δ 7.43-7.46 for one proton (ArH_a), multiplet at δ 7.36-7.39 for two protons (ArH_h), multiplet at δ 6.46-6.49 for one proton (ArH_l) and multiplet at δ 6.29-6.33 for one proton (ArH_j). It also displayed a singlet at δ 4.17 for two aliphatic protons attached to the carbon near the thio group (C$H_{2/e}$). Its mass spectrum showed $(M)^+$ peak at 504.29 m/z and $(M+2)^+$ peak at 506.26 m/z.

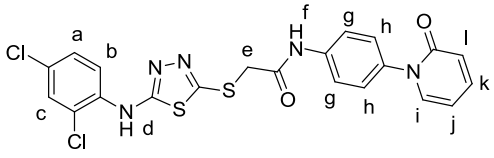

(244)

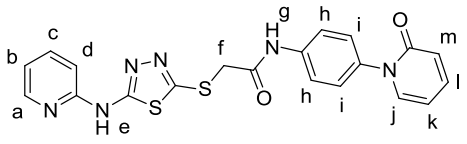

(245)

The ^{1}H-NMR spectrum of compound (**245**) showed a broad singlet at δ 11.75 and another singlet at δ 10.50 for two NH protons (N$H_{e,g}$). The aromatic protons appeared as multiplet at δ 8.27-8.29 for one proton (ArH_a), multiplet at δ 7.75-7.79 for one proton (ArH_c), multiplet at δ 7.68-7.72 for two protons (ArH_h), multiplet at δ 7.60-7.63 for one proton (ArH_j), multiplet at δ 7.48-7.5 for one proton (ArH_l), multiplet at δ 7.34-7.38 for two protons (ArH_i), multiplet at δ 7.07-7.10 for one proton (ArH_d), multiplet at δ 6.99-7.03 for one proton (ArH_b), multiplet at δ 6.46-6.49 for one proton (ArH_m) and multiplet at δ 6.29-6.33 for one proton (ArH_k). It also displayed a singlet at δ 4.18 for two

aliphatic protons attached to the carbon near the thio group (C*H*$_{2/f}$). Its mass spectrum showed $(M)^+$ peak at 437.0 m/z.

The ^{1}H-NMR spectrum of compound (**246**) showed a broad singlet at δ 11.63 and another singlet at δ 10.49 for two NH protons (N*H*$_{e,g}$). The aromatic protons appeared as multiplet at δ 8.10-8.11 for one proton (Ar*H*$_d$), multiplet at δ 7.67-7.71 for two protons (Ar*H*$_h$), multiplet at δ 7.60-7.63 for two protons (Ar*H*$_{b,j}$), multiplet at δ 7.48-7.53 for one proton (Ar*H*$_l$), multiplet at δ 7.34-7.38 for two protons (Ar*H*$_i$), multiplet at δ 6.99-7.02 for one proton (Ar*H*$_c$), multiplet at δ 6.46-6.49 for one proton (Ar*H*$_m$) and multiplet at δ 6.29-6.33 for one proton (Ar*H*$_k$). It also displayed a singlet at δ 4.16 for two aliphatic protons attached to the carbon near the thio group (C*H*$_{2/f}$) and another singlet at δ 2.24 for three methyl protons (C*H*$_{3/a}$). Its mass spectrum showed $(M)^+$ peak at 451.0 m/z.

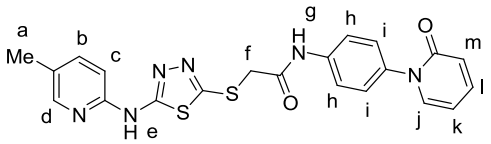

(246)

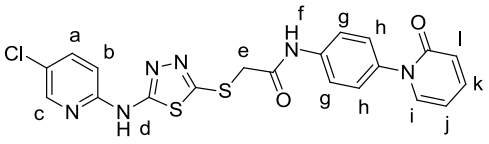

(247)

The ^{1}H-NMR spectrum of compound (**247**) showed a broad singlet at δ 11.92 and another singlet at δ 10.50 for two NH protons (N*H*$_{d,f}$). The aromatic protons appeared as multiplet at δ 8.32-8.33 for one proton (Ar*H*$_c$), multiplet at δ 7.86-7.89 for one proton (Ar*H*$_a$), multiplet at δ 7.67-7.71 for two protons (Ar*H*$_g$), multiplet at δ 7.60-7.62 for one proton (Ar*H*$_i$), multiplet at δ 7.48-7.52 for one proton (Ar*H*$_k$), multiplet at δ 7.34-7.38 for two protons (Ar*H*$_h$), multiplet at δ 7.10-7.13 for one proton (Ar*H*$_b$), multiplet at δ 6.46-6.49 for one proton (Ar*H*$_l$) and multiplet at δ 6.29-6.33 for one proton (Ar*H*$_j$). It also displayed a singlet at δ 4.18 for two aliphatic protons attached to the carbon near the thio group (C*H*$_{2/e}$). Its ^{13}C-NMR spectrum showed peak at δ 165.83 and δ 162.11 due to C=O carbon of the amide. Aromatic carbons appeared at δ 160.63, 154.77, 149.07, 144.47, 140.34, 138.96, 138.42, 138.28, 135.95, 127.03, 122.92, 120.33, 119.33, 112.42 and 105.37 whereas the

aliphatic carbon appeared at δ 38.50. Its mass spectrum showed $(M)^+$ peak at 471.0 m/z and $(M+2)^+$ peak at 473.0 m/z.

The ^{1}H-NMR spectrum of compound (**248**) showed a broad singlet at δ 10.48 for one proton attached to the amidic nitrogen (NH_g) and triplet at δ 8.27 for one amine proton (NH_e). The aromatic protons appeared as multiplet at δ 7.66-7.68 for two protons (ArH_h), multiplet at δ 7.60-7.62 for one proton (ArH_j), multiplet at δ 7.48-7.52 for one proton (ArH_l), multiplet at δ 7.34-7.38 for six protons (Ar$H_{b,c,i}$), multiplet at δ 7.26-7.28 for one proton (ArH_a), multiplet at δ 6.47-6.49 for one proton (ArH_m) and multiplet at δ 6.29-6.33 for one proton (ArH_k). Aliphatic protons were observed as doublet at δ 4.45 for two protons (NHC$H_{2/d}$) attached to the carbon near the amino group and singlet at δ 4.01 for two aliphatic protons attached to the carbon near the thio group (SC$H_{2/f}$). Its mass spectrum showed $(M)^+$ peak at 450.0 m/z.

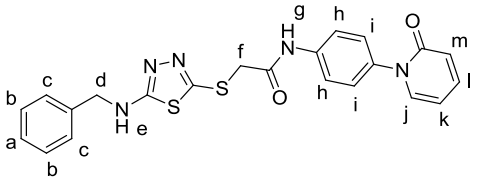

(248)

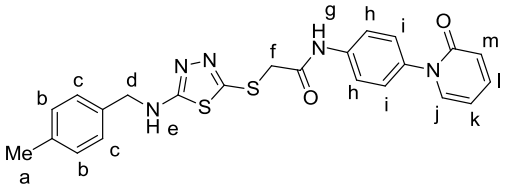

(249)

The ^{1}H-NMR spectrum of compound (**249**) showed a broad singlet at δ 10.44 for one proton attached to the amidic nitrogen (NH_g) and triplet at δ 8.27 for one amine proton (NH_e). The aromatic protons appeared as multiplet at δ 7.66-7.70 for two protons (ArH_h), multiplet at δ 7.61-7.63 for one proton (ArH_j), multiplet at δ 7.49-7.53 for one proton (ArH_l), multiplet at δ 7.34-7.38 for two protons (ArH_i), multiplet at δ 7.22-7.24 for two protons (ArH_c), multiplet at δ 7.14-7.16 for two protons (ArH_b), multiplet at δ 6.47-6.49 for one proton (ArH_m) and multiplet at δ 6.29-6.33 for one proton (ArH_k). Aliphatic protons were observed as doublet at δ 4.42 for two protons (NHC$H_{2/d}$) attached to the carbon near amino group, singlet at δ 4.03 for two aliphatic protons attached to the carbon near the thio group (SC$H_{2/f}$) and singlet at δ 2.29 for three methyl protons (C$H_{3/a}$). Its mass spectrum showed $(M)^+$ peak at 464.0 m/z.

The ^{1}H-NMR spectrum of compound (**250**) showed a broad singlet at δ 10.44 for one proton attached to the amidic nitrogen (NH_g) and triplet at δ 8.24 for one amine proton (NH_e). The aromatic protons appeared as multiplet at δ 7.68-7.71 for two protons (ArH_h), multiplet at δ 7.61-7.63 for one proton (ArH_j), multiplet at δ 7.49-7.53 for one proton (ArH_l), multiplet at δ 7.34-7.38 for two protons (ArH_i), multiplet at δ 7.26-7.30 for two protons (ArH_c), multiplet at δ 6.89-6.93 for two protons (ArH_b), multiplet at δ 6.47-6.49 for one proton (ArH_m) and multiplet at δ 6.29-6.33 for one proton (ArH_k). The aliphatic protons were observed as doublet at δ 4.39 for two protons (NHC$H_{2/d}$) attached to the carbon near amino group, singlet at δ 4.03 for two aliphatic protons attached to the carbon near the thio group (SC$H_{2/f}$) and singlet at δ 3.74 for three methoxy protons (OC$H_{3/a}$). Its mass spectrum showed $(M)^+$ peak at 480.0 m/z.

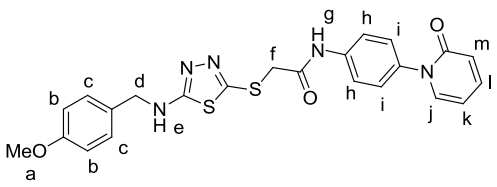

(250)

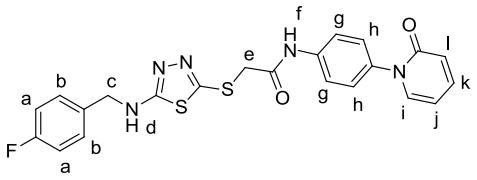

(251)

The ^{1}H-NMR spectrum of compound (**251**) showed a broad singlet at δ 10.44 for one proton attached to the amidic nitrogen (NH_f) and triplet at δ 8.31 for one amine proton (NH_d). The aromatic protons were observed as multiplet at δ 7.66-7.70 for two protons (ArH_g), multiplet at δ 7.61-7.63 for one proton (ArH_i), multiplet at δ 7.49-7.53 for one proton (ArH_k), multiplet at δ 7.34-7.41 for four protons (Ar$H_{b,h}$), multiplet at δ 7.15-7.20 for two protons (ArH_a), multiplet at δ 6.47-6.49 for one proton (ArH_l) and multiplet at δ 6.29-6.33 for one proton (ArH_j). The aliphatic protons were observed as doublet at δ 4.45 for two protons (NHC$H_{2/c}$) attached to carbon near amino group and singlet at δ 4.03 for two aliphatic protons attached to the carbon near the thio group (SC$H_{2/e}$). Its mass spectrum showed $(M)^+$ peak at 468.0 m/z.

The ^{1}H-NMR spectrum of compound (**252**) showed a broad singlet at δ 10.44 for one proton attached to the amidic nitrogen (NH_f) and triplet at δ 8.34 for one amine proton (NH_d). The aromatic protons appeared as multiplet at δ

7.66-7.70 for two protons (ArH_g), multiplet at δ 7.61-7.63 for one proton (ArH_i), multiplet at δ 7.49-7.53 for one proton (ArH_k), multiplet at δ 7.34-7.43 for six protons (Ar$H_{a,b,h}$), multiplet at δ 6.47-6.49 for one proton (ArH_l) and multiplet at δ 6.29-6.33 for one proton (ArH_j). The aliphatic protons were observed as doublet at δ 4.47 for two protons (NHC$H_{2/c}$) attached to carbon near amino group and singlet at δ 4.04 for two aliphatic protons attached to the carbon near the thio group (SC$H_{2/e}$). Its ^{13}C-NMR spectrum showed peak at δ 169.43 and δ 165.86 due to C=O carbon of the amide. Aromatic carbons appeared at δ 161.11, 149.48, 140.33, 138.95, 138.27, 137.43, 135.93, 131.53, 129.21, 128.17, 127.02, 120.31, 119.27 and 105.35 whereas the aliphatic carbons appeared at δ 46.87 and 38.50. Its mass spectrum showed $(M)^+$ peak at 484.0 m/z and $(M+2)^+$ peak at 486.0 m/z.

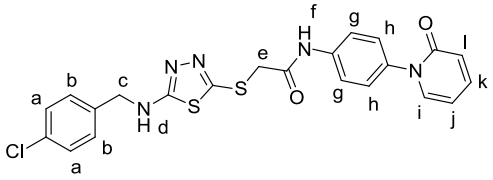

(252)

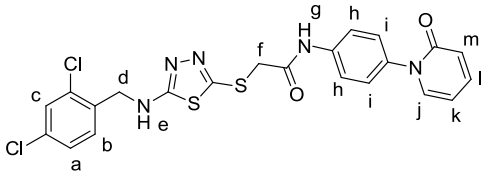

(253)

The ^{1}H-NMR spectrum of compound (**253**) showed a broad singlet at δ 10.48 for one proton attached to the amidic nitrogen (NH_g) and triplet at δ 8.38 for one amine proton (NH_e). The aromatic protons appeared as multiplet at δ 7.60-7.68 for four protons (Ar$H_{c,h,j}$), multiplet at δ 7.48-7.52 for one proton (ArH_l), multiplet at δ 7.41-7.43 for two protons (Ar$H_{a,b}$), multiplet at δ 7.33-7.35 for two protons (ArH_i), multiplet at δ 6.46-6.48 for one proton (ArH_m) and multiplet at δ 6.29-6.33 for one proton (ArH_k). The aliphatic protons appeared as doublet at δ 4.52 for two protons (NHC$H_{2/d}$) attached to carbon near amino group and singlet at δ 4.03 for two aliphatic protons attached to the carbon near thio group (SC$H_{2/f}$). Its mass spectrum showed $(M)^+$ peak at 518.0 m/z and $(M+2)^+$ peak at 520.0 m/z.

4.2.3. Biological evaluation

4.2.3.1. *In vitro* FXa inhibition assay

To check the antithrombotic potential of these 1,3,4-thiadiazole derivatives, all the synthesized compounds were screened against FXa at a concentration of 100 µM as per the previously reported procedure.[82] Those compounds with more than 50 % of the FXa inhibition were chosen for determination of their IC_{50} values. Simple benzyl substituted compounds (**159-165**) and amioalkyl derivatives (**178-186**) showed <50 % inhibition of the enzyme at a concentration of 100 µM (**Table 4.17** and **4.18**). Compound (**165**) having substituted biphenyl group as the P4 motif showed higher FXa inhibitory activity (IC_{50} = 9.55 µM) amongst the benzyl substituted compounds.

Table 4.17. IC_{50} values, nPT and naPTT time of compounds (**159-165**)

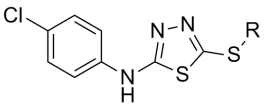

(159-165)

Comp	R	FXa IC_{50} ± SEM (µM)	nPT[a]	naPTT[a]
159	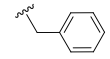	> 100	1.16	1.08
160	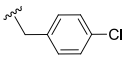	> 100	0.95	1.23
161	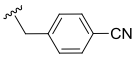	> 100	1.24	1.08
162	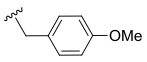	> 100	1.07	1.09
163	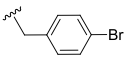	> 100	1.10	1.49
164	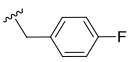	> 100	1.21	1.53
165	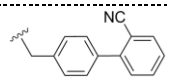	9.55 ± 1.3	1.64	1.44

[a]nPT = PT tested/ PT vehicle and naPTT = aPTT tested/aPTT vehicle at 1 mM concentration.

4.2.3.2. *In vitro* anticoagulant activity

All the target compounds were evaluated for their *in vitro* anticoagulant activity by using human plasma. PT measures the effect of a compound on the extrinsic pathway of coagulation, whereas aPTT represents the effect on the intrinsic pathway. Initially, all the synthesized compounds were screened at a concentration of 1 mM. The results were expressed as prothrombin time (nPT) and activated partial thromboplastin time (naPTT) in **Table 4.17-4.20**.

Table 4.18. IC_{50} values, nPT and naPTT time of compounds (**178-186**)

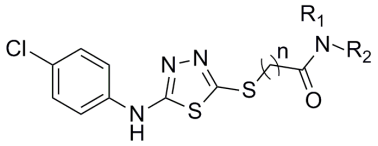

(178-186)

Comp	n	NR_1R_2	FXa IC_{50} ± SEM (µM)	nPT[a]	naPTT[a]
178	1		> 100	1.17	1.25
179	1	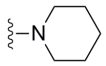	> 100	1.19	1.30
180	1	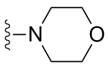	> 100	1.57	1.15
181	2		> 100	1.53	2.18
182	2	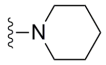	> 100	1.72	1.80
183	2	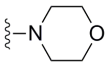	> 100	2.06	1.77
184	3		> 100	2.03	4.45
185	3	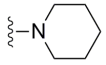	> 100	1.43	2.18
186	3	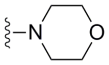	> 100	2.04	1.76

[a]nPT = PT tested/ PT vehicle and naPTT = aPTT tested/aPTT vehicle at 1 mM concentration.

Compounds (**227-229**) having 4-cholroaniline (**227**), 4-fluoroaniline (**228**) and 4-methoxyaniline (**229**) showed poor FXa inhibitory activity (IC_{50} >

100 µM). These substituents at *para* position of aniline were replaced by different heterocycles like pyrrolidine, piperidine, morpholine and *N*-methylpiperazine to get compounds (**230-233**). These compounds (**230-233**) offered good FXa inhibitory activity with IC_{50} values of 16.5 µM, 18.8 µM, 6.5 µM and 4.9 µM, respectively (**Table 4.19**).

Table 4.19. IC_{50} values, nPT and naPTT time of compounds (**227-239**)

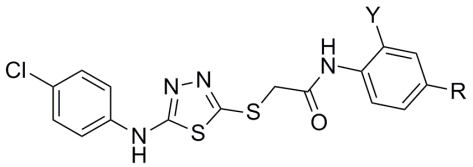

(227-239)

Comp	Y	R	FXa IC_{50} ± SEM (µM)	nPT[a]	naPTT[a]
227	H		> 100	1.18	1.23
228	H		> 100	0.92	1.35
229	H		> 100	1.43	1.34
230	H		16.5 ± 2.7	1.49	1.61
231	H	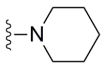	18.8 ± 1.8	1.43	1.52
232	H	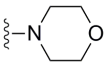	6.5 ± 1.1	1.96	2.06
233	H	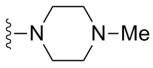	4.98 ± 1.0	1.30	1.66
234	H	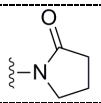	2.05 ± 0.8	2.75	2.36
235	H	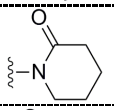	0.79 ± 0.13	2.96	3.00
236	H	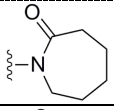	2.56 ± 1.3	2.03	2.18
237	H	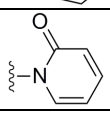	**0.22 ± 0.08**	**5.87**	**4.45**

Comp	Y	R	FXa IC_{50} ± SEM (µM)	nPT[a]	naPTT[a]
238	H	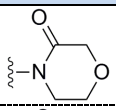	**0.35 ± 0.12**	**6.63**	**6.33**
239	F	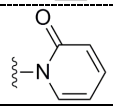	0.47 ± 0.13	3.61	3.08

[a]nPT = PT tested/ PT vehicle and naPTT = aPTT tested/aPTT vehicle at 1 mM concentration.

Replacement of simple pyrrolidine ring in compound (**230**, IC_{50} = 16.5 µM) with pyrrolidinone ring resulted in compound (**234**, IC_{50} = 2.05 µM) with much improved FXa inhibitory activity. Exchanging the pyrrolidinone to piperidinone and morpholinone resulted into compounds (**235**, IC_{50} = 0.79 µM) and (**238**, IC_{50} = 0.35 µM) enhancing the FXa inhibitory activity. Further replacement of piperidinone ring in compound (**235**) with caprolactam in compound (**236**) resulted in some loss of potency (IC_{50} = 2.56 µM). Aromatization of piperidinone ring in compound (**235**) resulted into the most potent compound (**237**) of the series. Compound (**237**, IC_{50} = 0.22 µM) showed even better FXa inhibitory activity than apixaban (IC_{50} = 0.32 µM). Incorporation of fluorine atom at ortho position of phenylpyridinone ring in compound (**237**) resulted into the compound (**239**) which exhibited 2-fold loss of FXa inhibitory activity.

Further modifications were carried out to explore favorable P1 motifs with pyridinone as the optimal P4 substituent, but all attempts proved unsuccessful (**Table 4.20**). Removal and replacement of chlorine atom of *p*-chlorophenyl group in compound (**237**) with methyl, methoxy and fluoro groups offered compounds (**240-243**) which exhibited significant loss of FXa inhibitory activity. Compound (**244**) containing additional chlorine atom at ortho position of *p*-chlorophenyl group showed a significant loss of activity (**244** vs **237**). 5-Chloro-2-pyridyl group as the P1 motif was expected to show better activity. But, the compound (**247**, IC_{50} = 4.6 µM) having 5-chloro-2-pyridyl group exhibited lesser potency than compound (**237**). To gauge the distance between Cl and Tyr228, compounds (**248-253**) with substituted benzyl groups as P1 moeities were synthesized. None of the compounds (**248-**

253) from this series showed any improvement in the activity over compound (**237**).

Table 4.20. IC_{50} values, nPT and naPTT time of compounds (**240-253**)

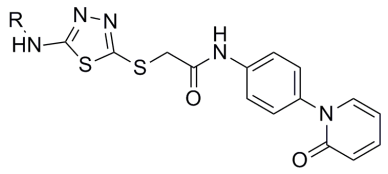

(240-253)

Comp	R	FXa IC_{50} ± SEM (µM)	nPT[a]	naPTT[a]
240	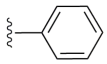	57 ± 4.8	1.54	2.12
241	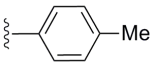	3.11 ± 1.6	1.43	1.52
242	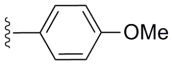	71.96 ± 4.1	1.24	1.34
243	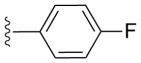	10.43 ± 1.2	2.08	2.29
244	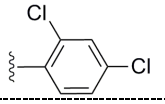	16.53 ± 2.1	1.51	1.62
245	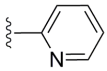	28.14 ± 3.8	1.78	1.89
246	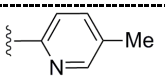	20.72 ± 2.9	1.91	1.66
247	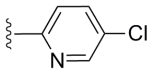	1.72 ± 1.0	2.29	2.82
248	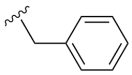	> 100	1.26	1.30
249	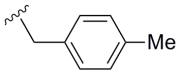	23.92 ± 3.1	1.31	1.62
250	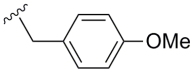	15.70 ± 2.1	1.58	1.69
251	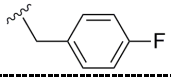	22.64 ± 3.6	2.03	1.78
252	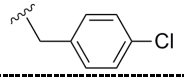	27.12 ± 2.4	1.53	1.39
253	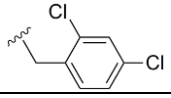	25.60 ± 2.1	1.41	1.36

[a]nPT = PT tested/ PT vehicle and naPTT = aPTT tested/aPTT vehicle at 1 mM concentration.

Compounds (**235**, **237-239**) exhibiting potent FXa inhibitory activity were selected for further assessment of their anticoagulant activity by determining the concentration of the compound required to double the clotting time (2 x PT and 2 x aPTT) in the PT and aPTT assay (**Figure 4.13**). All the four compounds showed lower anticoagulant activity than apixaban (2 x PT = 7.07 uM and 2 x aPTT = 9.21 uM) (**Table 4.21**) in these tests.

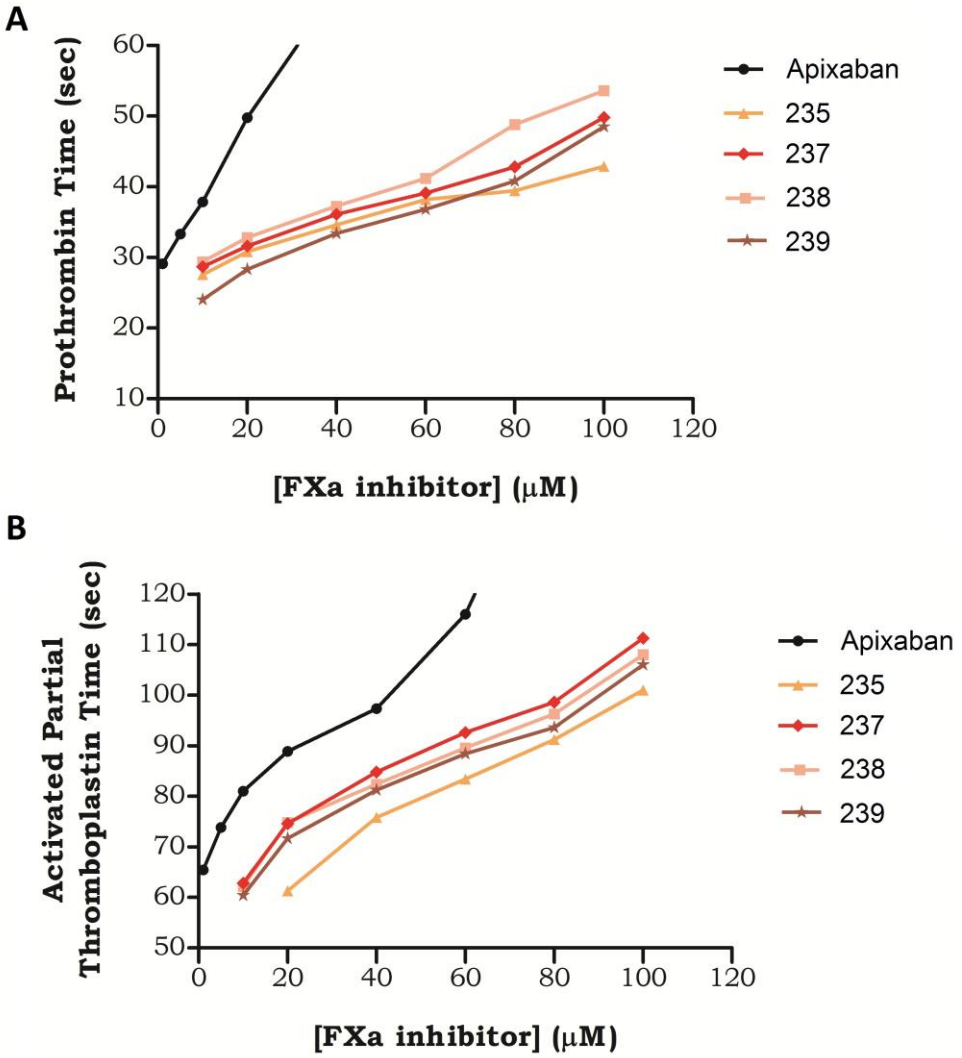

Figure 4.13. Prolongation of clotting time as a function of concentration of compounds (**235, 237-239**) in prothrombin time assay (PT) (A) or activated partial thromboplastin time assay (aPTT) (B).

Table 4.21. Anticoagulant activity of compounds (**235, 237-239**) in terms of 2 × PT and 2 × aPTT parameters

Comp	2 × PT (µM)	2 × aPTT (µM)
235	31.9	49.00
237	25.9	27.44
238	21.19	29.80
239	40.0	34.25
Apixaban	7.07	9.21

4.2.3.3. *In vivo* $FeCl_3$ induced arterial thrombosis

Based on *in vitro* FXa inhibitory activity and anticoagulant activity of compound (**237**), it was selected for *in vivo* evaluation of antithrombotic potential by $FeCl_3$ induced arterial thrombosis model in rats. The reduction in thrombus weight was considered as a preventive measure for *in vivo* efficacy of a compound. As shown in **Figure 4.14**, compound (**237**) displayed good *in vivo* antithrombotic activity in $FeCl_3$ induced arterial thrombosis model in dose-dependent manner. Compound (**237**) exhibited 49 % and 32 % inhibition of thrombus formation at 30 mg/kg and 15 mg/kg in rats. In the case of standard drug (apixaban) at dose of 30 mg/kg and 15 mg/kg, % inhibition of thrombus formation was found to be 57.25 % and 35.5 % respectively.

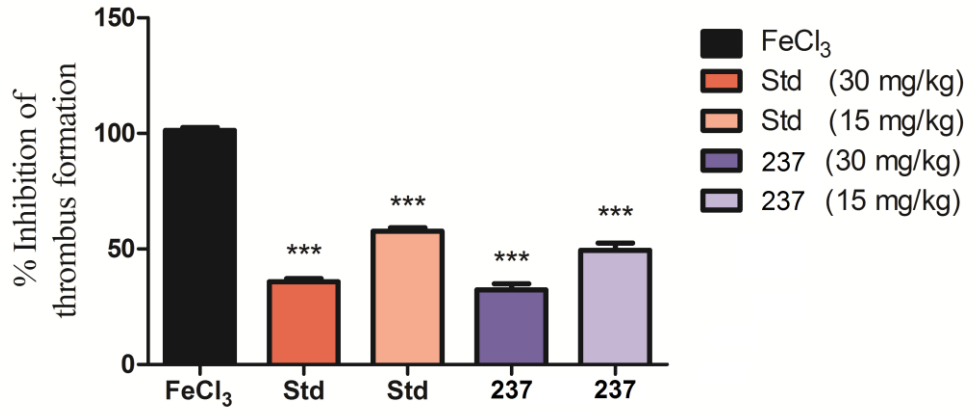

Figure 4.14. Effect of (**237**) and apixaban (15 and 30 mg/kg) on thrombus weight ($FeCl_3$ induced arterial thrombosis model). Statistical analysis was performed by One way ANOVA using Graph-pad prism 5.0 $^{*}p < 0.01$ vs. vehicle control. (n=3)

4.2.4. Molecular modeling studies

4.2.4.1. Docking studies of compound (237)

Docking studies were performed with FXa in order to assess molecular interactions of the synthesized compounds. The most active compound (**237**) offered the highest docking score which indicated its high affinity with the enzyme. The molecular interactions of the compound (**237**) are shown in **Figure 4.15**.

The *p*-chlorophenyl group occupied the S1 binding site with promising hydrophobic interactions. Also the chloro was observed in establishing non-covalent interactions with Tyr228. Further –NH- of acetamide and one of the =N- of thiadiazole ring of **237** interacted with Gly216 by forming hydrogen bonds that imparted stability to the ligand receptor complex. The phenylpyridinone system was observed to occupy S4 binding site, wherein the pyridinone ring of phenylpyridinone formed strong π-π interactions with Phe174 and Trp215.

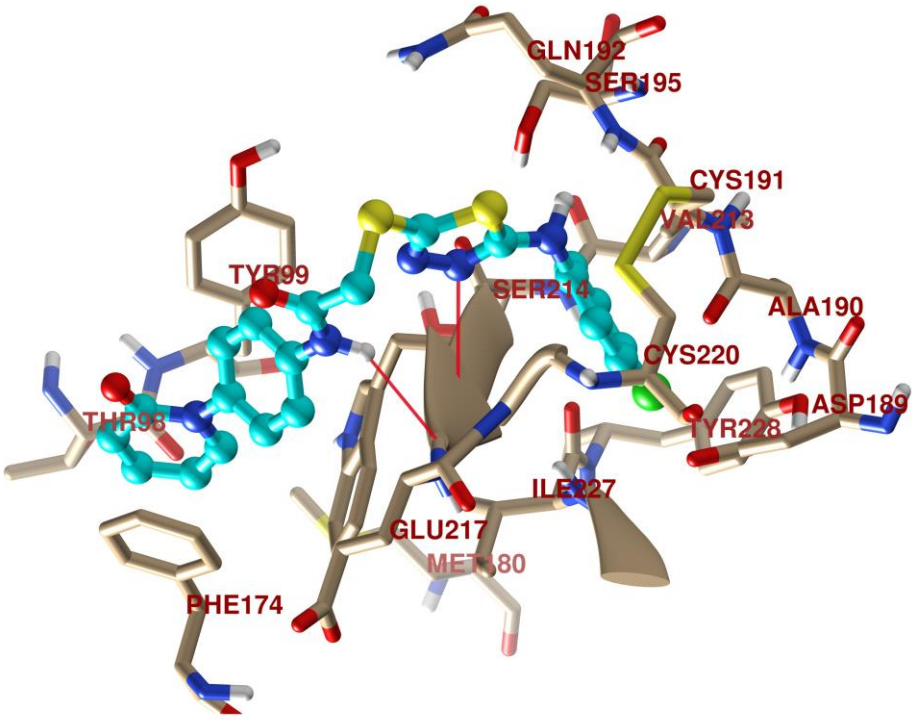

Figure 4.15. Docking pose of compound (**237**) within the active site of FXa.

4.2.4.2. Molecular dynamics simulations

Compound (**237**) exhibited promising binding affinity with the active site of the FXa receptor. Thus to verify and authenticate this interactive stability of the complex of active compound (**237**) and FXa over the period of time, molecular dynamics experiment was performed. The dynamic stability of **237** within the active site of the FXa receptor was evaluated over a period of 10 ns duration. After 10 ns period, the post dynamic analyses were carried out in order to recognize the stability of the ligand receptor complex. In order to evaluate the interactive binding stability of the ligand receptor complex over this period of time, RMSD-P, RMSF-P and RMSD-L (P = Protein; L = Ligand) were examined to support and validate the docking results. Considering the initial pose of ligand-receptor complex obtained from docking study as the reference frame, all these properties were calculated. RMSD-P explains the large scale movements in the protein when the ligand is present in the active site of the receptor and explains the protein structural conformation over the period of simulation time. Here the RMSD-P for FXa-(**237**) complex was found in the acceptable range with values from 0.7 to 2.2 Å with the average RMSD value of 1.55 Å (**Figure 4.16-A**). This assessment explained the stability of the protein backbone all through the simulation run and suggested that the existence of compound (**237**) in the receptor active site has not influenced the backbone stability. In order to determine how stable **237** is with respect to the protein and its active binding site, the Ligand fit on protein RMSD was computed. The Lig fit on Prot RMSD-L for the ligand was observed in the range of 0.6 to 2.2 Å with an average RMSD value of 1.4 Å (**Figure 4.16-B**). Despite having many rotatable bonds in the ligand structure the average RMSD value of ligand is significantly less than the RMSD-P, this suggested that the ligand is stable inside the active binding pocket and did not diffuse away from the active binding site of the receptor during the entire simulation run. Further, to understand the internal fluctuations of the ligand the Lig fit on Lig RMSD was calculated. It was observed in the acceptable range of 0.5 to 1.3 Å without any major deviation during the simulation time (**Figure 4.16-C**).

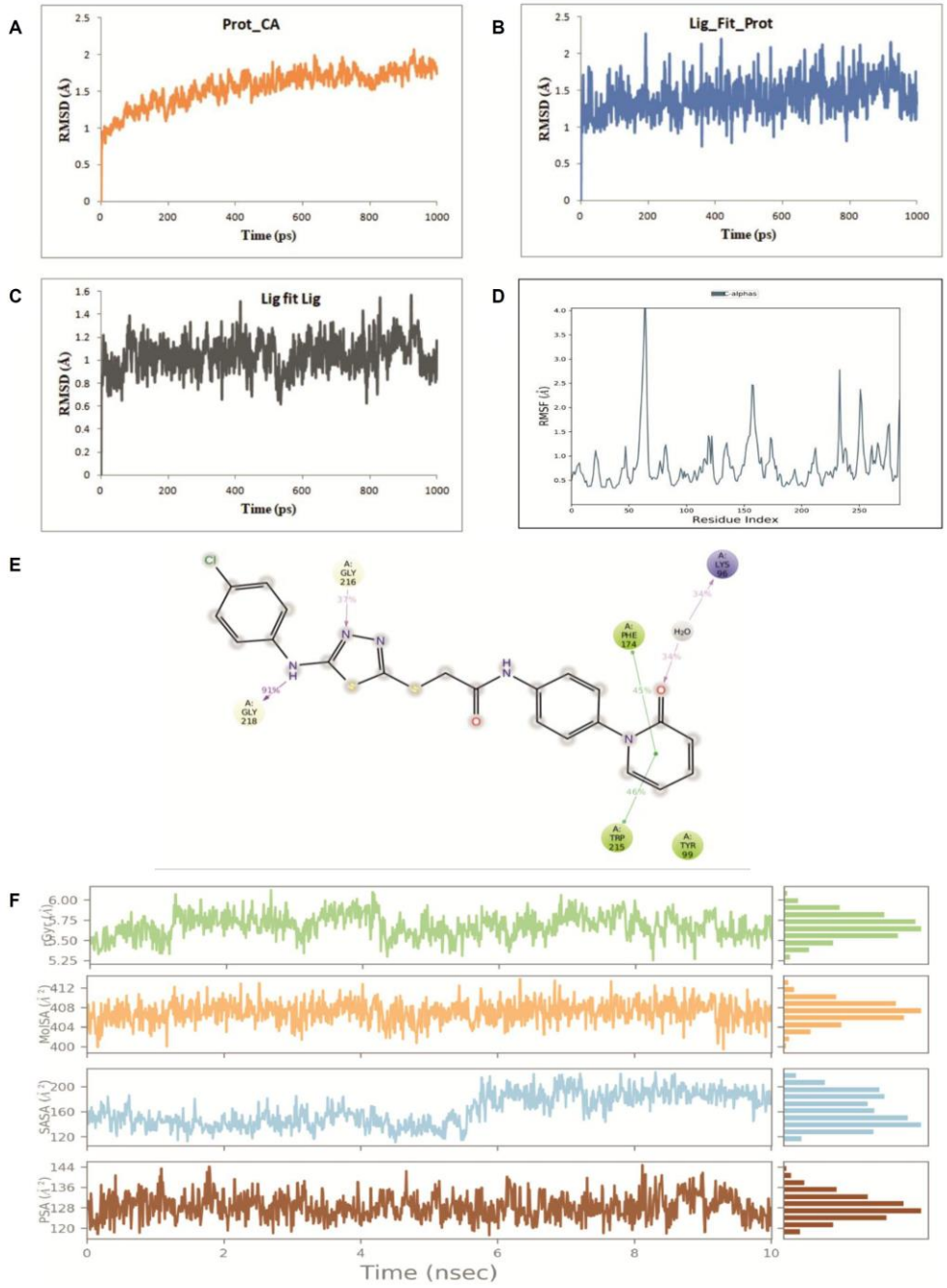

Figure 4.16. (**A**) RMSD-P for FXa with **237**; (**B**) RMSD-L for **237** with FXa; (**C**) Ligand (**237**) RMSD; (**D**) RMSF-P for FXa with **237**; (**E**) Ligand and receptor residue contact diagram for FXa with **237**; (**F**) rGyr, MolSA, SASA, and PSA for **237** for FXa.

Structural integrity of the receptor and the ligand residual mobility were quantitatively identified in terms of RMSF-P (**Figure 4.16-D**). Including the loop and terminal residues of receptor structure in complex with 16L in active site, the RMSF-P was below 4 Å. In addition to these studies, the

stability of the ligand receptor interactions over a period of time was also evaluated. In the molecular docking studies, the NH of acetamide and N of the thiadiazole ring of the most active ligand (**237**) forms a H-bond with Gly216. Whereas no such hydrogen bond interaction was observed between –NH- of chlorophenylamino group and Gly218 in the docking study. In the simulation study, it was observed that over a period of time, the hydrogen bond between the nitrogen of the thiadiazole and Gly216 was maintained stable over 37% of simulation time. Whereas, the hydrogen bond between NH of acetamide and Gly216 was not so promising over this period of time. The –NH- of chlorophenylamino part of the ligand exhibited very strong hydrogen bond with Gly218 in the simulation study. This was maintained stable over 91% of the simulation time. All the H-bonds observed in simulation study were having distances within 2.5 Å, and donor angle of ≥120° and acceptor angle of ≥ 90°. Further, the MD study explained the stability of π-π interactions of oxopyridine ring of the ligand with Phe174 and Trp215 of S4 binding pocket of receptor active site. These π-π stacking interactions were observed to be 45% and 46% stable over the simulation time with Phe174 and Trp215 respectively (**Figure 4.17-E**). The other ligand parameters like rGyr, MolSA, SASA and PSA were found to be in the acceptable range (**Figure 4.17-F**).

4.3. Carbazole derivatives as FXa inhibitors

Design, synthesis and biological evaluation of the carbazole derivatives have been described under the following headings:

4.3.1. Designing of carbazole derivatives as FXa inhibitors

4.3.2. Synthesis of carbazole derivatives

4.3.3. Biological evaluation

4.3.1. Designing of carbazole derivatives as FXa inhibitors

Various nitrogen-containing heterocycles, especially alkaloids, have been recognized as promising candidates in our quest for new drug leads for the treatment of thrombosis. Some indole alkaloids like *β*-carboline, tetrahydro-*β*-carboline and carbazoles were reported to possess a wide spectrum of pharmacological actions. Harmalol, harmaline, norharmane,

harmol, harmine and harmane belonging to *β*-carboline, were capable of inhibiting the platelet aggregation induced by collagen.[118] Various research group utilized *β*-carboline and carbazole for the development of antiplatelet and anticoagulant agents. Compound (**254**) was reported to exhibit good inhibition with the IC_{50} values of 20.8 ± 2.1, 2.0 ± 0.2 and 0.3 ± 0.01 for ADP, PAF and AA induced platelet aggregation respectively.[119]

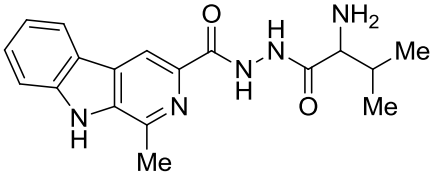

(254)

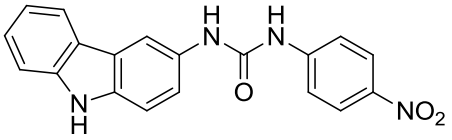

(255)

Based on the antiplatelet activity of murrayafoline A (1-methoxy-3-methyl-9*H*-carbazole), Kim et al. synthesized novel 3-*N*-substituted carbazole derivatives to check their inhibitory action on platelet aggregation. Compound (**255**), with a urea linkage to the carbazole framework, exhibited the strongest inhibitory activity (98.25% at 30 μM).[120]

A series of several indole and carbazole based FXa inhibitor has been identified by Arnaiz et al. Indole ring containing compound (**256**) was found as the most potent FXa inhibitor with a K_i value of 0.2 nM. Compound (**257**), having carbazole scaffold also showed good inhibition against FXa having K_i value of 0.9 nM.[121]

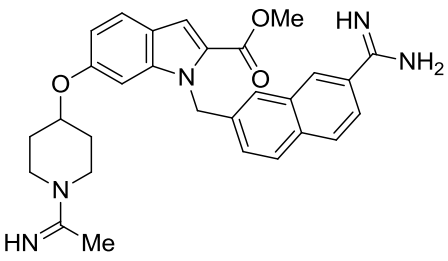

(256)

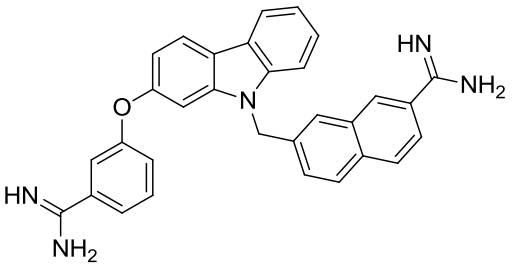

(257)

Certain dibenzofuran derivatives were reported to have a great variety of pharmacological effects, including inhibition of the clotting activity of thrombin[122] and inhibition of serotonin (5-hydroxytryptamine; 5HT)-induced bradycardia in rats.[123] Based on these findings, Wang et al. identified

dibenzofuran and carbazole derivatives possessing antiplatelet activity. Among the series, compound (**258**) and compound (**259**) exhibited potent inhibitory activities against platelet aggregation induced by arachidonic acid, with IC_{50} values of 14.87 µM and 14.60 µM, respectively.[124]

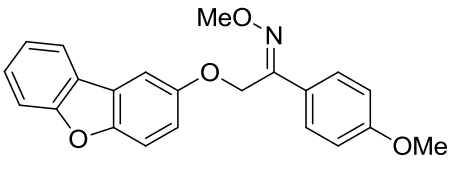

(258)

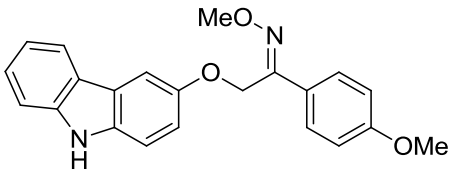

(259)

For reducing the side effects and increasing the potency, one of the strategies used in drug designing is to design a compound with multitarget activity. Combining anticoagulant and antiplatelet activities of drugs would have an additive effect by suppressing both blood coagulation and platelet function, thus making the drug more effective than the treatment directed against thrombin/FXa or against platelets alone.

Thus, antiplatelet and anticoagulant activities of carbazole derivatives suggested carbazole ring as an important privileged scaffold for the development of multitarget directed antithrombotic agents.

To develop orally active antithrombotic agents, it was contemplated to introduce monoaryls or biaryls as S4 binding ligands in the carbazole scaffold, and the chloroaromatic group as the S1 binding ligand as represented in **Figure 4.17**.

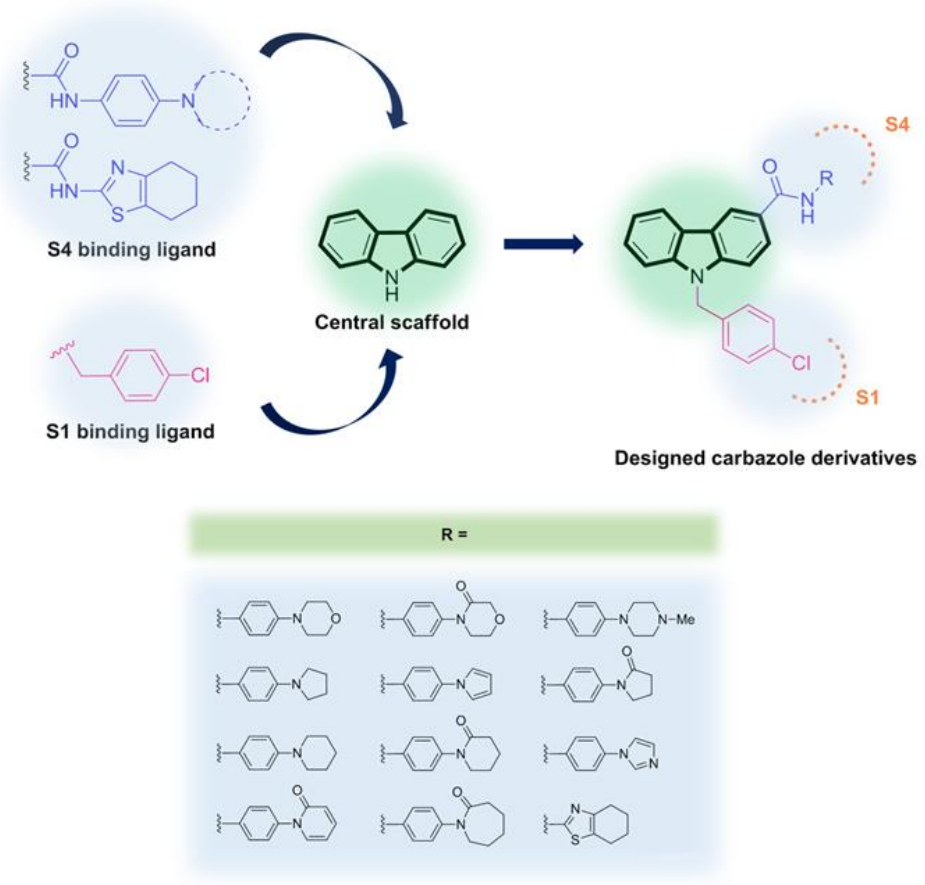

Figure 4.17. Designing of novel carbazole derivatives as FXa inhibitors.

4.3.2. Synthesis of carbazole derivatives

4.3.2.1. Synthesis of 9-(4-chlorobenzyl)-9*H*-carbazole-3-carboxylic acid (263)

The desired key intermediate (**263**) was synthesized from commercially available carbazole (**260**) in three steps (**Scheme 4.12**). In the first step, carbazole was reacted with 4-chlorobenzylchloride in the presence of aqueous NaOH using DMSO as a solvent to give 9-(4-chlorobenzyl)-9*H*-carbazole (**261**)**.** Formylation of the compound (**261**) was carried out with the help of phosphorus oxychloride and dimethylformamide to offer the mono-formylated product 9-(4-chlorobenzyl)-9*H*-carbazole-3-carbaldehyde (**262**). Compound (**262**) was oxidized with the help of *tert*-butyl hydroperoxide (TBHP) in which DMSO used as solvent to get 9-(4-chlorobenzyl)-9*H*-carbazole-3-carboxylic acid (**263**).

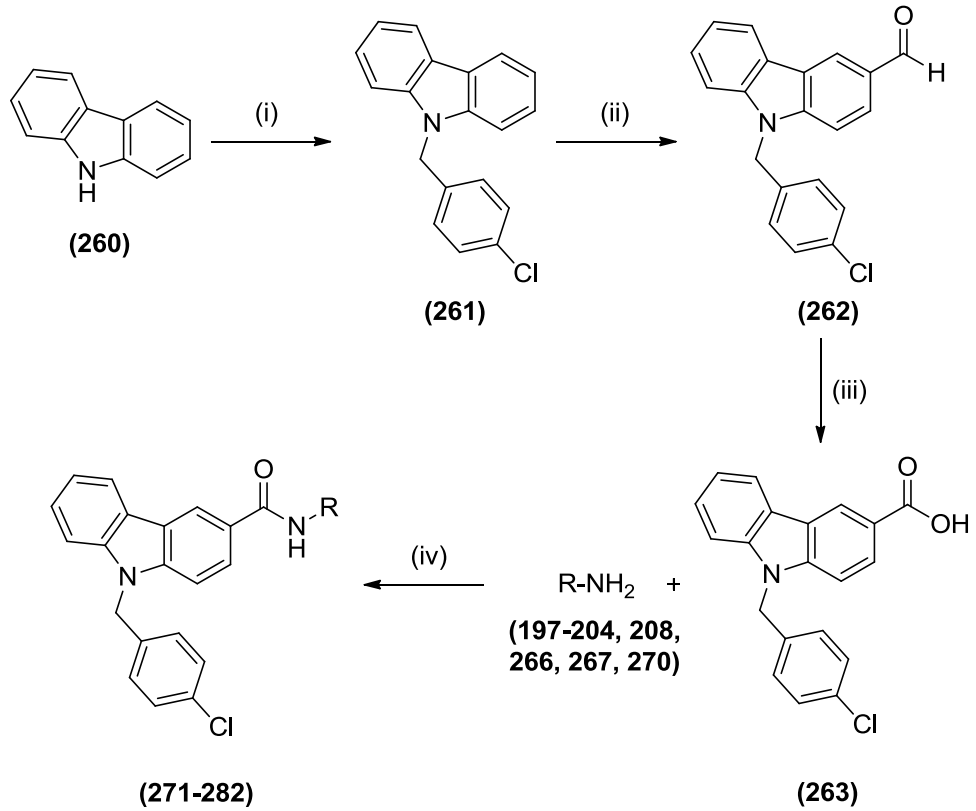

Scheme 4.12. Synthetic route for the preparation of compounds (**271-282**). Reagents and conditions: (i) 4-Chlorobenzylchloride, NaOH, DMSO, 2-3 h, rt; (ii) DMF, $POCl_3$, $CHCl_3$, reflux 12-15 h; (iii) TBHP, DMSO, stirred overnight at 110 °C; (iv) Anhydrous HOBt, EDCI, DMAP, DMF, overnight, rt.

The IR spectrum of 9-(4-chlorobenzyl)-9*H*-carbazole (**261**) showed peaks (cm^{-1}) at 3049 (aromatic C-H stretch), 2935 (aliphatic C-H stretch) and 1594 (C=C stretch). The -NH stretching vibration peak of carbazole disappeared in *N*-substituted carbazole. Its ^{1}H-NMR spectrum showed doublet at δ 8.20 for two protons (ArH_a), doublet at δ 7.65 for two protons (ArH_e), triplet at δ 7.45 for two proton (ArH_b), doublet at δ 7.35 for two protons (ArH_d), triplet at δ 7.23 for two protons (ArH_c) and doublet at δ 7.19 for two protons (ArH_f) confirming total twelve aromatic protons in structure. Singlet at δ 5.68 also appeared for two methylene protons (NC$H_{2/g}$). The mass spectrum showed $(M)^+$ peak at 292.0 m/z and $(M+2)^+$ peak at 294.1 m/z.

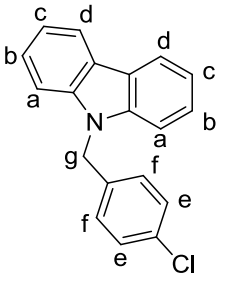

(261)

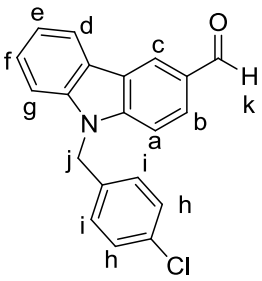

(262)

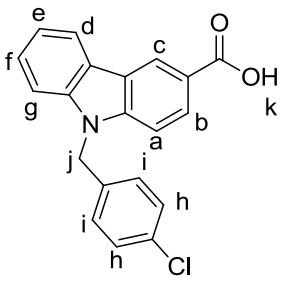

(263)

The IR spectrum of 9-(4-chlorobenzyl)-9*H*-carbazole-3-carbaldehyde (**262**) showed peaks (cm^{-1}) at 3055 (aromatic C-H stretch), 2924 (aliphatic C-H stretch) and 1703 (C=O stretch). Its ^{1}H-NMR spectrum showed a singlet at δ 10.07 for aldehyde proton (CH_kO). The aromatic protons appeared as singlet at δ 8.80 for one proton (ArH_c), doublet at δ 8.32 for one proton (ArH_g), doublet at δ 7.98 for one proton (ArH_b), doublet at δ 7.82 for one proton (ArH_a), doublet at δ 7.70 for one proton (ArH_d), triplet at δ 7.50 for one proton (ArH_f), multiplet at δ 7.28-7.32 for three protons (Ar$H_{e,h}$) and doublet at δ 7.18 for two protons (ArH_i). Aliphatic protons were observed as singlet at δ 5.76 for two methylene protons (NC$H_{2/j}$). Its mass spectrum showed $(M)^+$ peak at 320.22 m/z and $(M+2)^+$ peak at 322.23 m/z.

The IR spectrum of 9-(4-chlorobenzyl)-9*H*-carbazole-3-carboxylic acid (**263**) showed peaks (cm^{-1}) at 3400 (OH stretch), 3053 (aromatic C-H stretch, 2833 (aliphatic C-H stretch) and 1682 (C=O stretch). Its ^{1}H-NMR spectrum showed a singlet at δ 12.69 for one proton of carboxylic acid group (COOH_k). The aromatic protons appeared as singlet at δ 8.83 for one proton (ArH_c), doublet at δ 8.33 for one proton (ArH_g), doublet at δ 8.06 for one proton (ArH_b), multiplet at δ 7.69-7.73 for two protons (Ar$H_{a,d}$), triplet at δ 7.51 for one proton (ArH_f), doublet at δ 7.35 for two protons (ArH_h), triplet at δ 7.28 for one proton (ArH_e) and doublet at δ 7.19 for two protons (ArH_i). Singlet at δ 5.76 appeared for two methylene protons (NC$H_{2/j}$). The mass spectrum showed $(M-1)^+$ peak at 334.19 m/z.

4.3.2.2. Synthesis of necessary aromatic amines (194-201, 205, 266, 267, 270)

Different aromatic amines required for the synthesis of targeted carbazole derivatives were synthesized as per the reported procedure. The synthetic routes for the preparation of compounds (**194-201** and **205**) were depicted in **Scheme 4.9**. In a similar manner, 4-(1*H*-pyrrol-1-yl)benzenamine **(266)** and 4-(1*H*-imidazol-1-yl)benzenamine **(267)** were also prepared from commercially available 4-fluoro-1-nitrobenzene (**187**) using pyrrole and imidazole respectively (**Scheme 4.13**). Another aromatic amine (**270**) was prepared in microwave irradiation condition at 195 W for 10 min in presence of iodine (**Scheme 4.14**). All these intermediates were characterized by their physical data and IR spectroscopy.

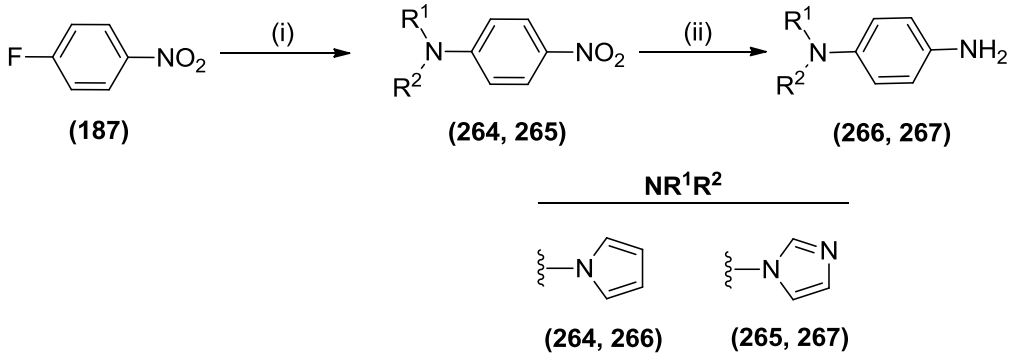

Scheme 4.13. Synthetic routes for the preparation of compounds **(266** and **267)**. Reagents and conditions: (i) Pyrrole/imidazole, potassium carbonate, DMF, 110 °C, 12-15 h; (ii) Pd/C, ethanol, hydrazine hydrate, reflux 2-3 h.

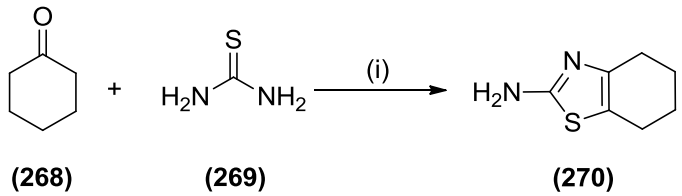

Scheme 4.14. Synthetic route for preparation of 4,5,6,7-tetrahydrobenzo[*d*]thiazol-2-amine (**270**). Reagents and conditions: (i) Iodine, methanol, 195 W for 10 min in M.W.

4.3.2.3. Synthesis of 9-(4-chlorobenzyl)-*N*-substituted-9*H*-carbazole-3-carboxamides (271-282)

As per the **Scheme 4.12**, the intermediate (**263**) was reacted with different amines (**194-201, 205, 266, 267** and **270**) to obtain the desired

carbazole derivatives (**271-282**). IR spectra of all the synthesized compounds showed one peak at 3275-3330 cm^{-1} for –NH stretching and another one around 1650 for C=O stretching of the amide group. Melting points, IR spectral data and purity data are given in **Table 4.22**.

Table 4.22. Analytical data of compounds (**271-282**)

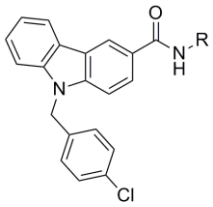

(271-282)

Comp	R	M.P.	IR characteristic peaks (cm^{-1})	HPLC Data
271	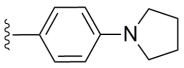	259-261 °C	3289, 3046, 2830, 1631, 1327, 805, 751	Purity: 99.7% t_R = 6.70 min
272	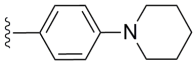	240-242 °C	3282, 3048, 2852, 1632, 1129, 817, 750	Purity: 98.5% t_R = 3.70 min
273	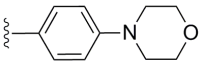	234-236 °C	3269, 3010, 2854, 1632, 1116, 816, 752	Purity: 99.2% t_R = 6.55 min
274	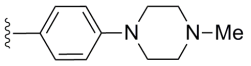	254-256 °C	3284, 3050, 2932, 1628, 1520, 1329, 816, 750	Purity: 99.2% t_R = 4.40 min
275	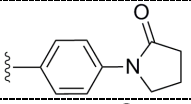	252-254 °C	3297, 1672, 1524, 1408, 1239, 832, 755	Purity: 99.3% t_R = 6.20 min
276	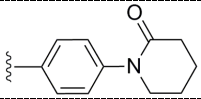	266-268 °C	3295, 3053, 2931, 1655, 1620, 1013, 834, 749	Purity: 98.1% t_R = 5.81 min
277	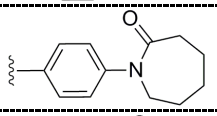	243-245 °C	3304, 3050, 2928, 1633, 1516, 1324, 827, 752	Purity: 98.7% t_R = 6.99 min
278	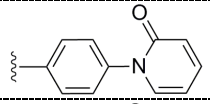	256-258 °C	3305, 3046, 1660, 1515, 1322, 801	Purity: 98.9% t_R = 5.38 min
279	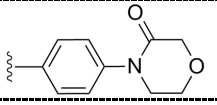	243-245 °C	3327, 3054, 2865, 1643, 1600, 1238, 1100, 810	Purity: 99.1% t_R = 5.17 min
280	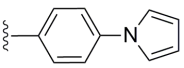	229-231 °C	3302, 1648, 1527, 1325, 824, 750	Purity: 95.5% t_R = 15.3 min
281	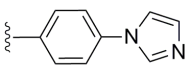	>260 °C	3219, 3116, 3000, 1671, 1521, 1329, 823, 746	Purity: 99.2% t_R = 4.60 min
282	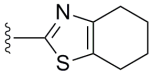	220-222	3138, 3048, 2928, 1662, 1550, 1323, 801, 748	Purity: 99.0% t_R = 5.72 min

The ^{1}H-NMR spectrum of compound (**271**) showed a singlet at δ 9.95 for one proton of amide group (CONH_k). The aromatic protons appeared as singlet at δ 8.84 for one proton (ArH_c), doublet at δ 8.28 for one proton (ArH_g), doublet at δ 8.08 for one proton (ArH_b), doublet at δ 7.75 for one proton (ArH_a), doublet at δ 7.69 for one proton (ArH_d), doublet at δ 7.61 for two protons (ArH_h), multiplet at δ 7.47-7.52 for one proton (ArH_f), doublet at δ 7.37 for two protons (ArH_l), multiplet at δ 7.27-7.34 for one proton (ArH_e), doublet at δ 7.20 for two protons (ArH_m) and doublet at δ 6.57 for two protons (ArH_i). Aliphatic protons appeared as singlet at δ 5.74 for two methylene protons (NC$H_{2/j}$), multiplet at δ 3.20-3.24 for four protons (NC$H_{2/n}$) and multiplet at δ 1.96-1.98 for four protons (C$H_{2/o}$). Its mass spectrum showed $(M)^+$ peak at 480 m/z.

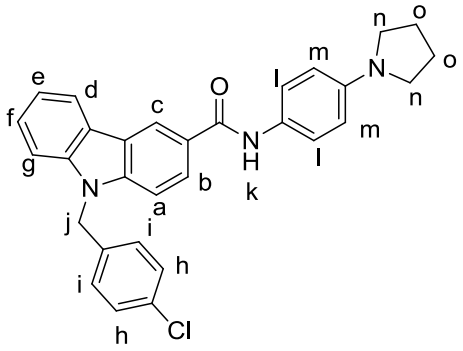

(271)

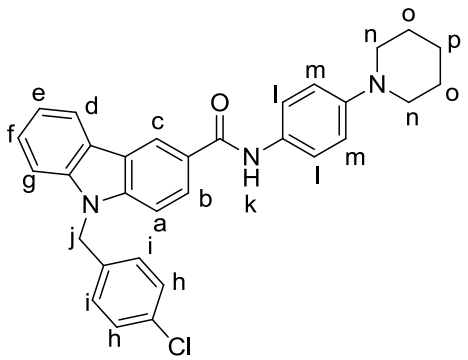

(272)

The ^{1}H-NMR spectrum of compound (**272**) showed a singlet at δ 10.04 for one proton of the amide group (CONH_k). The aromatic protons were observed as singlet at δ 8.84 for one proton (ArH_c), doublet at δ 8.28 for one proton (ArH_g), doublet at δ 8.08 for one proton (ArH_b), doublet at δ 7.76 for one proton (ArH_a), multiplet at δ 7.63-7.69 for three protons (Ar$H_{d,h}$), triplet at δ 7.50 for one proton (ArH_f), doublet at δ 7.37 for two protons (ArH_l), triplet at δ 7.30 for one proton (ArH_e), doublet at δ 7.20 for two protons (ArH_m) and doublet at δ 6.95 for two protons (ArH_i). Aliphatic protons appeared as singlet at δ 5.75 for two methylene protons (NCH_{2j}), multiplet at δ 3.09-3.11 for four protons (NC$H_{2/n}$), multiplet at δ 1.61-1.67 for four protons (C$H_{2/o}$), and multiplet at δ 1.51-1.56 for two protons (C$H_{2/p}$). Its mass spectrum showed $(M)^+$ peak at 494.2 m/z and $(M+2)^+$ peak at 496.2 m/z.

The ^{1}H-NMR spectrum of compound (**273**) showed a singlet at δ 10.09 for one proton of the amide group (CON*H*$_k$). The aromatic protons appeared as singlet at δ 8.85 for one proton (Ar*H*$_c$), doublet at δ 8.29 for one proton (Ar*H*$_g$), doublet at δ 8.09 for one proton (Ar*H*$_b$), doublet at δ 7.77 for one proton (Ar*H*$_a$), multiplet at δ 6.66-6.72 for three protons (Ar*H*$_{d,h}$), triplet at δ 7.50 for one proton (Ar*H*$_f$), doublet at δ 7.36 for two protons (Ar*H*$_l$), triplet at δ 7.31 for one proton (Ar*H*$_e$), doublet at δ 7.20 for two protons (Ar*H*$_m$), doublet at δ 6.97 for two protons (Ar*H*$_i$) confirming the total fifteen aromatic protons in structure. The aliphatic protons appeared as singlet at δ 5.76 for two methylene protons (NC*H*$_{2/j}$), triplet at δ 3.75 for four methylene protons (OC*H*$_{2/o}$) and triplet at δ 3.08 for four protons (NC*H*$_{2/n}$). Its mass spectrum showed $(M)^+$ peak at 496 m/z.

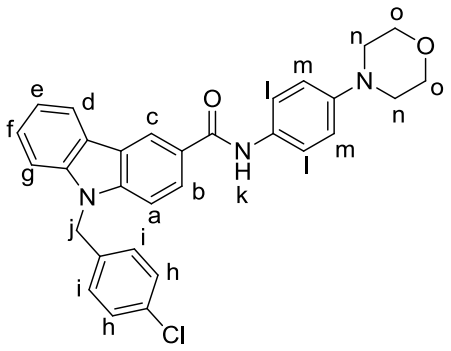

(273)

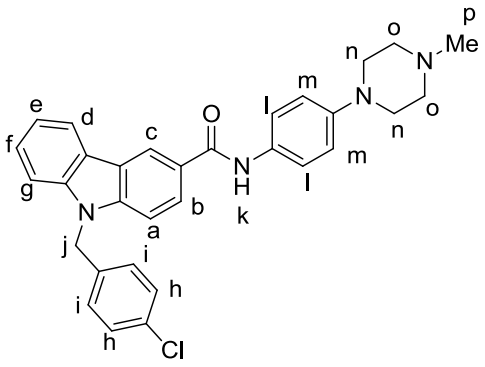

(274)

The ^{1}H-NMR spectrum of compound (**274**) showed a singlet at δ 10.03 for one proton of the amide group (CON*H*$_k$). The aromatic protons were observed as singlet at δ 8.84 for one proton (Ar*H*$_c$), doublet at δ 8.27 for one proton (Ar*H*$_g$), doublet at δ 8.08 for one proton (Ar*H*$_b$), doublet at δ 7.75 for one proton (Ar*H*$_a$), multiplet at δ 6.65-6.68 for three protons (Ar*H*$_{d,h}$), triplet at δ 7.51 for one proton (Ar*H*$_f$), multiplet at δ 7.28-7.36 for three protons (Ar*H*$_{e,l}$), doublet at δ 7.20 for two protons (Ar*H*$_m$) and doublet at δ 6.95 for two protons (Ar*H*$_i$). Aliphatic protons appeared as singlet at δ 5.74 for two protons (NC*H*$_{2/j}$), multiplet at δ 3.09-3.12 for four protons (NC*H*$_{2/n}$), multiplet at δ 2.42-2.48 for four protons (NC*H*$_{2/o}$) and singlet at δ 2.23 for three protons of methyl group (NC*H*$_{3/p}$). Its mass spectrum showed $(M)^+$ peak at 509 m/z.

The ^{1}H NMR spectrum of compound (**275**) showed a singlet at δ 10.26 for proton of the amide group (CONH_k). The aromatic protons were observed as singlet at δ 8.87 for one proton (ArH_c), doublet at δ 8.30 for one proton (ArH_g), doublet at δ 8.10 for one proton (ArH_b), doublet at δ 7.84 for two protons (ArH_h), doublet at δ 7.78 for one proton (ArH_a), multiplet at δ 7.65-7.70 for three protons (Ar$H_{d,l}$), triplet at δ 7.51 for one proton (ArH_f), doublet at δ 7.37 for two protons (ArH_m), triplet at δ 7.31 for one proton (ArH_e) and doublet at δ 7.21 for two protons (ArH_i). Aliphatic protons appeared as singlet at δ 5.75 for two methylene protons (NC$H_{2/j}$), triplet at δ 3.85 for two protons (NC$H_{2/n}$), multiplet at δ 2.48-2.52 for one proton (C$H_{2/o}$) and triplet at δ 2.08 for two protons (ArH_p). Its mass spectrum showed $(M)^+$ peak at 494.33 m/z and $(M+2)^+$ peak at 496.32 m/z.

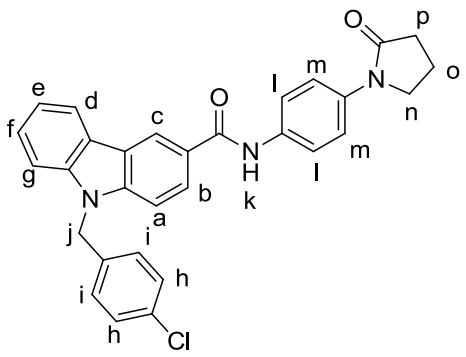

(275)

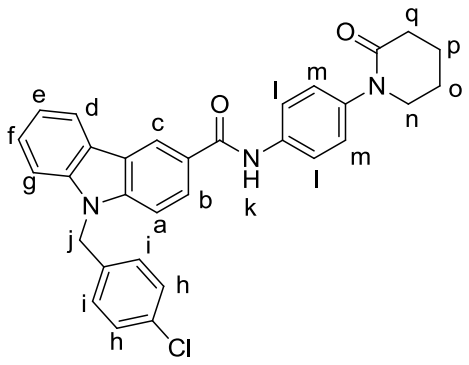

(276)

The ^{1}H-NMR spectrum of compound (**276**) showed a singlet at δ 10.29 for one proton of the amide group (CONH_k). The aromatic protons appeared as singlet at δ 8.87 for one proton (ArH_c), doublet at δ 8.30 for one proton (ArH_g), doublet at δ 8.10 for one proton (ArH_b), doublet at δ 7.83 for two protons (ArH_h), doublet at δ 7.79 for one proton (ArH_a), doublet at δ 7.70 for one proton (ArH_d), multiplet at δ 7.48-7.52 for one proton (ArH_f), doublet at δ 7.37 for two protons (ArH_l), multiplet at δ 7.26-7.34 for one proton (ArH_e), doublet at δ 7.27 for two protons (ArH_m) and doublet at δ 7.21 for two protons (ArH_i). Aliphatic protons appeared as singlet at δ 5.76 for two methylene protons (NC$H_{2/j}$), multiplet at δ 3.60-3.62 for two protons (NC$H_{2/n}$), triplet at δ 2.40 for two protons (COC$H_{2/q}$), multiplet at δ 1.84-1.88 for four protons

(C$H_{2/o,p}$). Its mass spectrum showed $(M)^+$ peak at 508.35 m/z and $(M+2)^+$ peak at 510.29 m/z.

The ^{1}H-NMR spectrum of compound (**277**) showed a singlet δ at 10.26 for proton of the amide group (CONH_k). The aromatic protons appeared as singlet at δ 8.86 for one proton (ArH_c), doublet at δ 8.29 for one proton (ArH_g), doublet at δ 8.10 for one proton (ArH_b), multiplet at δ 7.76-7.81 for three protons (Ar$H_{a,h}$), doublet at δ 7.69 for one proton (ArH_d), triplet at δ 7.50 for one proton (ArH_f), multiplet at δ 7.29-7.36 for three protons (Ar$H_{e.l}$) and multiplet at δ 7.18-7.20 for four protons (Ar$H_{i,m}$). The aliphatic protons were observed as singlet at δ 5.75 for two protons (NC$H_{2/j}$), multiplet at δ 3.69-3.77 for two protons (NC$H_{2/r}$), multiplet at δ 2.59-2.61 for two protons (COC$H_{2/n}$) and multiplet at δ 1.65-1.81 for six protons (C$H_{2/o,p,q}$). Its mass spectrum showed $(M+1)^+$ peak at 522.2 m/z and $(M+2)^+$ peak at 523.2 m/z.

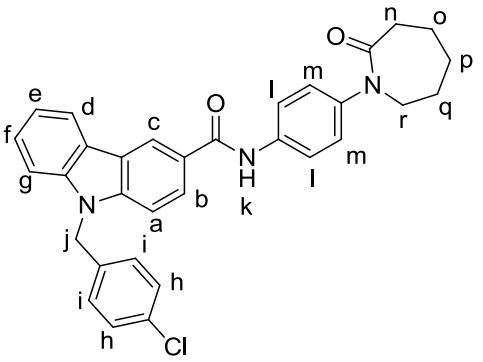

(277)

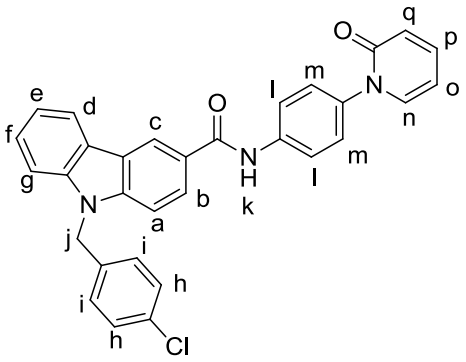

(278)

The ^{1}H-NMR spectrum of compound (**278**) showed a singlet at δ 10.42 for proton of the amide group (CONH_k). The aromatic protons appeared as singlet at δ 8.88 for one proton (ArH_c), doublet at δ 8.31 for one proton (ArH_g), doublet at δ 8.12 for one proton (ArH_b), multiplet at δ 7.93-7.97 for two protons (ArH_h), doublet at δ 7.80 for one proton (ArH_a), doublet at δ 7.70 for one proton (ArH_d), multiplet at δ 7.66-7.68 for one proton (ArH_p), multiplet at δ 7.49-7.53 for two protons (Ar$H_{f,q}$), multiplet at δ 7.31-7.41 for five protons (Ar$H_{e,l,m}$), doublet at δ 7.20 for two protons (ArH_i), doublet at δ 6.50 for one proton (ArH_o) and multiplet at δ 6.30-6.34 for one proton (ArH_n). The aliphatic protons were observed as a singlet at δ 5.76 for two methylene

protons (NC$H_{2/j}$). Its mass spectrum showed $(M)^+$ peak at 504.35 m/z and $(M+2)^+$ peak at 506.34 m/z.

The ^{1}H-NMR spectrum of compound (**279**) showed a singlet at δ 10.35 for proton of amide (CONH$_k$). The aromatic protons appeared as singlet at δ 8.87 for one proton (ArH_c), doublet at δ 8.30 for one proton (ArH_g), doublet at δ 8.10 for one proton (ArH_b), doublet at δ 7.87 for two protons (ArH_h), doublet at δ 7.79 for one proton (ArH_d), doublet at δ 7.70 for one proton (ArH_a), triplet at δ 7.50 for one proton (ArH_f), multiplet at δ 7.29-7.40 for five protons (Ar$H_{e,l,i}$) and doublet at δ 7.20 for two protons (ArH_m). Aliphatic protons appeared as singlet at δ 5.75 for two protons (NC$H_{2/j}$), singlet at δ 4.21 for two protons (OC$H_{2/p}$), triplet at δ 3.98 for two protons (OC$H_{2/o}$), triplet at δ 3.74 for two protons (OC$H_{2/n}$). Its mass spectrum showed $(M)^+$ peak at 510.40 m/z and $(M+2)^+$ peak at 512.36 m/z.

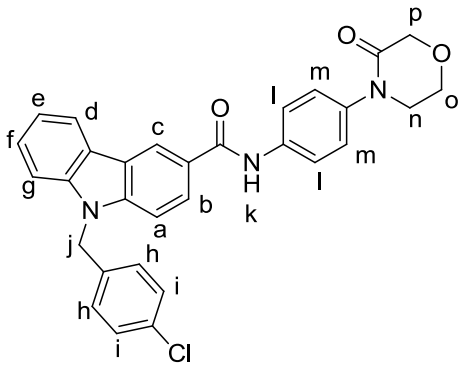

(279)

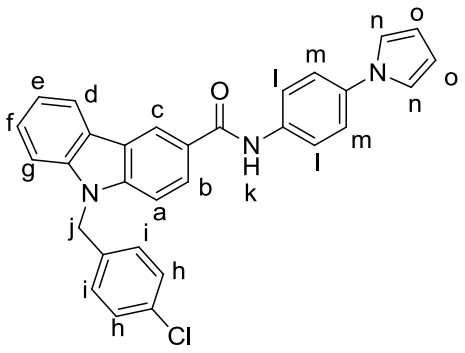

(280)

The ^{1}H NMR spectrum of compound (**280**) showed a singlet at δ 10.35 for one proton of the amide (CONH$_k$). The aromatic protons appeared at δ 8.88 for one proton (ArH_c), doublet at δ 8.31 for one proton (ArH_g), doublet at δ 8.11 for one proton (ArH_b), doublet at δ 7.94 for two protons (ArH_h), doublet at δ 7.80 for one proton (ArH_a), doublet at δ 7.71 for one proton (ArH_d), doublet at δ 7.60 for two protons (ArH_n), triplet at δ 7.53 for one proton (ArH_f), multiplet at δ 7.30-7.37 for five protons (Ar$H_{l,m,e}$), doublet at δ 7.21 for two protons (ArH_i) and multiplet at δ 6.24-6.28 for two protons (ArH_o). A singlet at δ 5.76 was appeared for two methylene protons (NC$H_{2/j}$). Its mass spectrum showed $(M)^+$ peak at 476.39 m/z.

The ^{1}H-NMR spectrum of compound (**281**) showed a singlet at δ 10.40 for one proton of the amide (CON*H*$_k$). The aromatic protons appeared as singlet at δ 8.88 for one proton (Ar*H*$_c$), doublet at δ 8.30 for one proton (Ar*H*$_g$), singlet at δ 8.22 for one proton (Ar*H*$_p$), doublet at δ 8.11 for one proton (Ar*H*$_b$), doublet at δ 7.99 for two protons (Ar*H*$_h$), doublet at δ 7.79 for one proton (Ar*H*$_a$), multiplet at δ 7.64-7.73 for four protons (Ar*H*$_{d,m.o}$), triplet at δ 7.51 for one proton (Ar*H*$_f$), multiplet at δ 7.31-7.37 for three protons (Ar*H*$_{l,e}$), doublet at δ 7.21 for two protons (Ar*H*$_i$) and multiplet at δ 7.10-7.12 for one proton (Ar*H*$_n$). A singlet at δ 5.76 was observed for two methylene protons (NC*H*$_{2j}$). Its mass spectrum showed $(M+1)^+$ peak at 477.1 m/z and $(M+2)^+$ peak at 478.2 m/z.

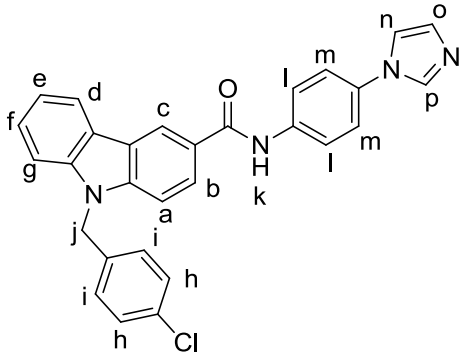

(281)

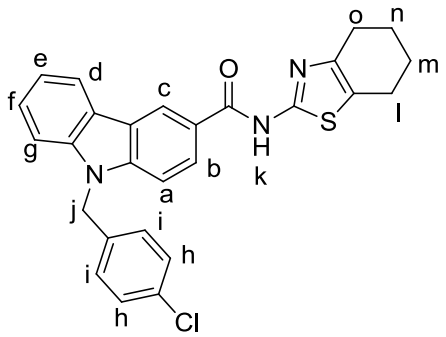

(282)

The ^{1}H-NMR spectrum of compound (**282**) showed a singlet at δ 12.34 for one proton of the amide (CON*H*$_k$). Aromatic protons appeared as singlet at δ 9.07 for one proton (Ar*H*$_c$), multiplet at δ 8.20-8.33 for two protons (Ar*H*$_{g,b}$), doublet at δ 7.78 for one proton (Ar*H*$_a$), multiplet at δ 7.67-7.73 for one proton (Ar*H*$_d$), triplet at δ 7.52 for one proton (Ar*H*$_f$), multiplet at δ 7.29-7.37 for three protons (Ar*H*$_{e,h}$) and doublet at δ 7.20 for two protons (Ar*H*$_i$). Aliphatic protons were observed as singlet at δ 5.75 for two methylene protons (NC*H*$_{2/j}$), multiplet at δ 2.63-2.69 for four protons (C*H*$_{2/l,o}$), multiplet at δ 1.40-1.80 for four protons (C*H*$_{2/m,n}$). Its mass spectrum showed $(M)^+$ peak at 472.1 m/z and $(M+2)^+$ peak at 474.2 m/z.

4.3.3. Biological evaluation of the synthesized compounds (271-282)

The synthesized compounds were evaluated for their *in vitro* anticoagulant and antithrombotic activities. For the evaluation of anticoagulant activity PT and aPTT times were determined. The FXa inhibition assay was performed to assess the antithrombotic potential of the synthesized compounds.

4.3.3.1. *In vitro* anticoagulant activity

The anticoagulation potential of the newly synthesized FXa inhibitors was assessed by measuring the prothrombin time (PT) and activated partial thromboplastin time (aPTT). PT and aPTT estimate the effect of an inhibitor on the extrinsic and intrinsic pathways respectively. Significant prolongation in both PT and aPTT by inhibitors shows their effect on both the pathways and indicate selectivity towards FXa, which is common in both pathways. All the synthesized compounds were subjected to determination of PT and aPTT at a concentration of 1 mM in human plasma. The *in vitro* anticoagulant activities of compounds (**271-282**) were given in **Table 4.23**.

All the synthesized compounds were evaluated for PT and aPTT time measurements. All the compounds exhibited moderate anticoagulant activity. Among the tested compounds, compound (**278**) having 2-oxopyridine moiety showed good activity with PT (39.4 sec) and aPTT (69.6 sec) time. Compound (**276**) having 2-piperidinone moiety also showed notable activity with PT (33.5 sec) and aPTT (66.1 sec) time.

4.3.3.2. *In vitro* FXa inhibition assay for evaluation of antithrombotic activity

In vitro enzyme inhibition assay for FXa was performed for the synthesized compounds at a concentration of 100 µM by using a chromogenic substrate (S-2765) as per the previously reported procedure.[82] The enzyme inhibition was determined from the change in the absorbance at 405 nm with hydrolysis of the substrate by the enzyme. Those compounds with more than 50 % inhibition of FXa were chosen for determination of their IC_{50} values. Compounds (**275**, **276**, **278-282**) showed good inhibition of FXa in

preliminary screening. **Table 4.23** represents IC_{50} values of compounds (**275**, **276**, **278-282**) against FXa. Among the tested compounds, compound (**278**) having 2-oxopyridine moiety showed the highest FXa inhibitory activity (7.49 µM).

Table 4.23. FXa inhibitory activity, PT and aPTT time of compounds (**271-282**)

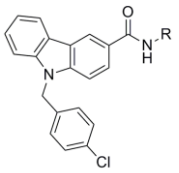

(271-282)

Comp	R	FXa IC_{50} ± SEM (µM)	PT Time (Sec)	aPTT Time (Sec)
271	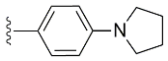	>100	22.1	40.8
272	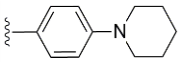	>100	20.7	41.1
273	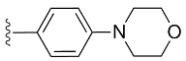	>100	21.5	43.1
274	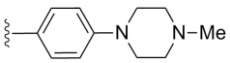	>100	20.02	44.2
275	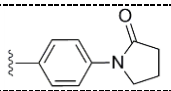	63.15 ± 3.6	23.4	42.7
276	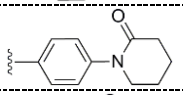	**15.87 ± 1.8**	**33.5**	**66.1**
277	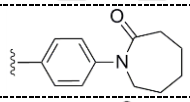	ND	21.76	41.0
278	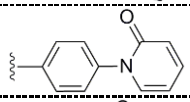	**7.49 ± 0.9**	**39.9**	**69.6**
279	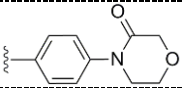	47.20 ± 4.2	29.7	62.6
280	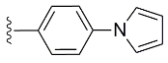	29.40 ± 2.2	22.6	42.8
281	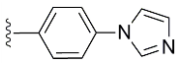	16.60 ± 1.4	24.1	47.7
282	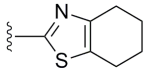	33.10 ± 2.6	29.7	49.8
Blank (DMSO)			18.9	39.0
Apixaban			>180	>180